

液晶の構造と物性(2)

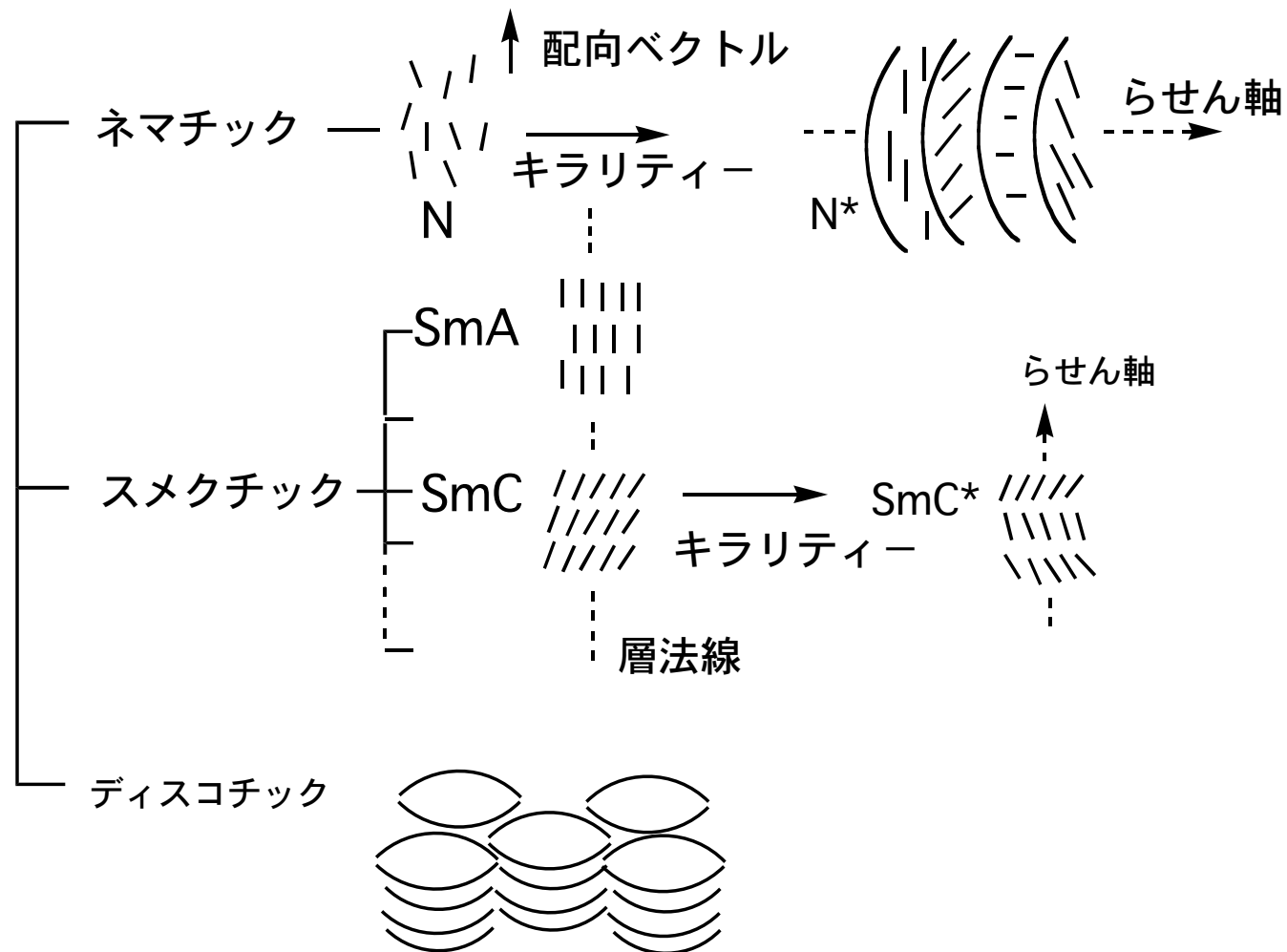
平成23年 9月 6日

弘前大院・理工
吉澤 篤

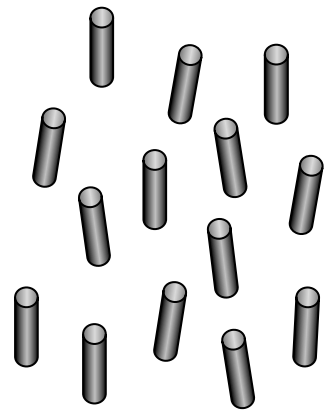
内容

1. C-13 NMR による観測
2. 「分子内に秩序を持つ液晶分子」による階層構造の構築

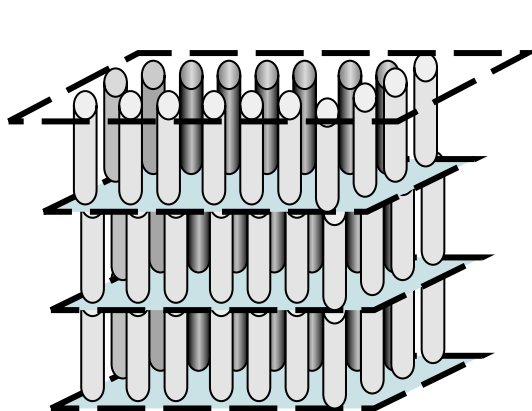
サーモトロピック液晶相の分類



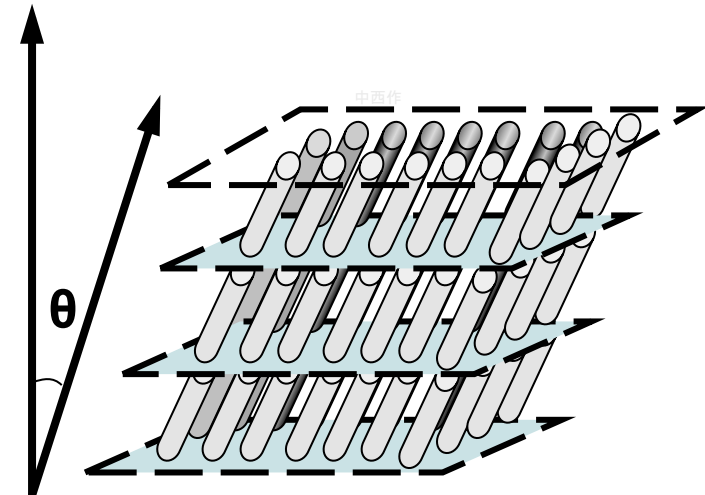
偏光顯微鏡觀察



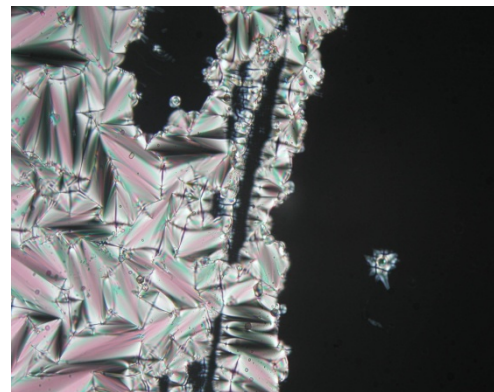
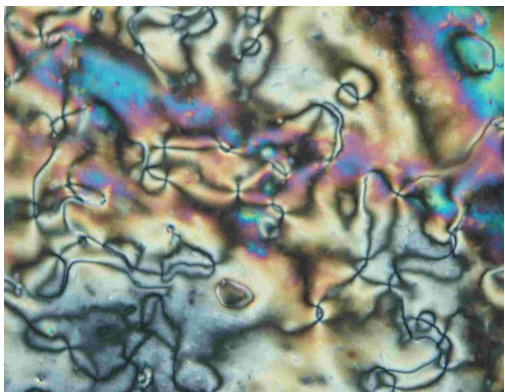
N相



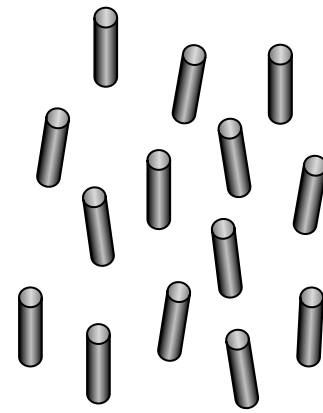
SmA相



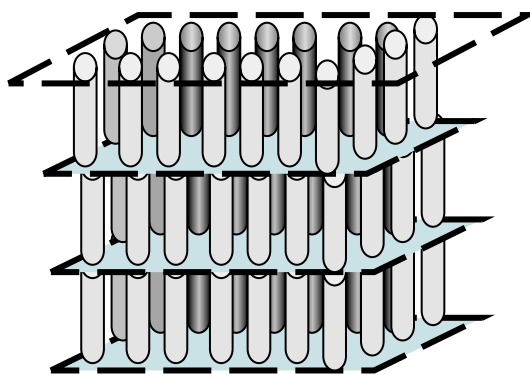
SmC相



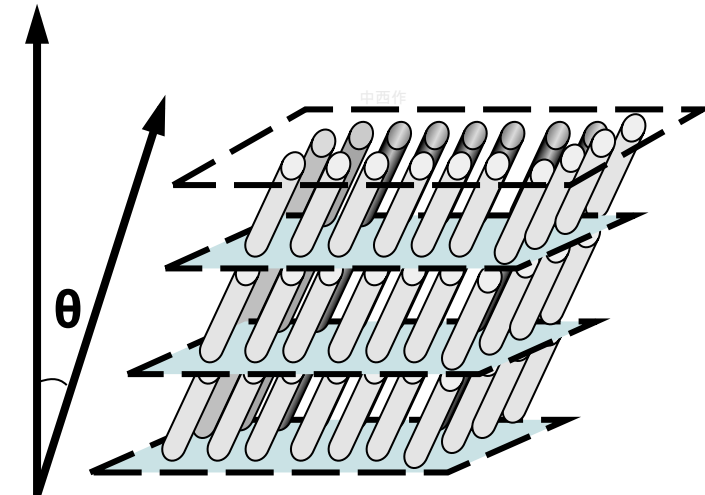
X線回折測定



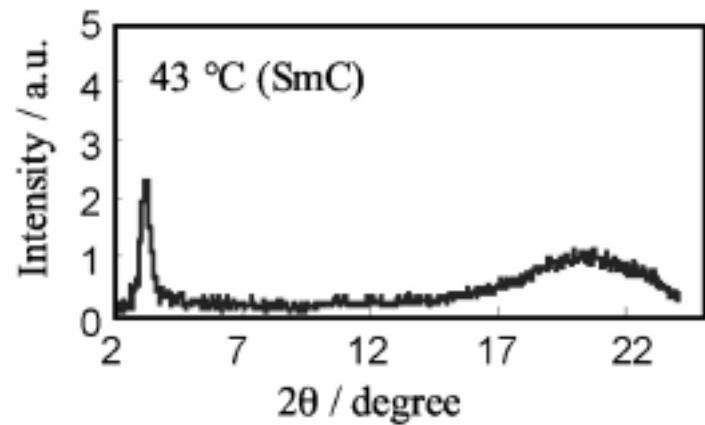
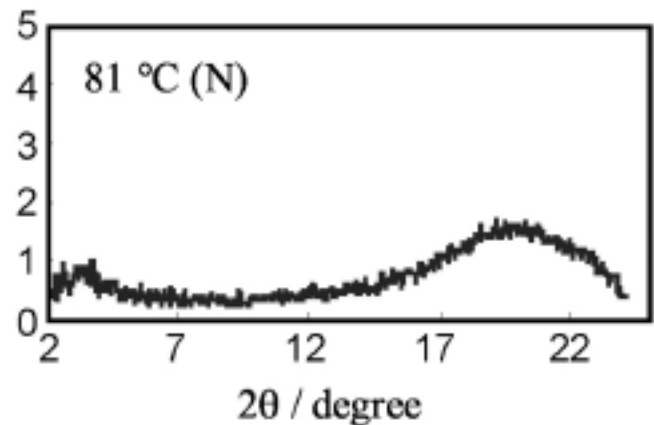
N相



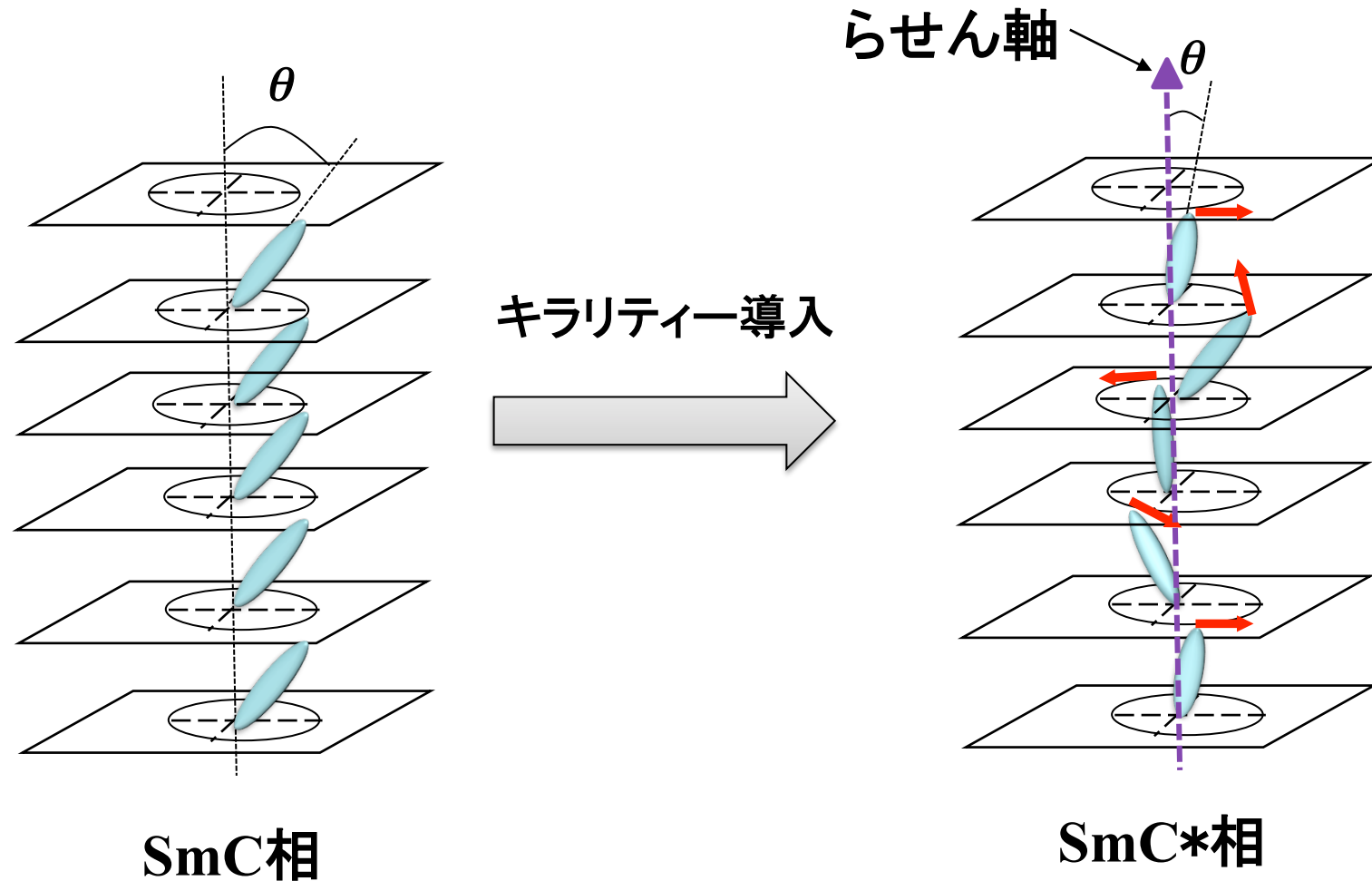
SmA相



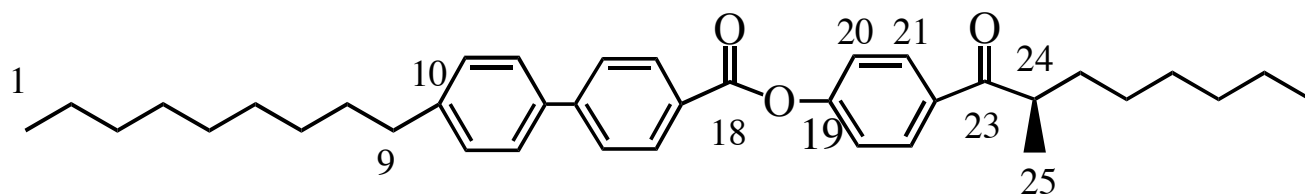
SmC相



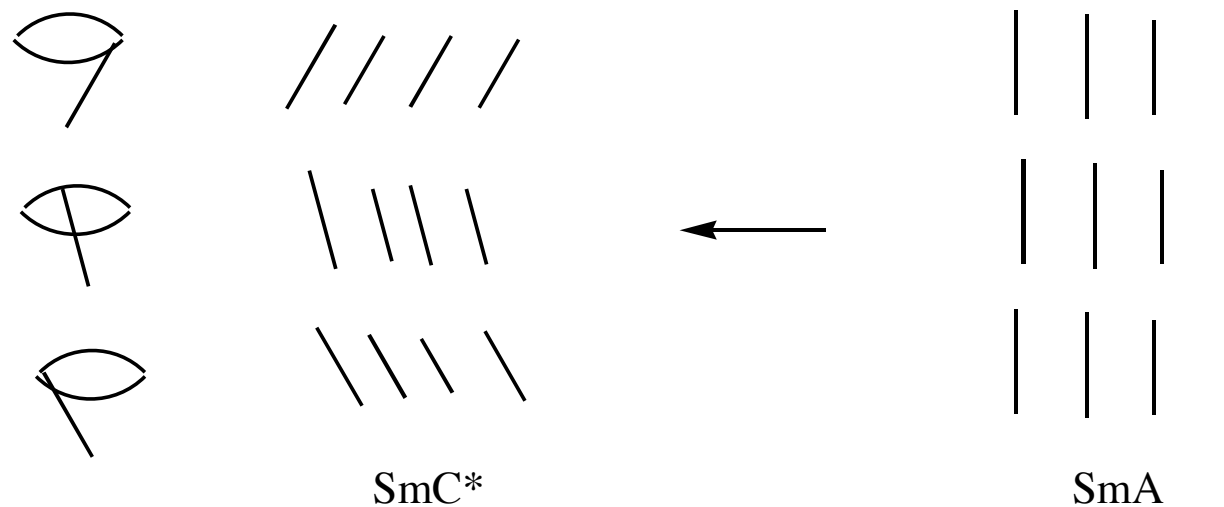
SmC相へのキラリティーの導入



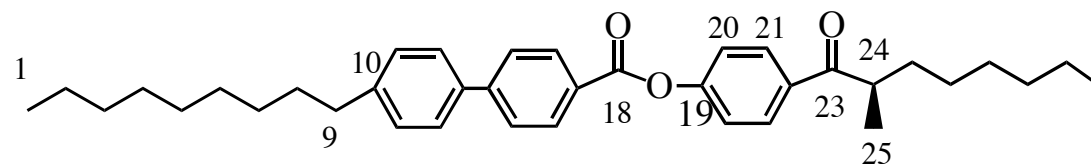
固体NMRから得られた情報 SmA-SmC*相転移



MONBIC: Cryst 79°C SmC* 101 SmA 118 Iso Liq



A. Yoshizawa, H. Kikuzaki, M. Fukumasa, *Liquid Crystals*, 1995, **18**, 351.



MONBIC: Cryst 79°C SmC* 101 SmA 118 Iso Liq

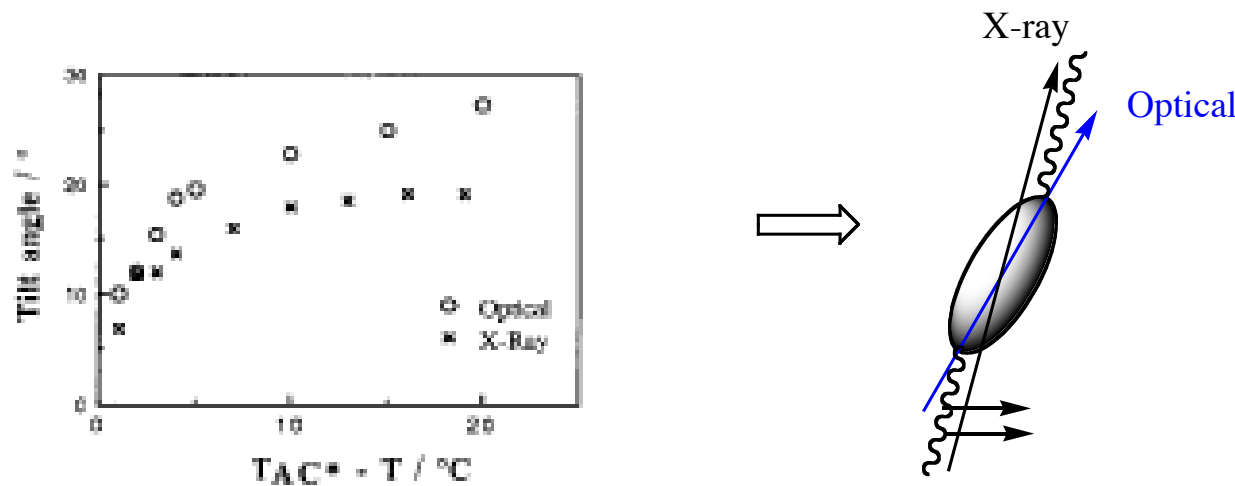
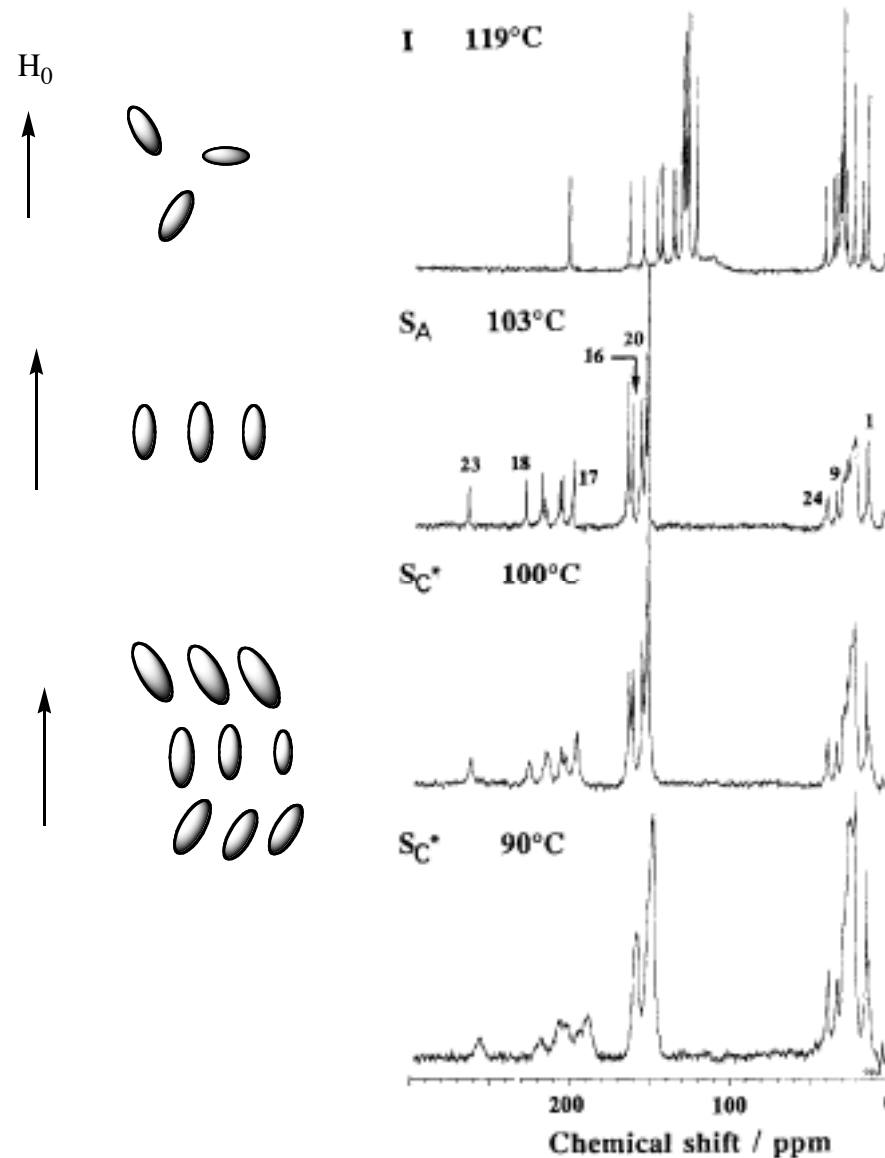
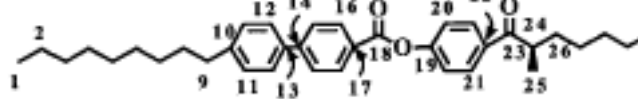
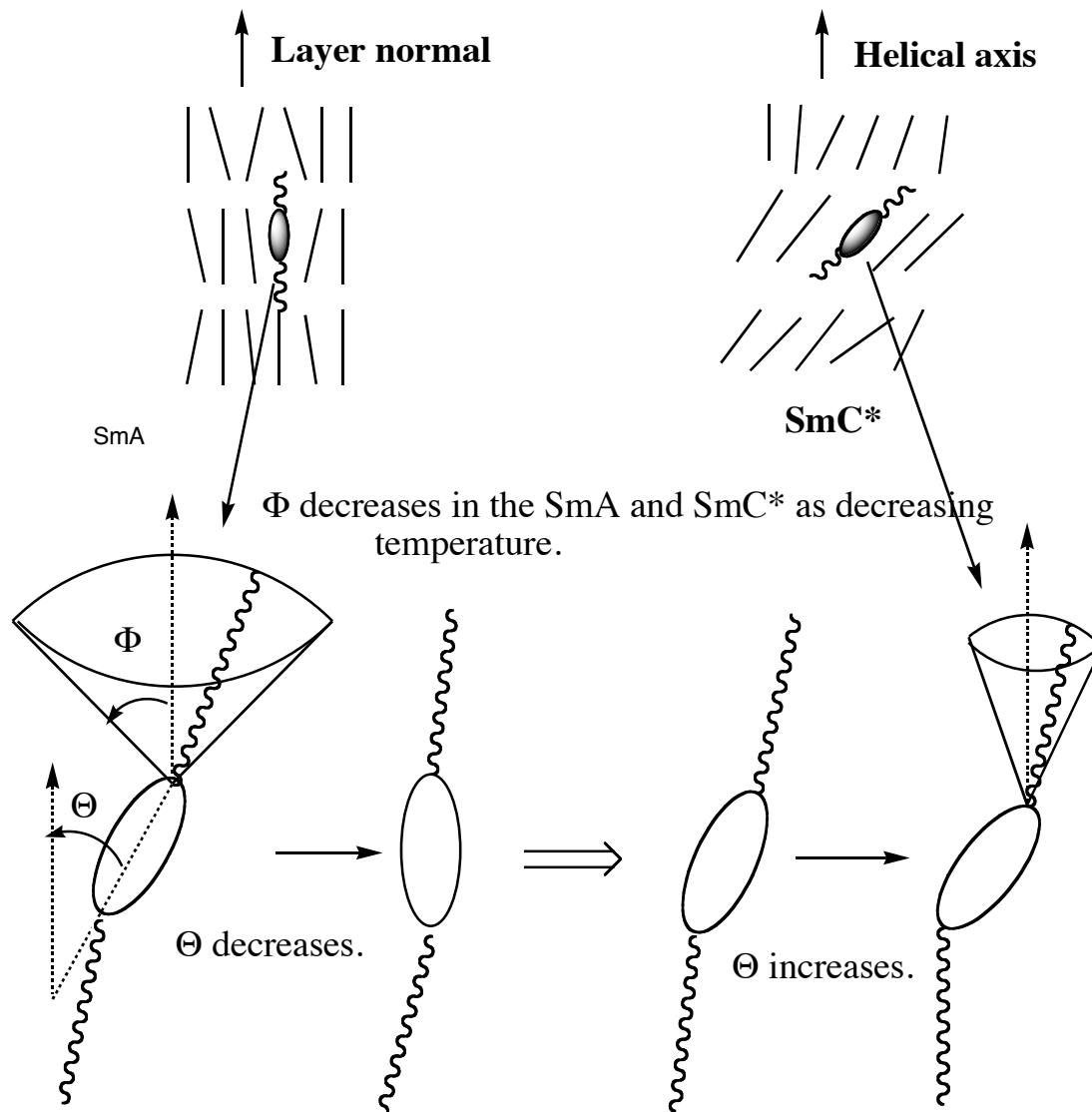


Figure 7. The temperature dependence of the tilt angle determined by optical microscopy and X-ray measurements.

C-13 NMR spectra without MAS



磁場配向スペクトルからわかったこと



C-13 NMR spectra with MAS

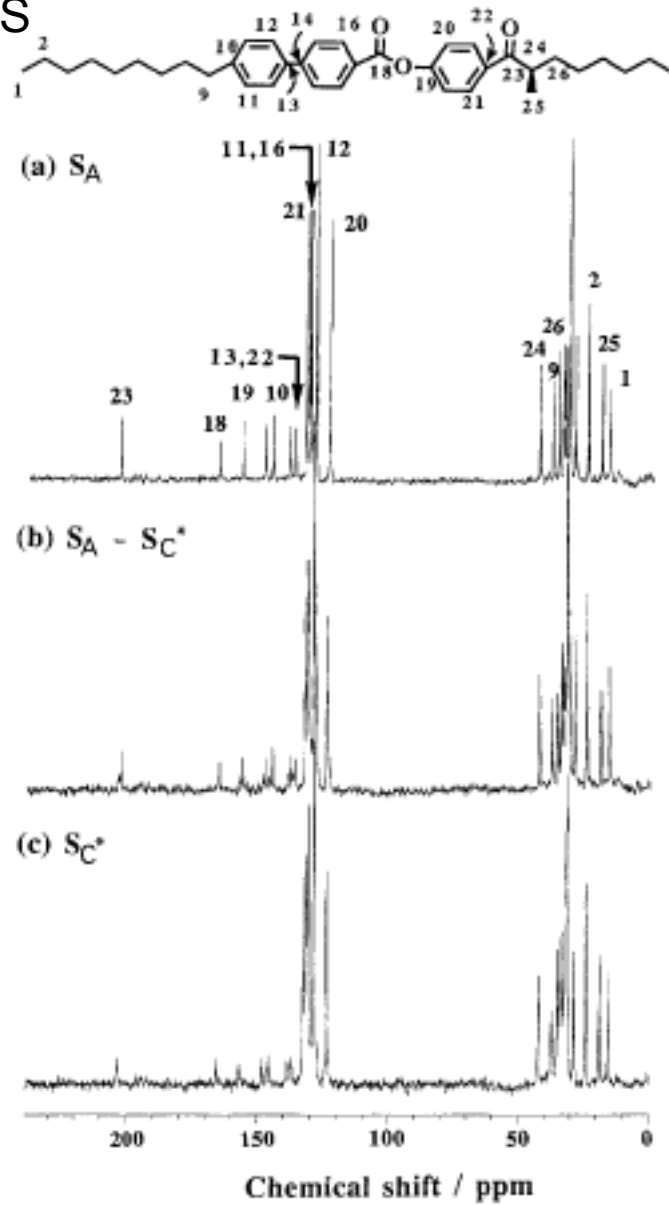


Figure 11. The C-13 NMR spectra of (S)-MONBIC (a) in the S_A phase (112°C), (b) at the $S_A - S_C^*$ coexistence (100°C), and (c) in the S_C^* phase (96°C) with sample spinning.

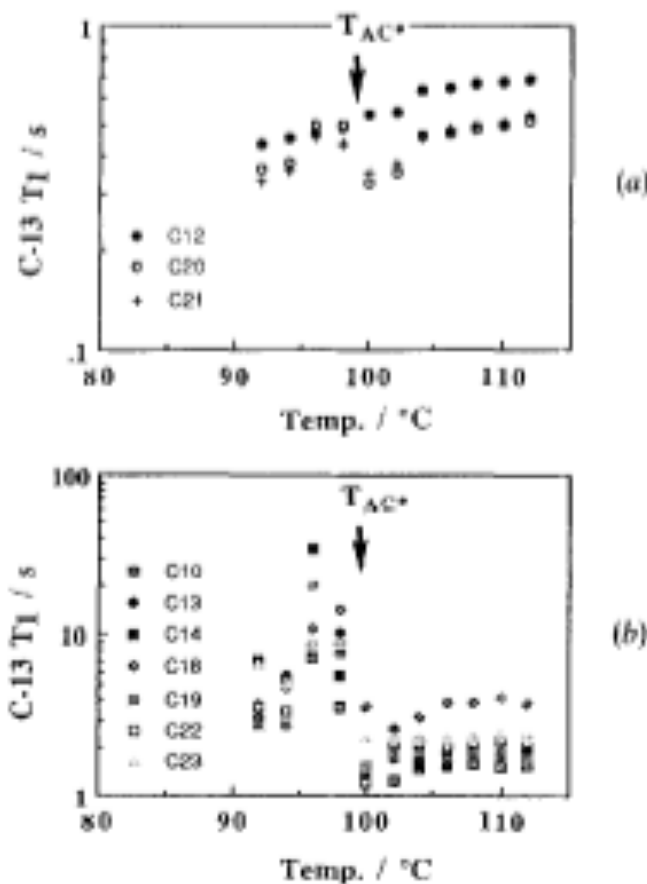
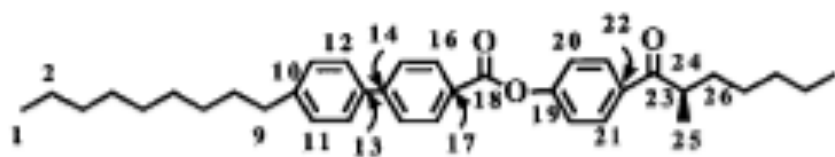


Figure 12. The temperature dependence of C-13 T_1 of (a) the protonated-aromatic carbons and (b) the unprotonated carbons of (S)-MONBIC in S_A and S_C^* phases with MAS.

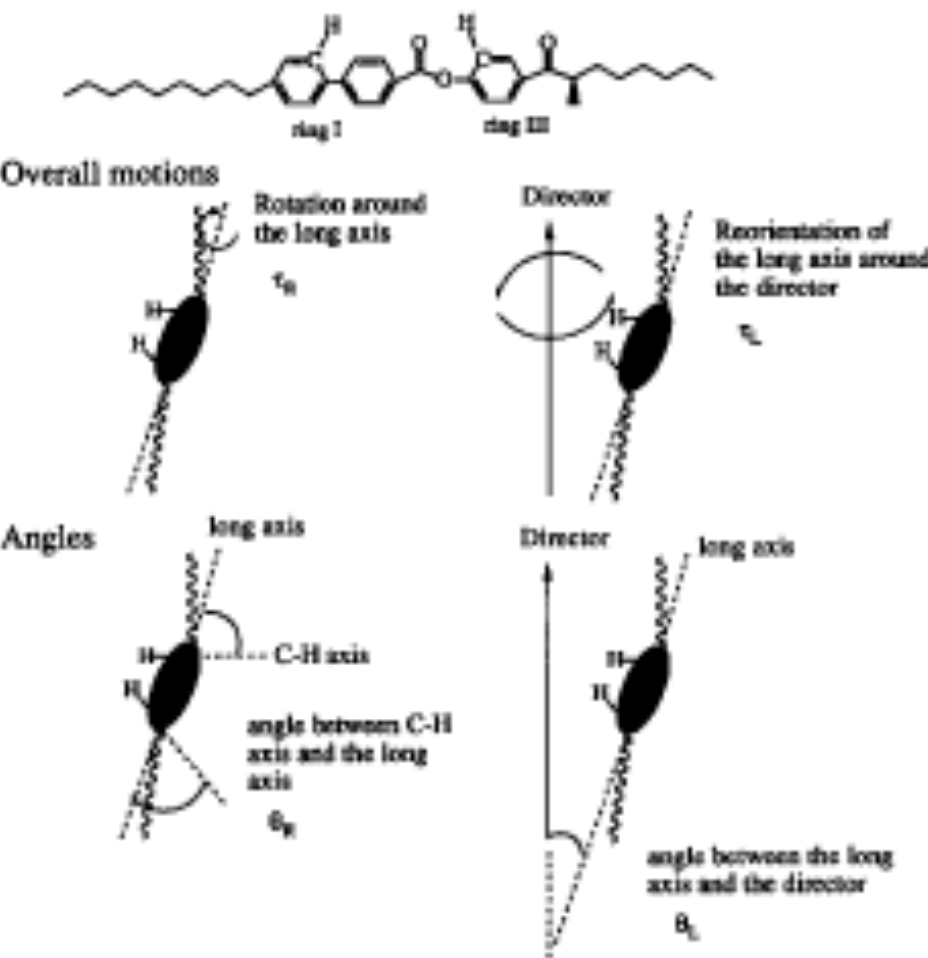


Figure 15. The factors that may effect C-13 T_1 values.

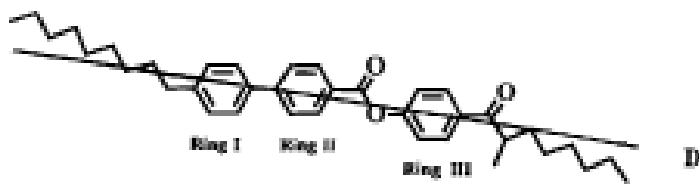


Figure 10. Definition of the molecular long axis, D .

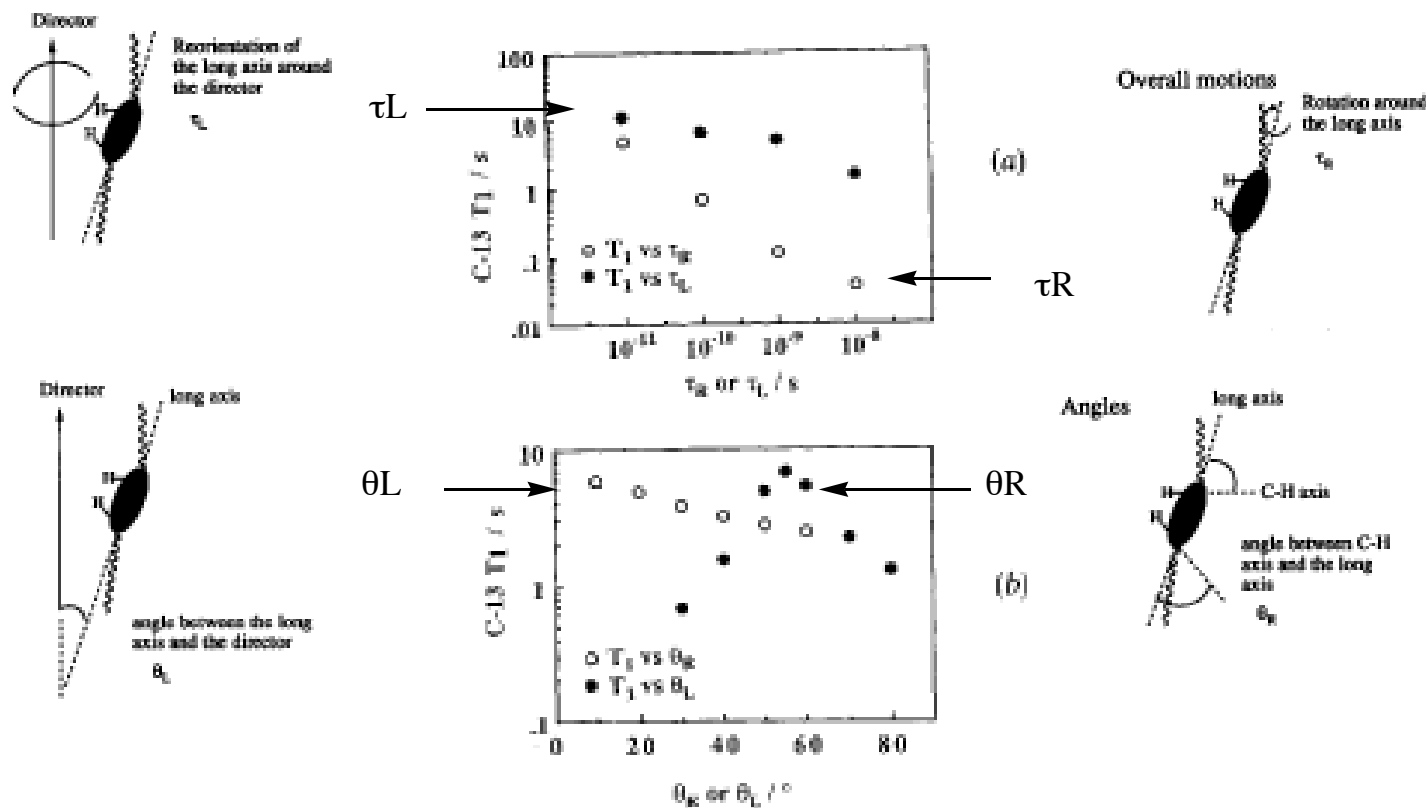


Figure 14. The calculated dependence of a protonated aromatic $C-13 T_1$ on (a) τ_R or τ_L , and (b) θ_R or θ_L .

緩和時間T1の測定からわかったこと

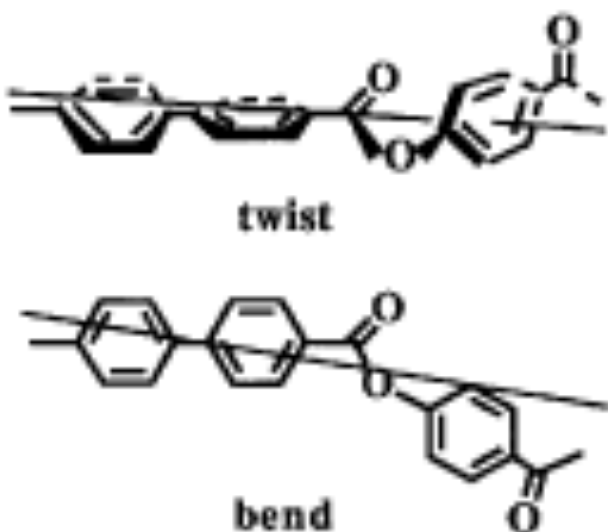


Figure 16. The molecular deformation for the core part. The estimated long axis is shown.

緩和時間T_{1ρ}の測定からわかったこと

Table 7. C-13 T_{1ρ} (ms) for (S_i)-MONBIC in the S_A and S_C^{*} phases with MAS†.

Temperature/°C	C ₁₀	C ₁₈	C ₂₁	C ₂₂	C ₂₃
S _A					
110	0.32 (0.29)	0.29 (0.23)	1.33 (1.08)	0.33 (0.28)	0.45 (0.48)
105	0.29	0.24	1.34	0.31	0.40
100‡	0.10	0.09	0.30	0.11	0.13
S _C [*] (S _C)					
95	0.14	0.13	0.48	0.16	0.14
90	0.13 (0.10)	0.14 (0.13)	0.49 (0.86)	0.15 (0.12)	0.17 (0.15)

† The values in parentheses are C-13 T_{1ρ} (ms) for (S, R)-MONBIC in the S_A and S_C phases with MAS.

‡ The S_A-S_C^{*} coexistence was observed at 100°C. The C-13 T_{1ρ} values were obtained from the peaks in the S_A phase.

- 1) 相間時間が10⁻⁴s程度の協同的な分子運動がコア部分に存在する。側鎖にはない。
- 2) T_{1ρ}がSmA-SmC*相転移近傍のSmA相で急激に減少する。ダイレクターの再配向を反映している。

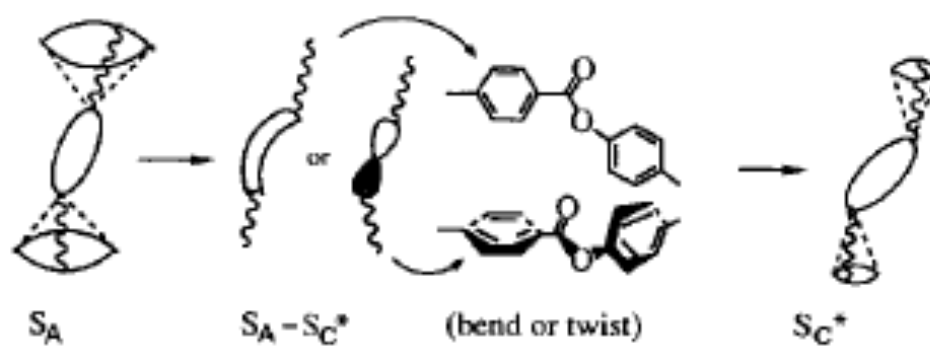


Figure 17. The schematic representation of the molecular orientation of (*S*)-MONBIC in the S_A and S_C^* phases.

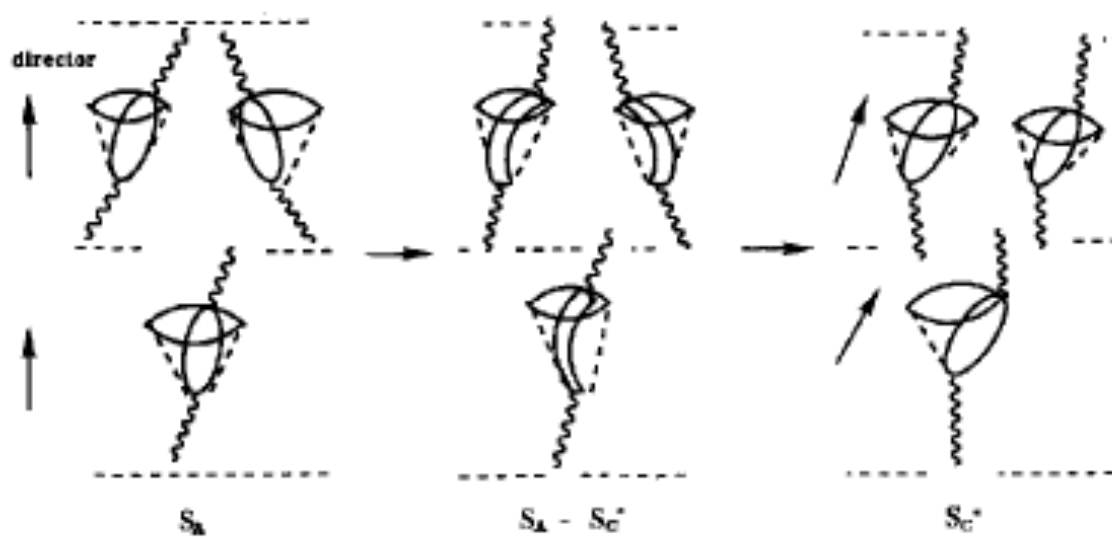
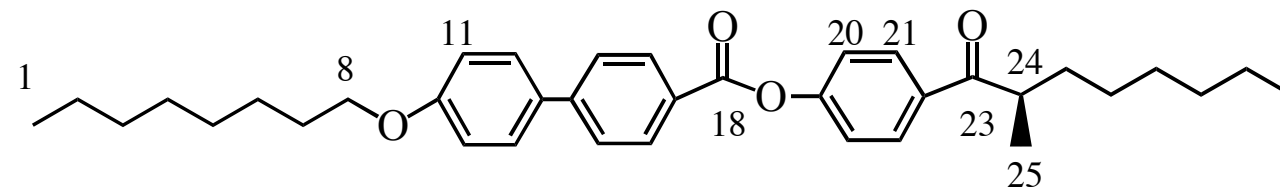
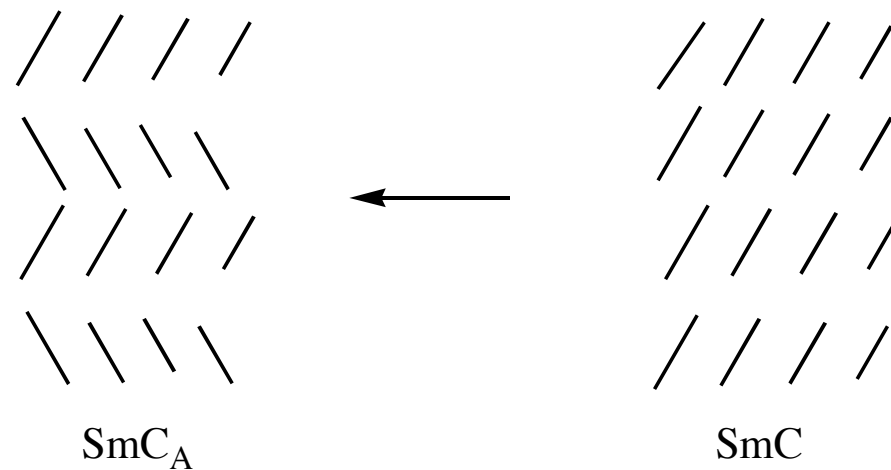


Figure 18. The dynamic molecular deformation effect on the reorientation of the director near the S_A to S_C^* transition.

固体NMRから得られた情報 SmC*-SmCA*相転移



MOPBIC: Cryst 82 (SmI_A* 64 SmC_A* 81) SmC* 138 SmA 157 Iso Liq



A. Yoshizawa, I. Nishiyama, H. Kikuzaki, N. Ise, *Jpn. J. Appl. Phys.*, 1992, **31**, L862.

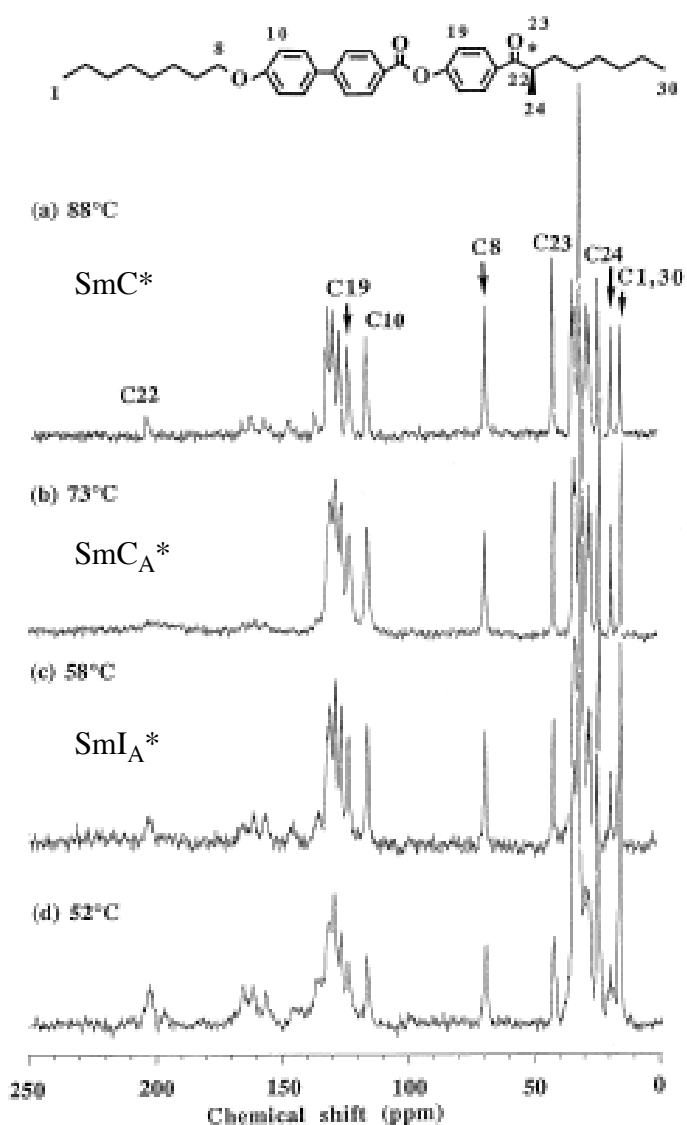


Fig. 2. Temperature-dependent CP/MAS C-13 NMR spectra of MOPBIC on cooling.

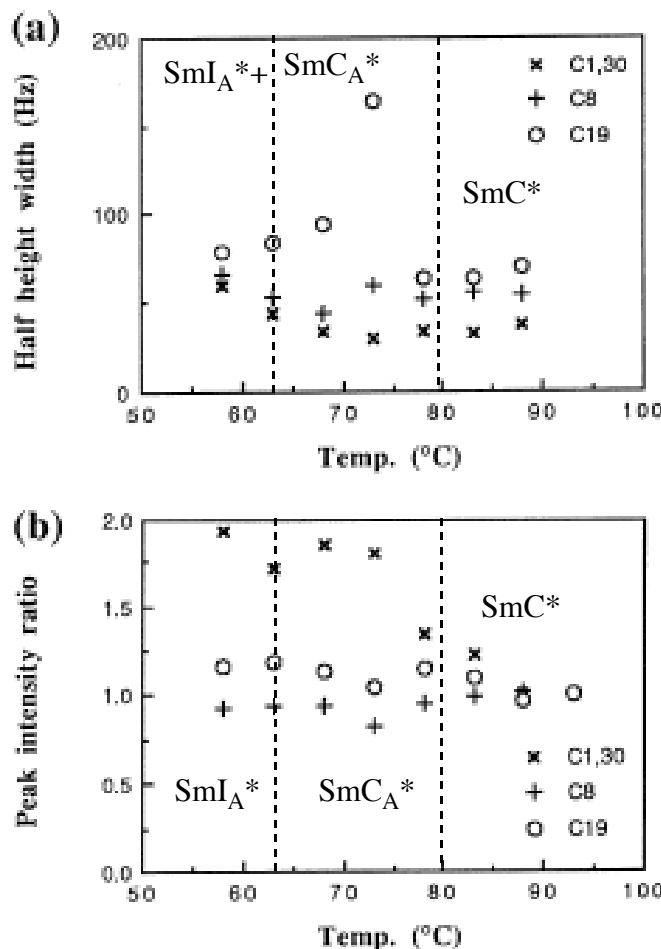
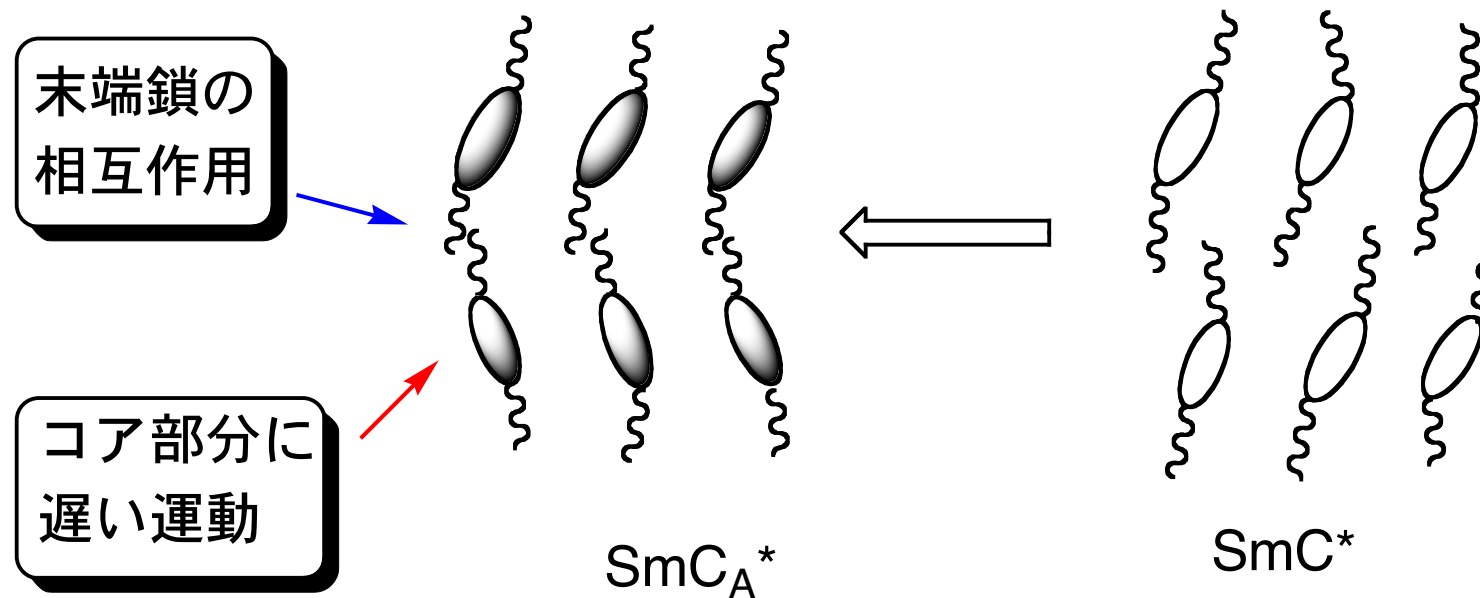
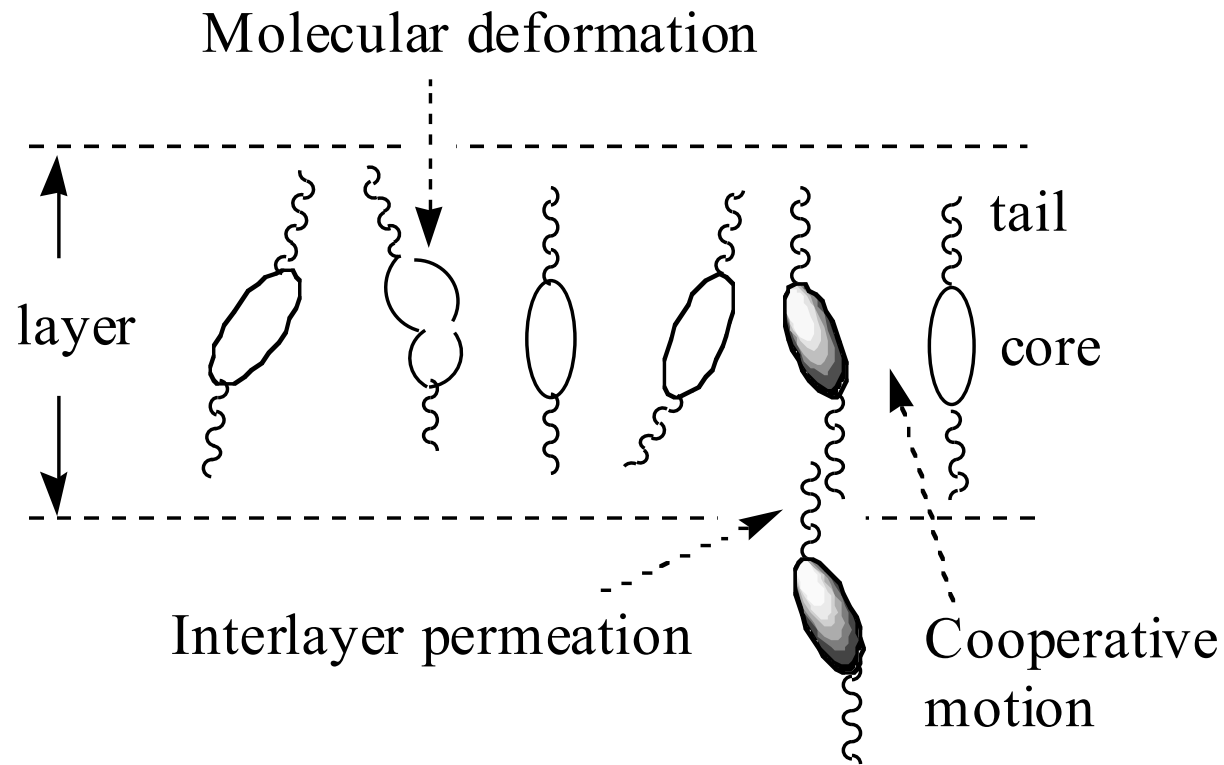


Fig. 3. The temperature dependence of (a) half-height widths and (b) peak intensity ratios for core and chain carbons of MOPBIC on cooling. The half-height width of the peak is calculated assuming that the line sharp can be approximated by a Gaussian equation. Peak intensity at observed temperature divided by that at 93°C is peak intensity ratio.

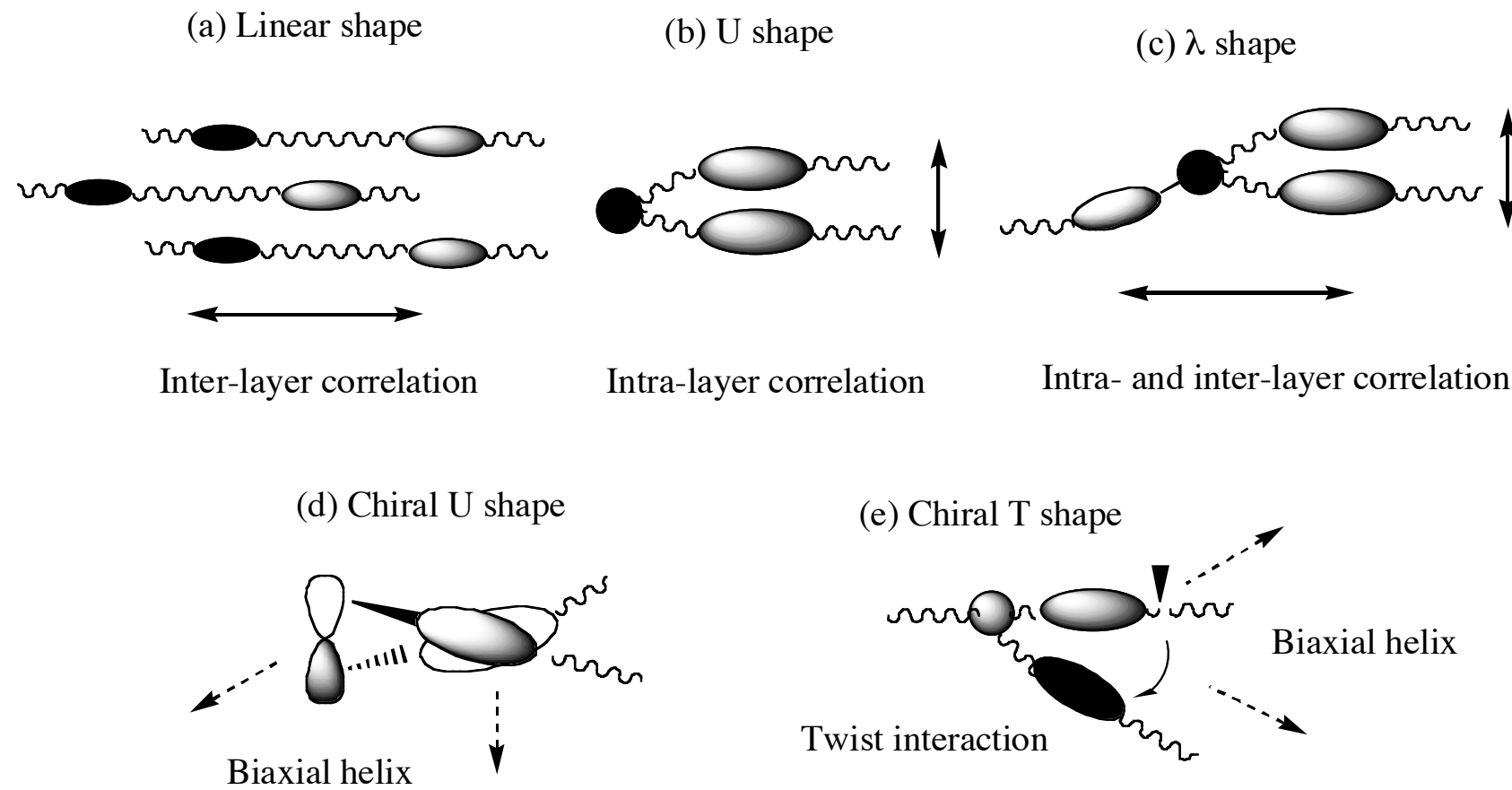
CP/MAS NMR スペクトルからわかったこと



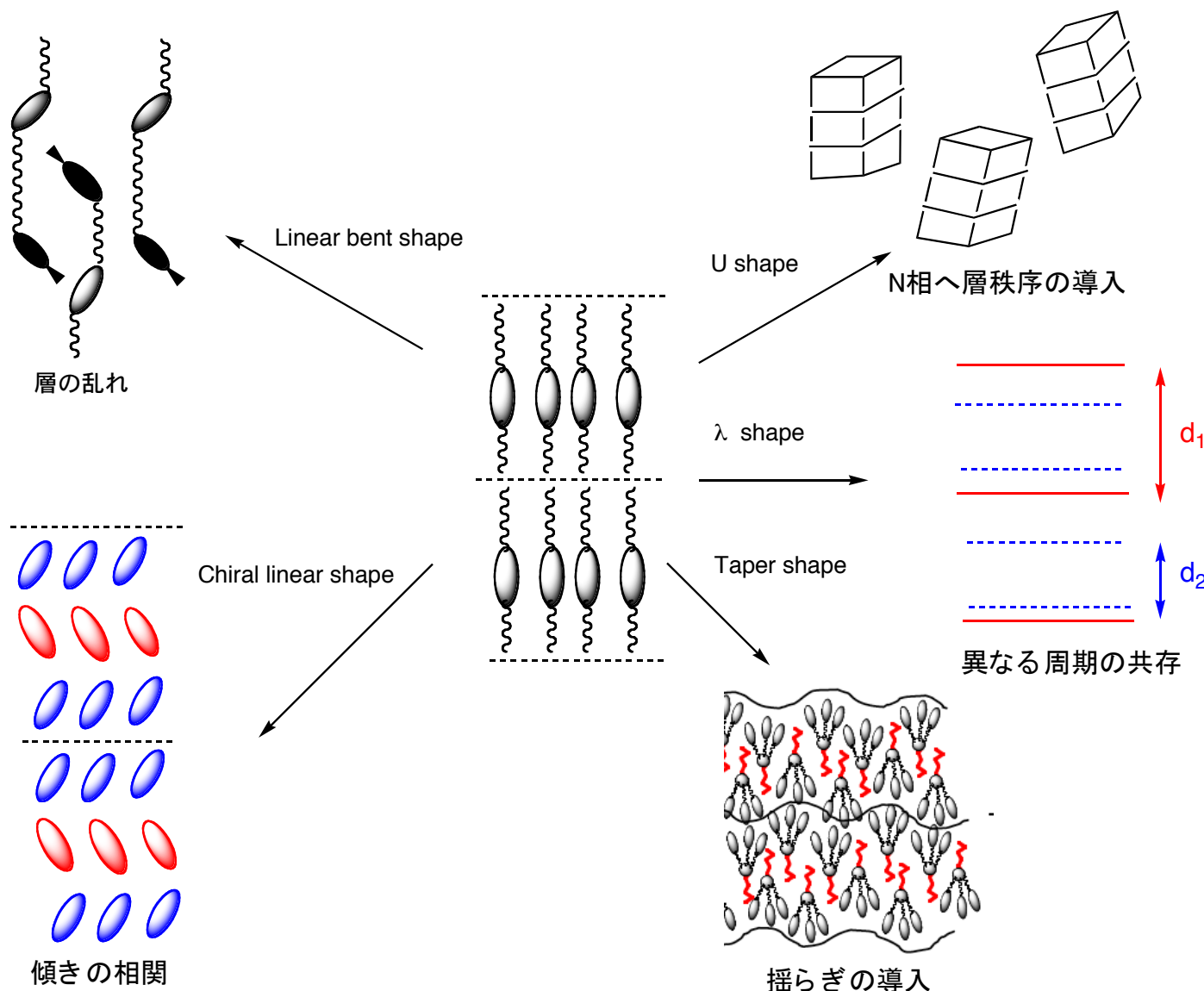
Molecular organization model by C-13 NMR study



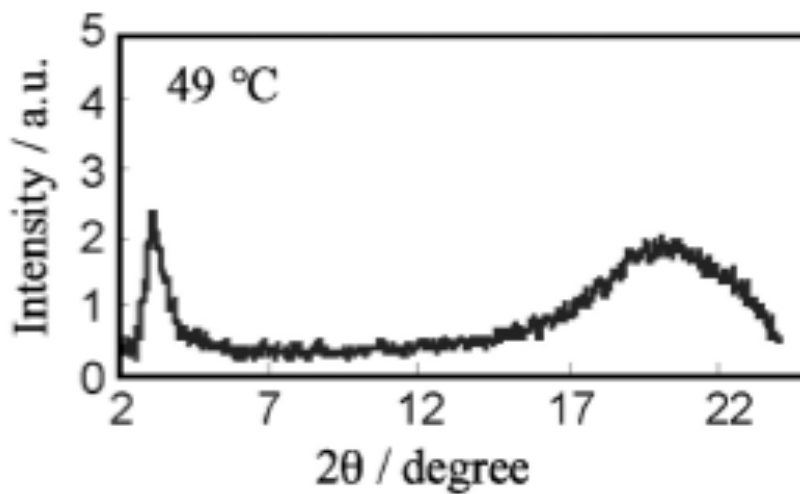
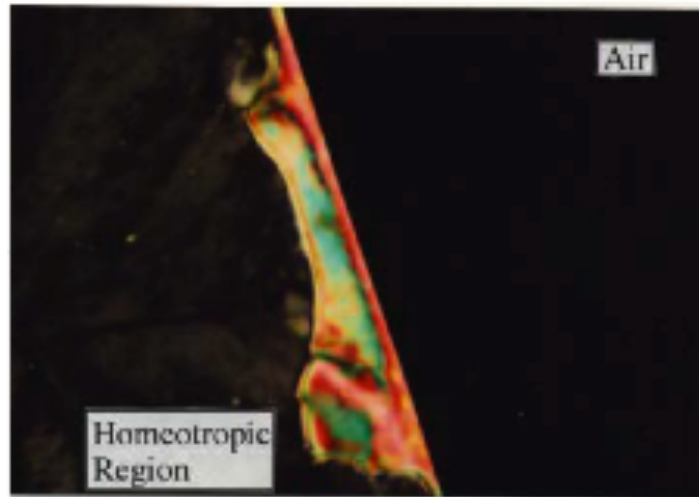
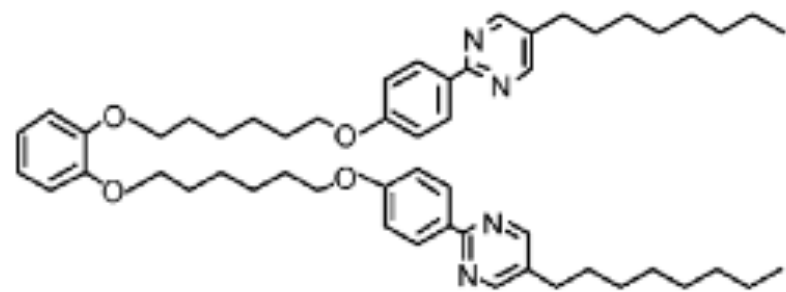
液晶オリゴマーの設計指針 一分子内への秩序導入一



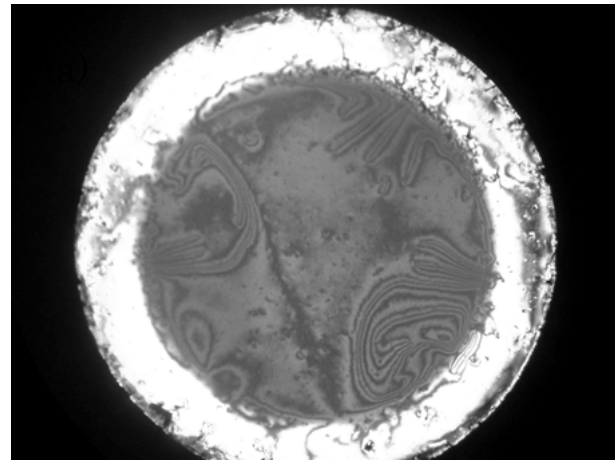
層秩序の調節による階層構造の形成



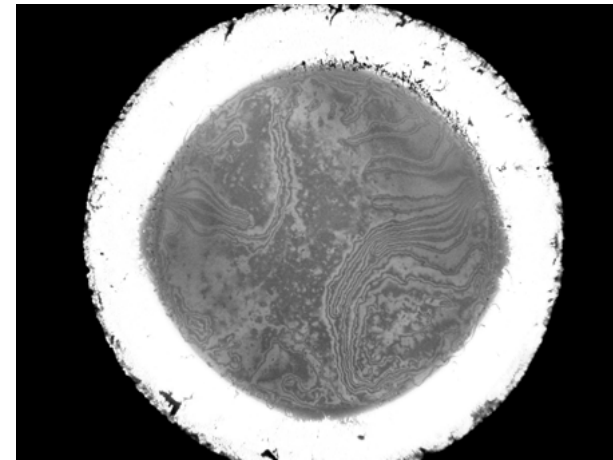
層秩序を持つN相



A. Yoshizawa & A. Yamaguchi, *Chem. Commun.*, 2002, 2060.

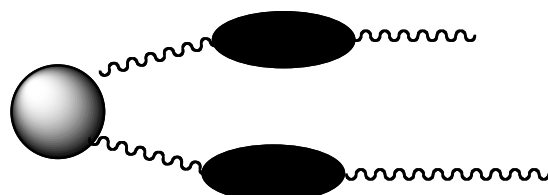


N (80 °C)

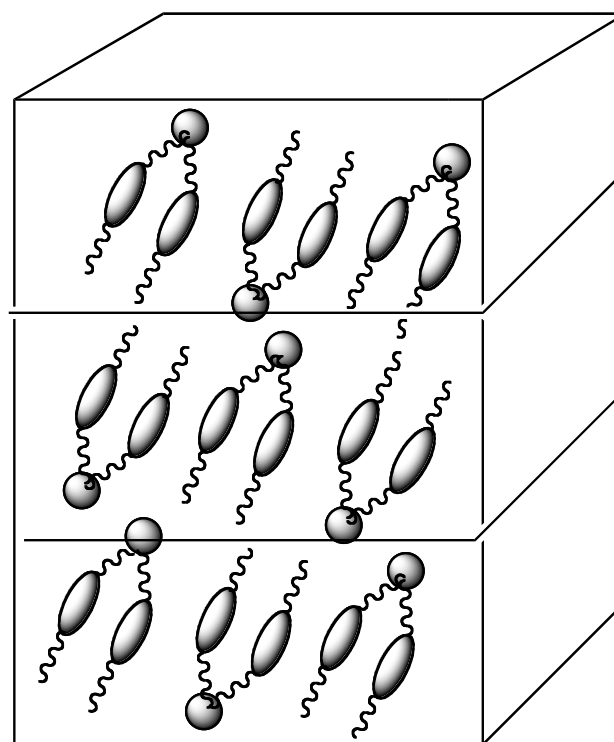


SmC (40.8 °C)

コアを揃える

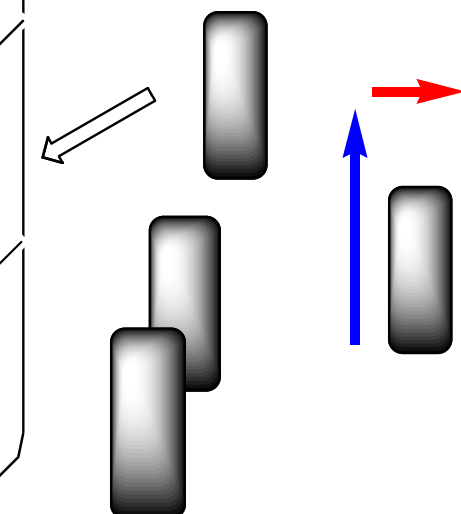


層内の相互作用強い →



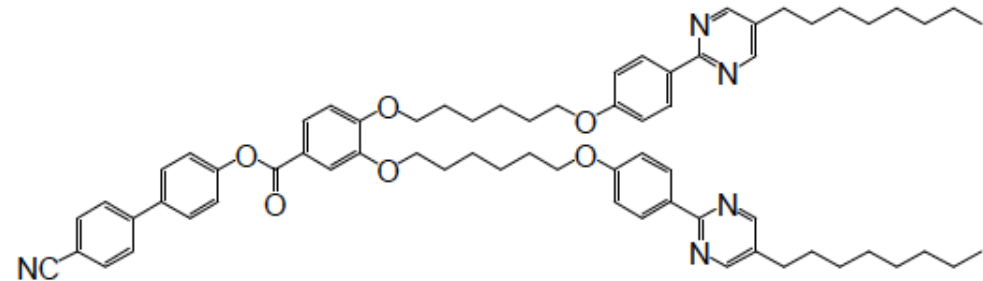
層間の相互作用弱い
相関長が短い →

N (1 軸性)

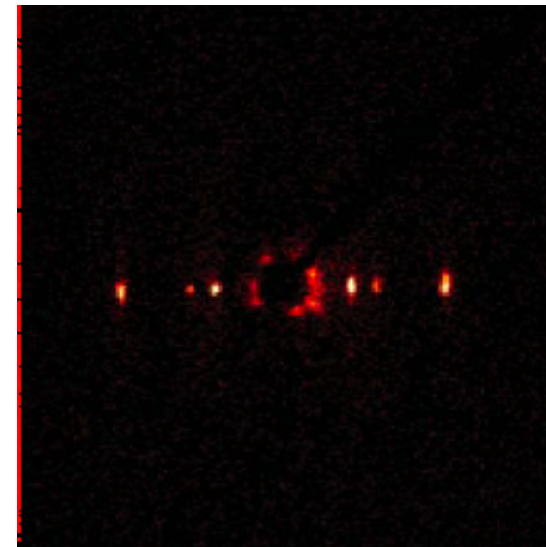
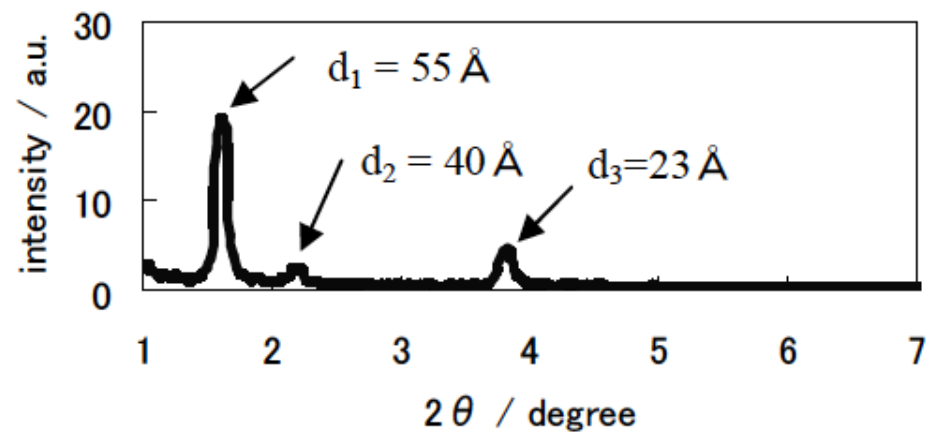


N (2 軸性)

不整合なSmA 相一λ型分子

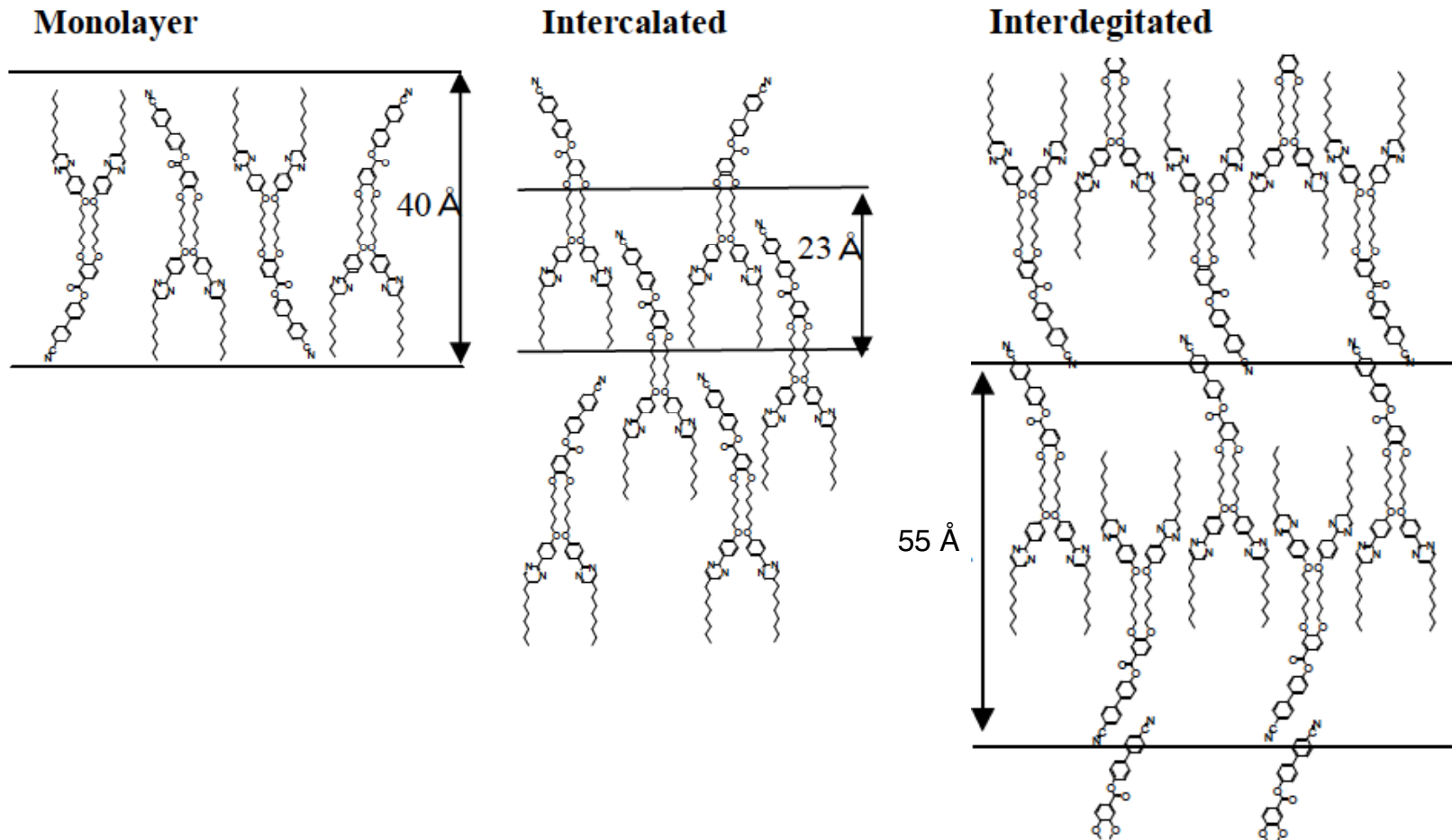


Incommensurate SmA

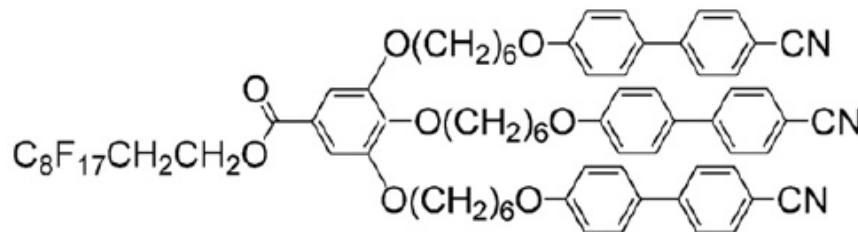


A. Yamaguchi, I. Nishiyama, J. Yamamoto, H. Yokoyama and A. Yoshizawa,
J. Mater. Chem., 2005, **15**, 2580.

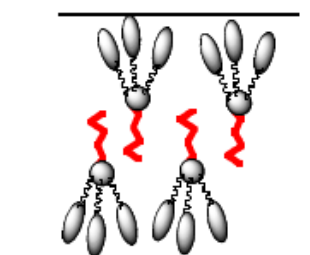
エントロピーの不利をエンタルピーで補償



Shape amphiphilicity & C-H/C-F amphiphilicity

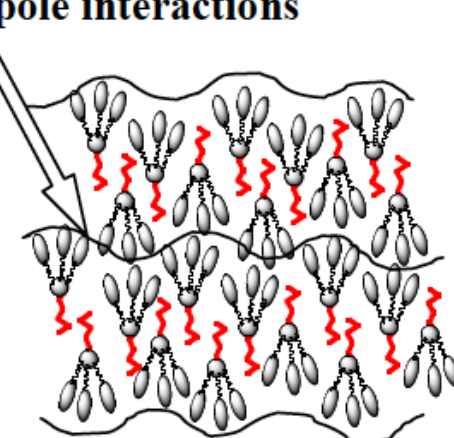


Segregation effect



Dipole-dipole interactions

Competition



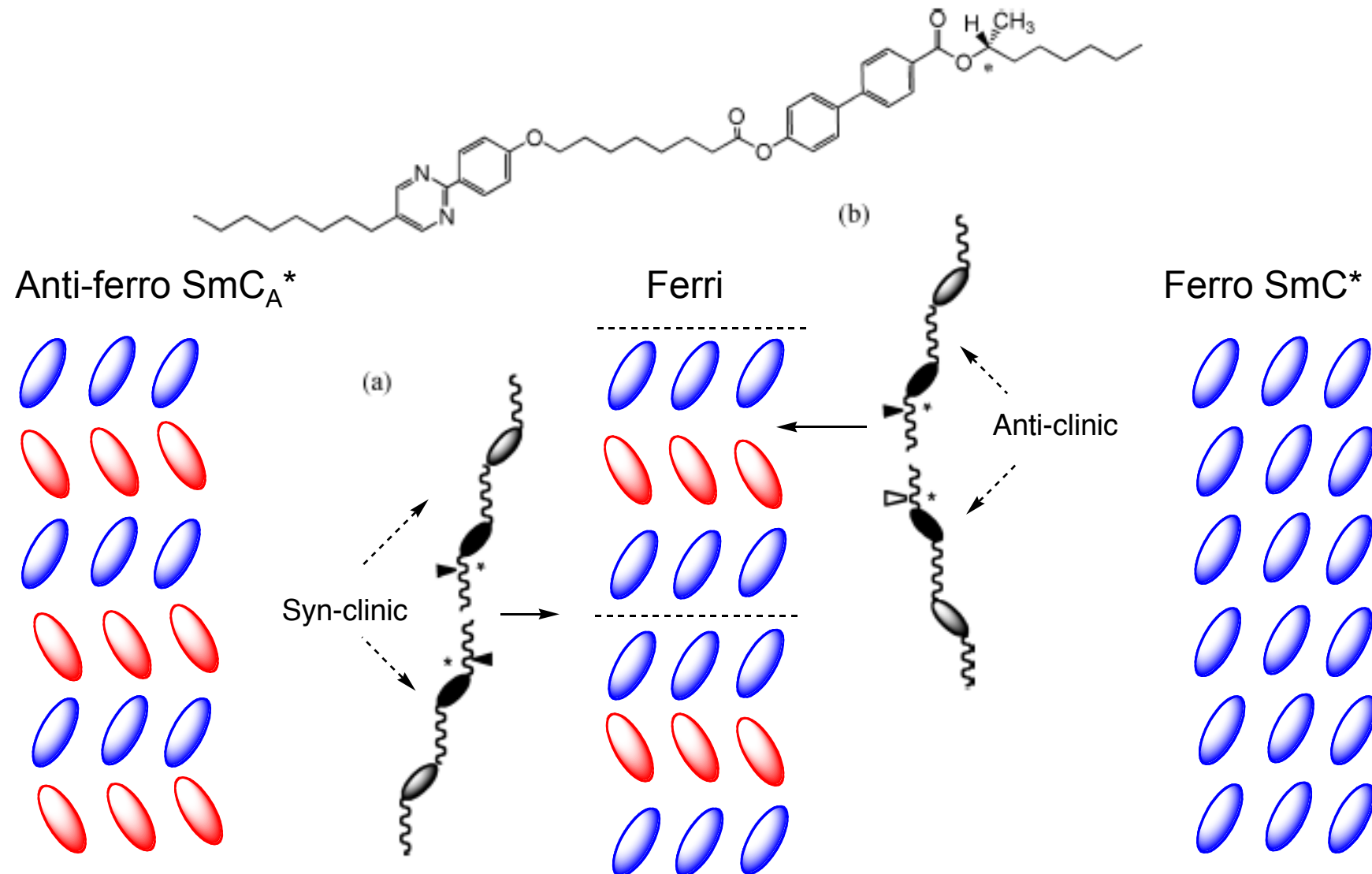
Fluctuated lamellar structure

Bicontinuous cubic phase

Order through fluctuations

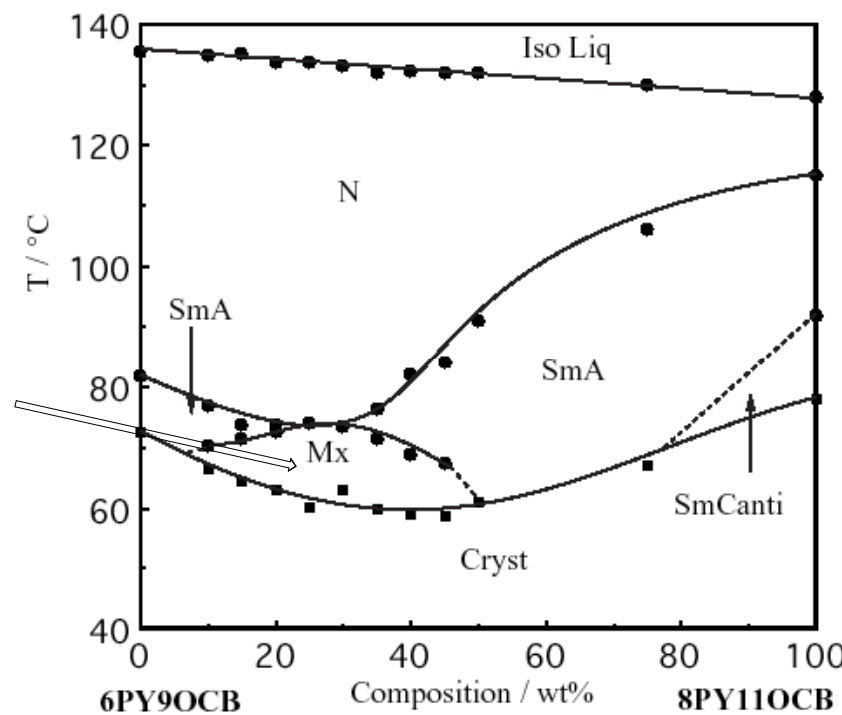
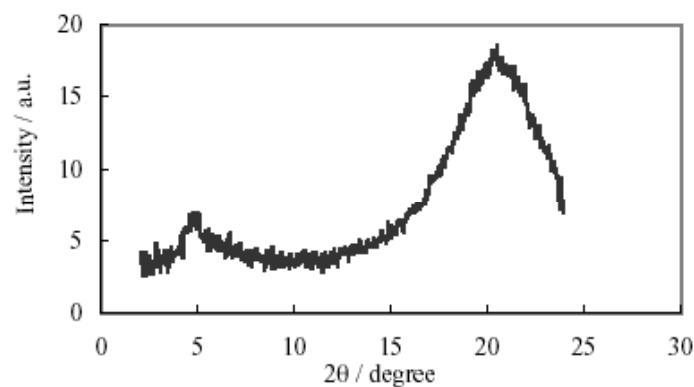
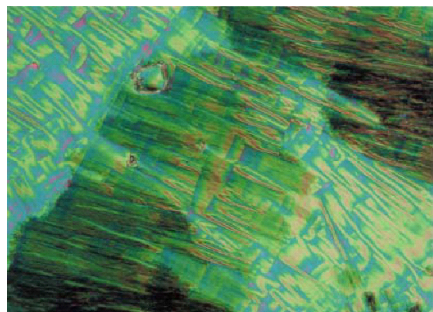
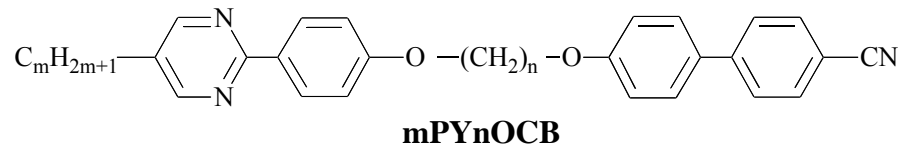
A. Yamaguchi, Y. Maeda, H. Yokoyama and A. Yoshizawa,
Chem., Mater., 2006, **18**, 5704.

分子内の傾きの相関と分子間のキラル認識によるフェリ相の安定化



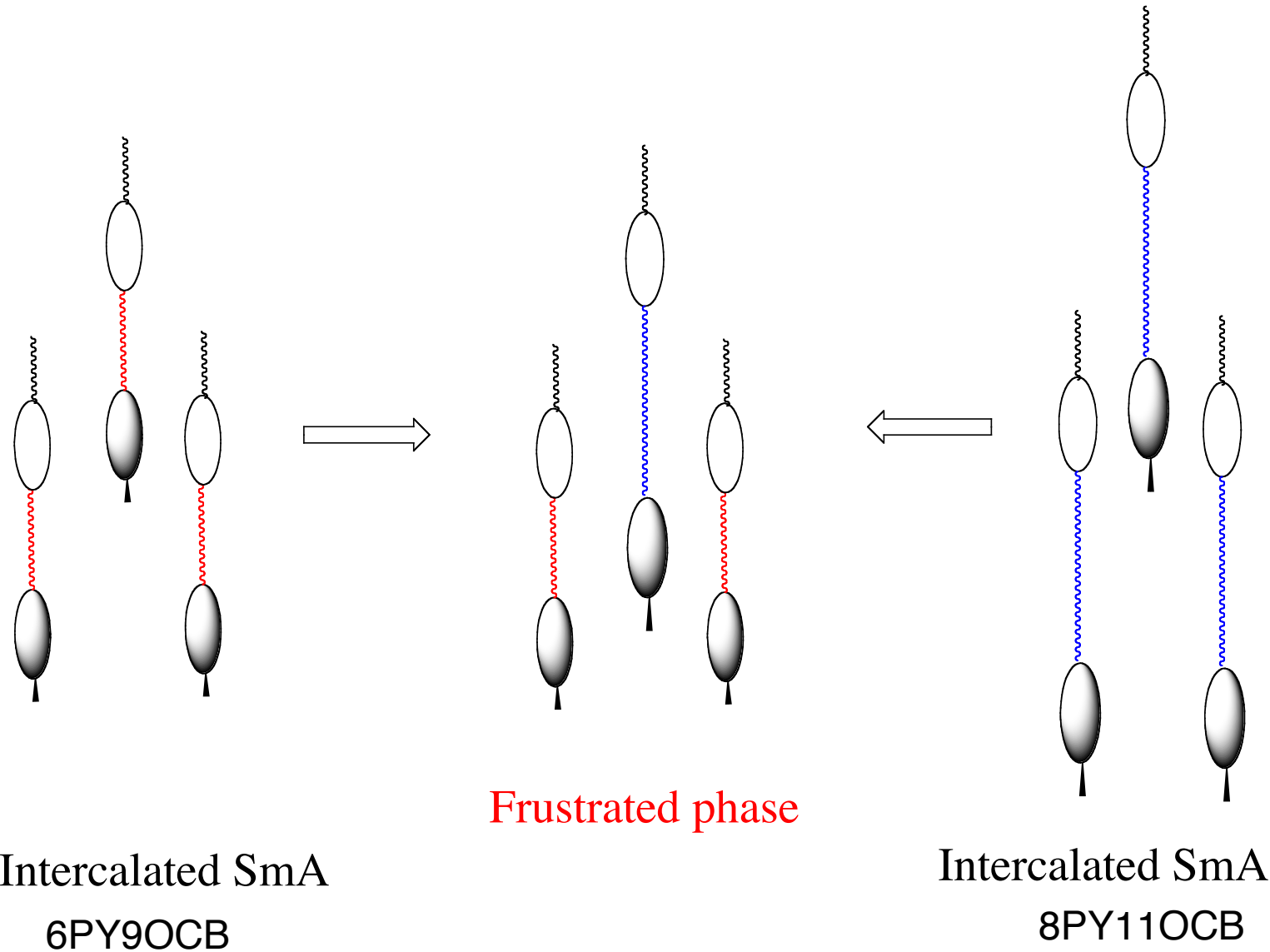
A. Noji, N. Uehara, Y. Takanishi, J. Yamamoto, and A. Yoshizawa,
J. Phys. Chem. B, 2009, **113**, 16142.

スペーサー長の異なる非対称二量体液晶の混合による
フラストレート相の誘起 $m < n$, n : odd

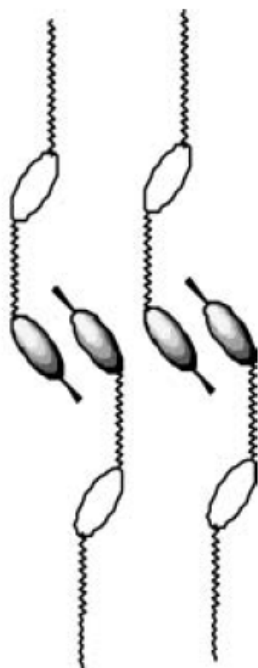
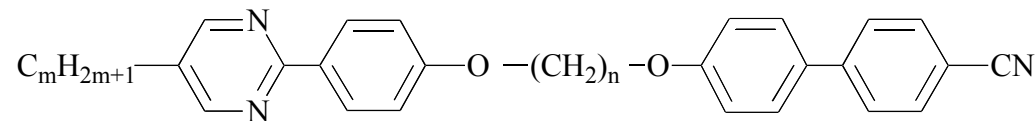


A. Yoshizawa, K. Yamamoto, H. Dewa, I. Nishiyama, H. Yokoyama: *J. Mater. Chem.*, **13**, 172 (2003).

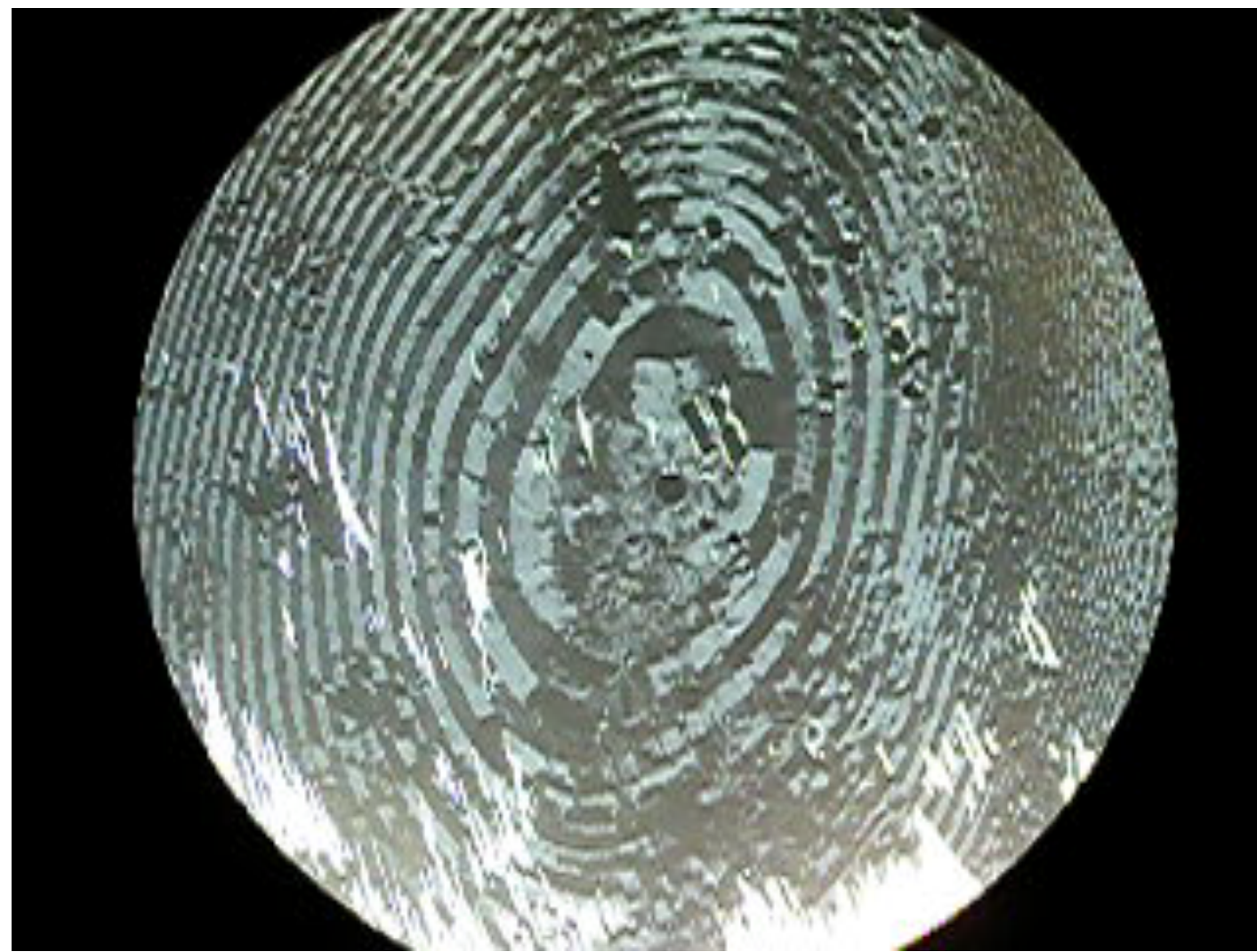
Frustration between packing entropy and electrostatic core-core interaction

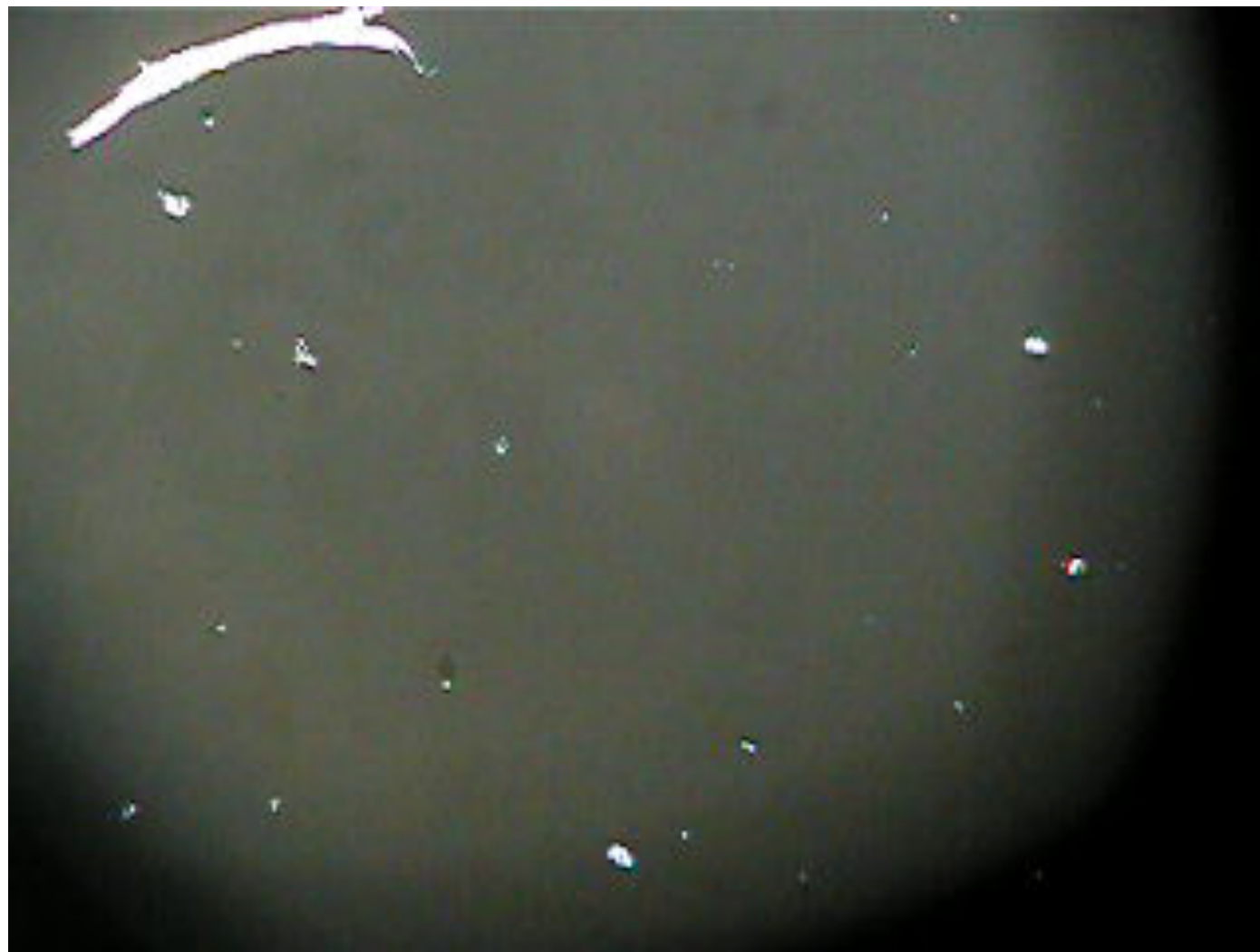


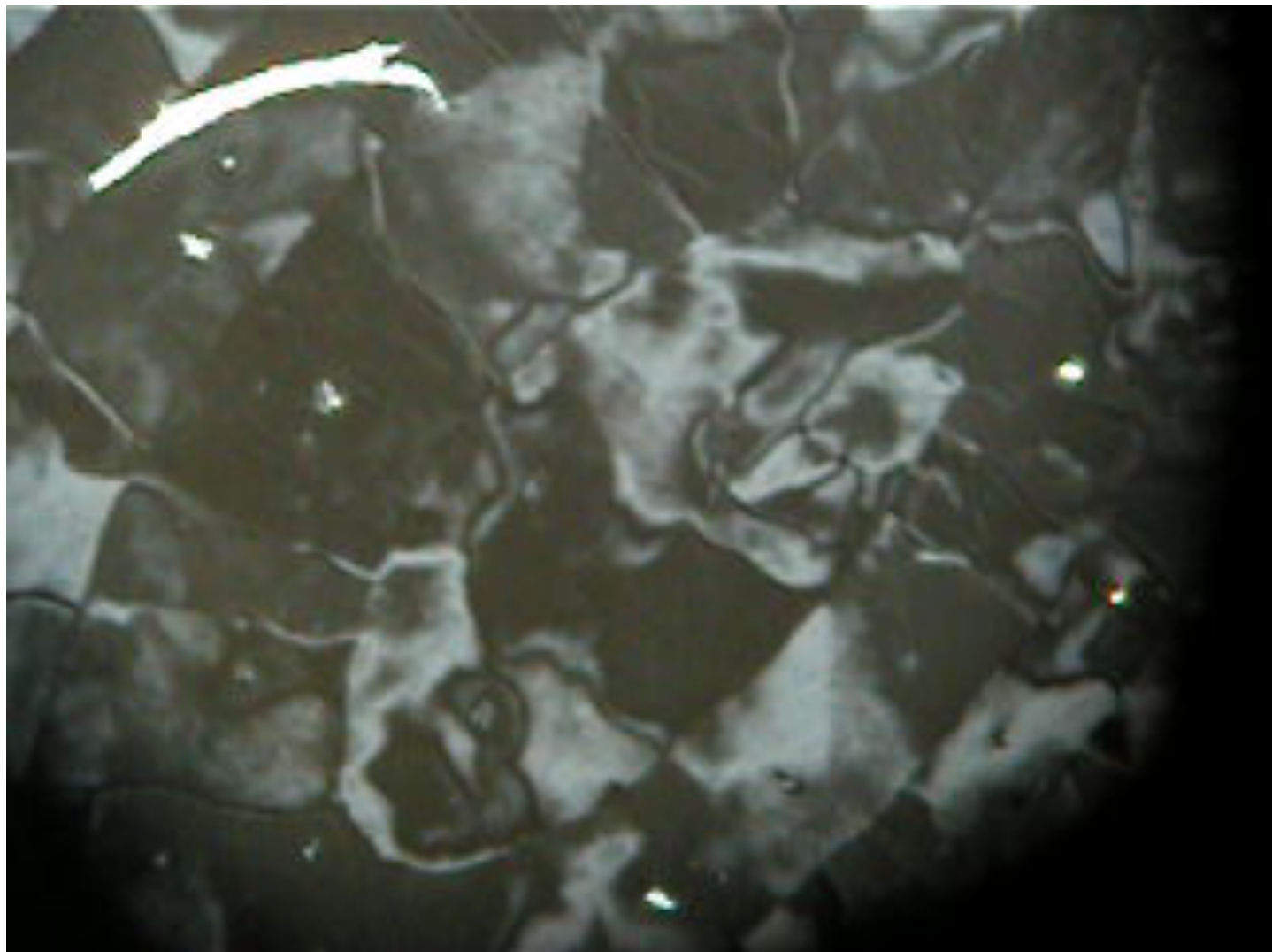
12PY7OCBと12PY9OCB等量混合物のホメオトロピック領域
においてパターン形成が形成し、温度によって振動した。 $m > n$, n :odd

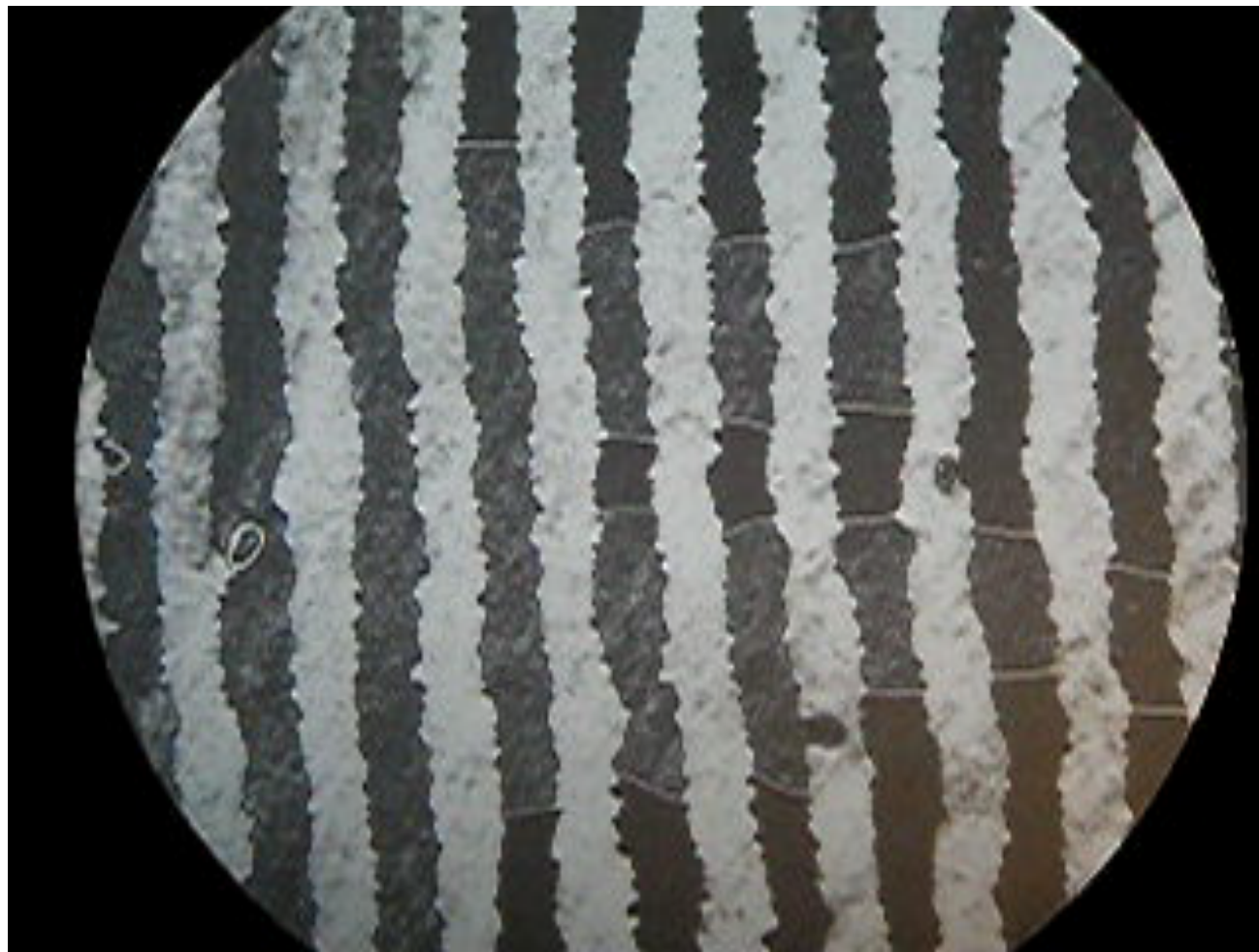


A. Yoshizawa, M. Kurauchi, Y. Kohama, H. Dewa, K. Yamamoto, I. Nishiyama, T. Yamamot, J. Yamamoto,
H. Yokoyama: *Liq. Cryst.*, **33**, 611 (2006).

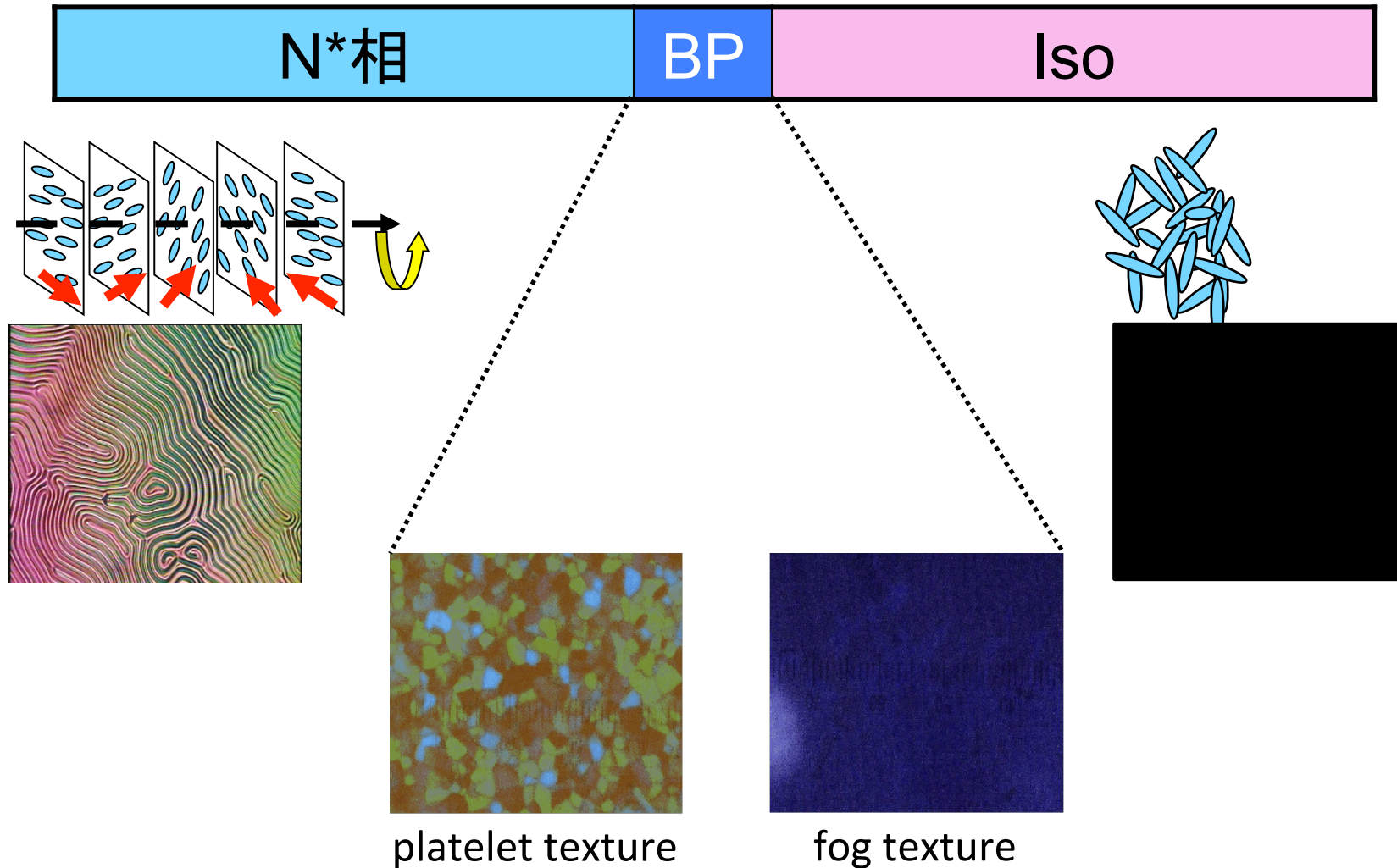




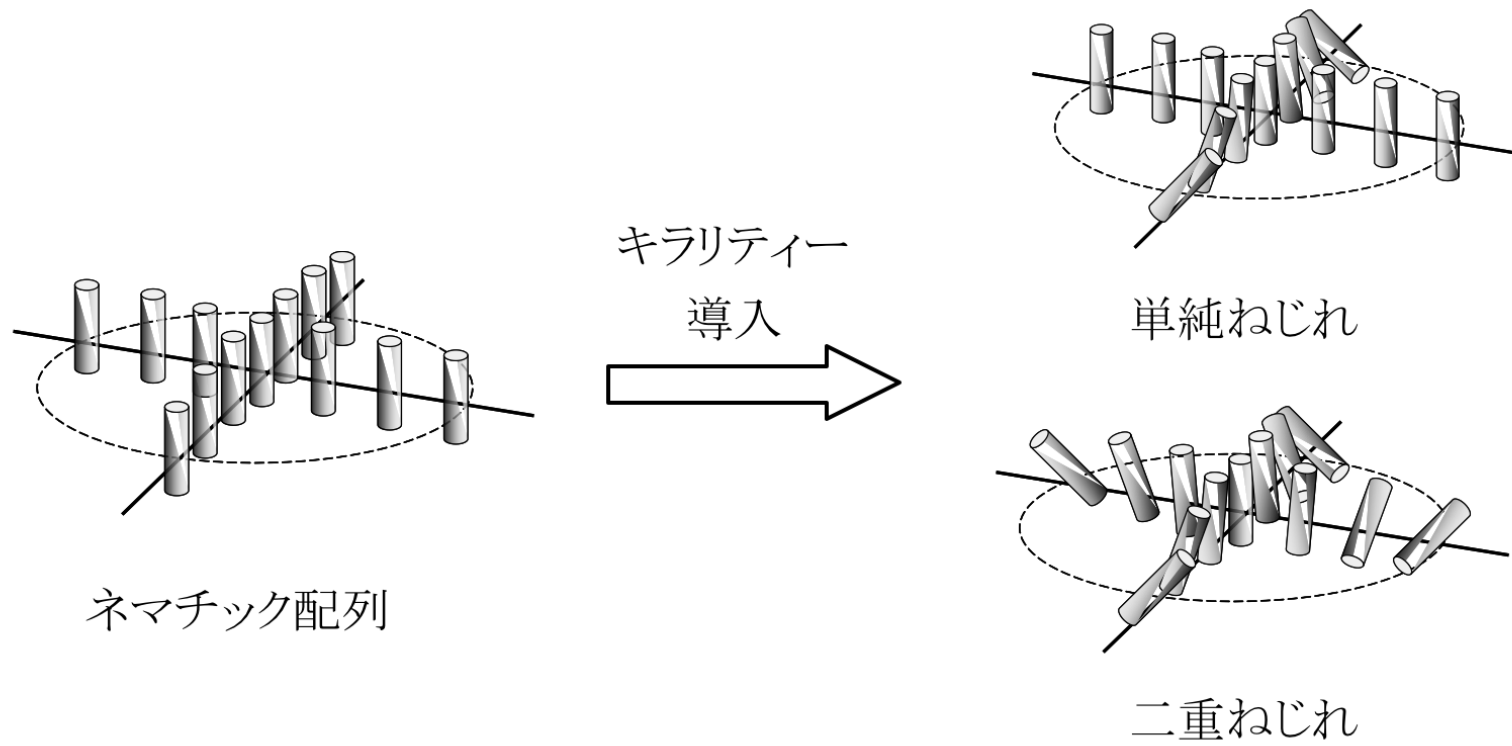




ブルー相

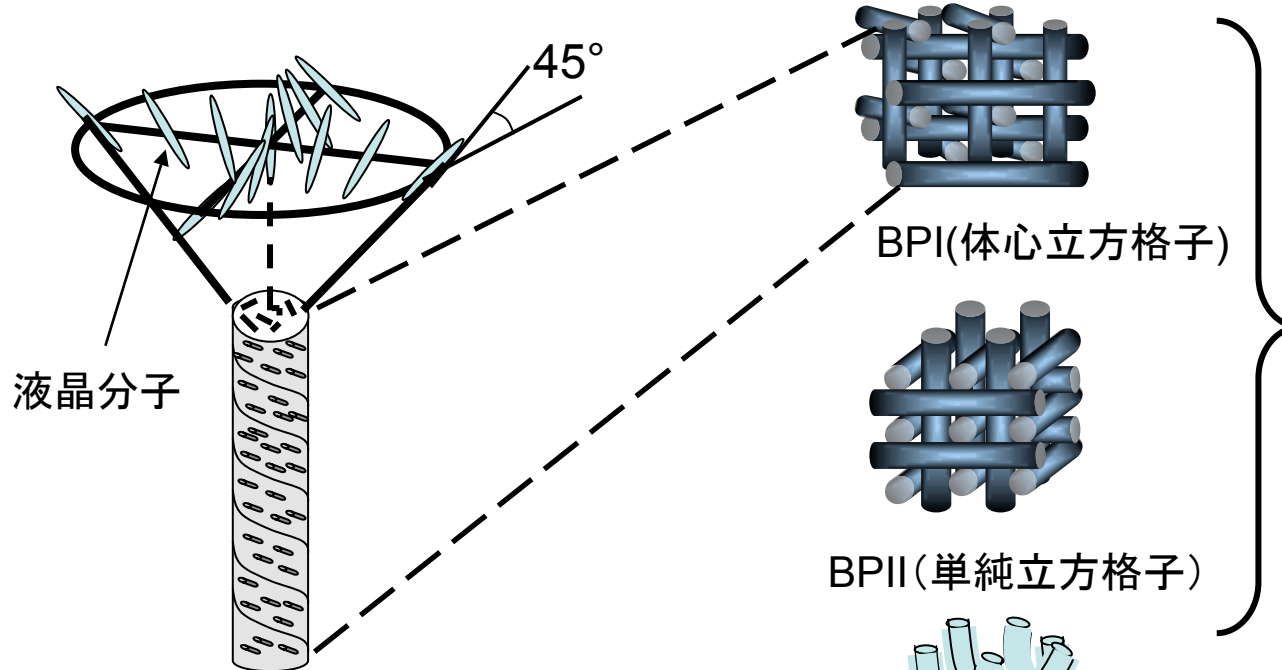


極狭い温度範囲で発現 (0.5~2K程度)

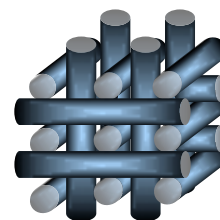


単純ねじれと二重ねじれの分子配向モデル

ブルー相



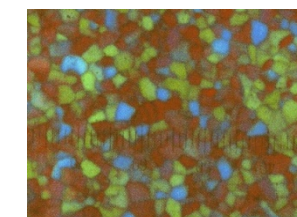
BPI(体心立方格子)



BPII(単純立方格子)



BPIII(アモルファス)



platelet texture
(cubic BP)

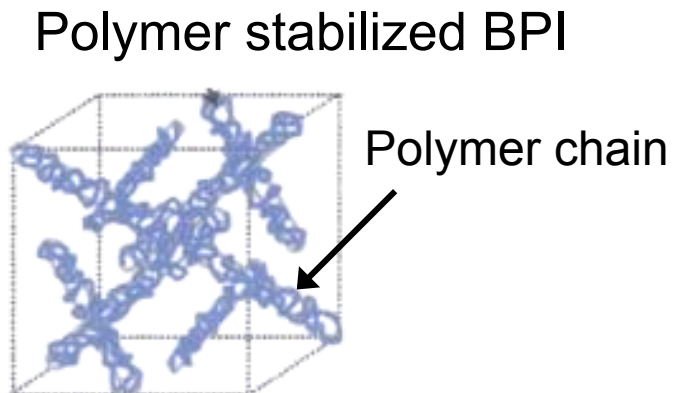
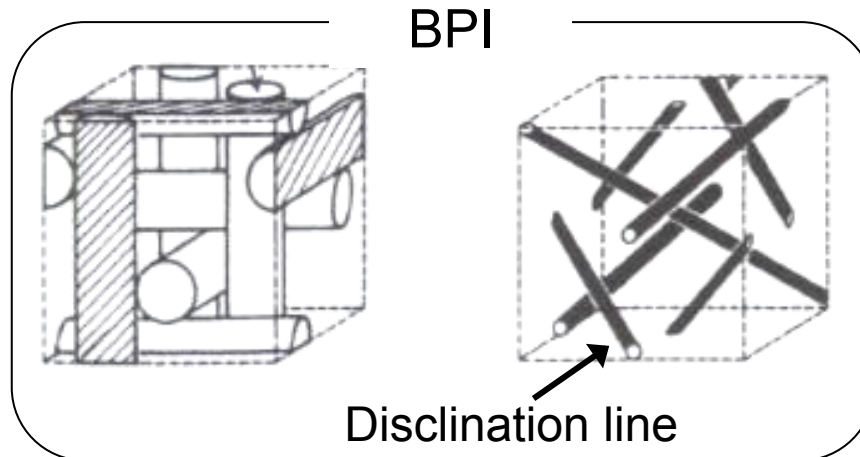
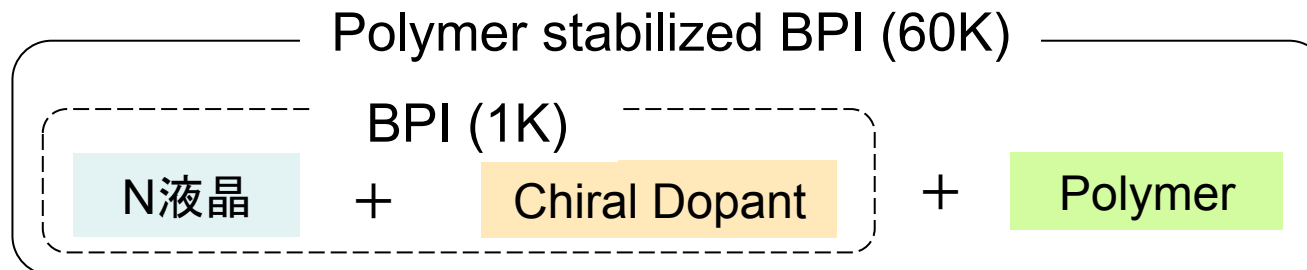


fog texture
(amorphous BP)

三次元らせん構造
(2重ねじれ円柱構造)

- ・光学的に等方性(クロスニコル偏光子で光を通さない)
- ・発現する温度範囲が狭い(通常1K程度)

高分子安定化ブルー相



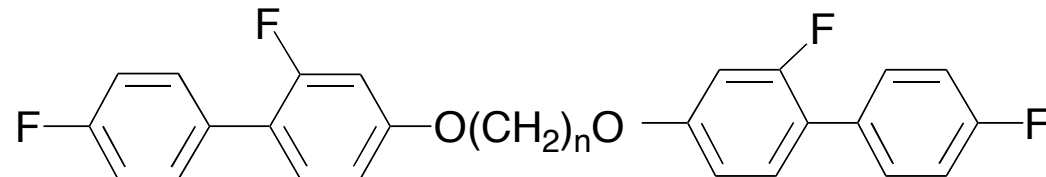
BPの欠陥部分を高分子で埋めることによってBPを安定化させる

- ・60K以上の温度範囲でBPIを発現
- ・μ秒オーダーのスイッチングを確認

H. Kikuchi, M. Yokota, Y. Hisakado, H. Yang and T. Kajiyama, *Nature Materials.*, 2002, **1**, 64.
Y. Hisakado, H. Kikuchi, T. Nagamura, and T. Kajiyama. *Adv. Mater.*, 2005, **17**, 96.

Liquid crystal 'blue phases' with a wide temperature range

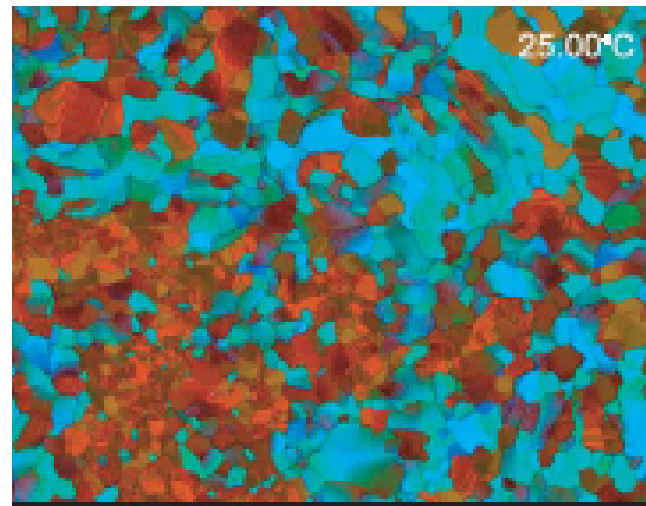
H. J. Coles & M. N. Pivnenko Nature 2005, 436, 997

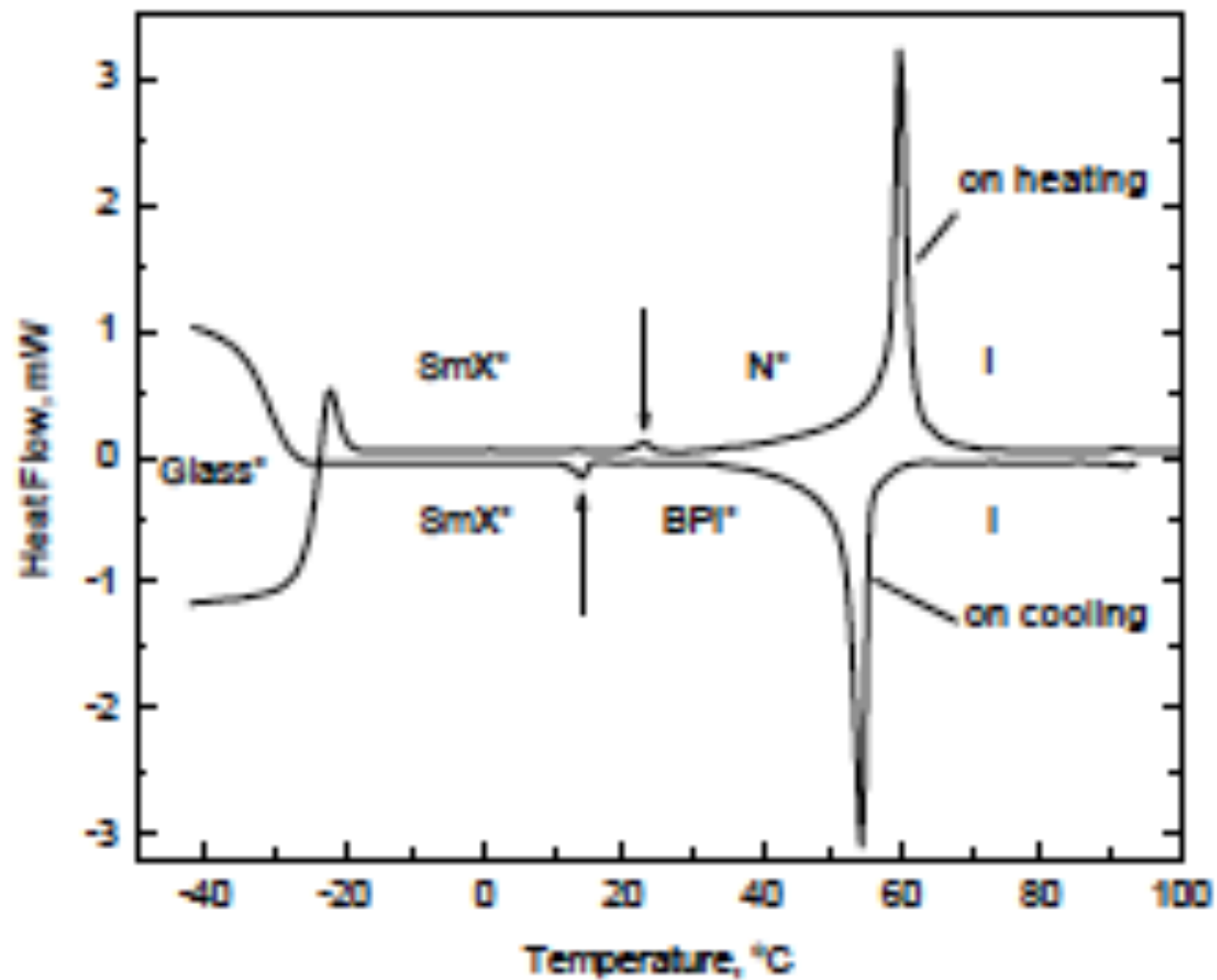


n = 7: 30.4wt%, n=9: 35.1wt%, n=11: 30.6wt%

Chiral dopant BDH1281: 3.9wt%

Iso liq 57.72°C BPIII* 57.58°C BPII* **57.22°C BPI*** 16.5°C SmX* -28°C glass





Stabilizing blue phases

1. Polymer-stabilized blue phases (Cubic BP)
H. Kikuchi et al., *Nature Mater.*, 2002, 1, 64.
2. Chiral T-shaped compound (Amorphous BP)
A. Yoshizawa, M. Sato et al., *J. Mater. Chem.*, 2005, 15, 3285.
3. Mixture of fluoro-substituted bimesogenic compounds and chiral dopant
H. J. Coles & M. N. Pivnenko, *Nature*, 2005, 436, 997. (Cubic BP)
4. Chiral compound possessing a bent core (Amorphous BP)
C. V. Yelamaggad et al.. *Chem. Mater.*, 2006, 18, 6100.
5. Hydrogen-bonded self-assembled complex of chiral fluoro-substituted benzoic acid and pyridine derivative (Cubic BP)
W. He, et al., *Adv. Mater.*, 2009, 21, 1.
6. Binaphthyl derivative (Cubic BP)
A. Yoshizawa, Y. Kogawa et al., *J. Mater. Chem.*, 2009, 19, 5759.
7. Pinning effect of mixed cellulose ester membrane (Cubic BP)
M. Ojima, et al., *Appl. Phys. Express*, 2009, 2, 021502.

8. Nanoparticle-induced widening of the temperature range of liquid-crystalline phases (Amorphous BP)

E. Karatari & Z. Kutnjak et al., *Phys. Rev. E*, 2010, 81, 041703.

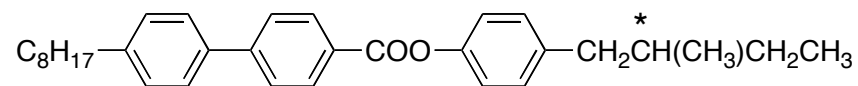
9. Stable amorphous blue phase of bent-core nematic liquid crystals doped with a chiral material (Amorphous BP)

S. Taushanoff, H. Takezoe, A. Jakli et al., *J. Mater. Chem.*, 2010, 20, 5893.

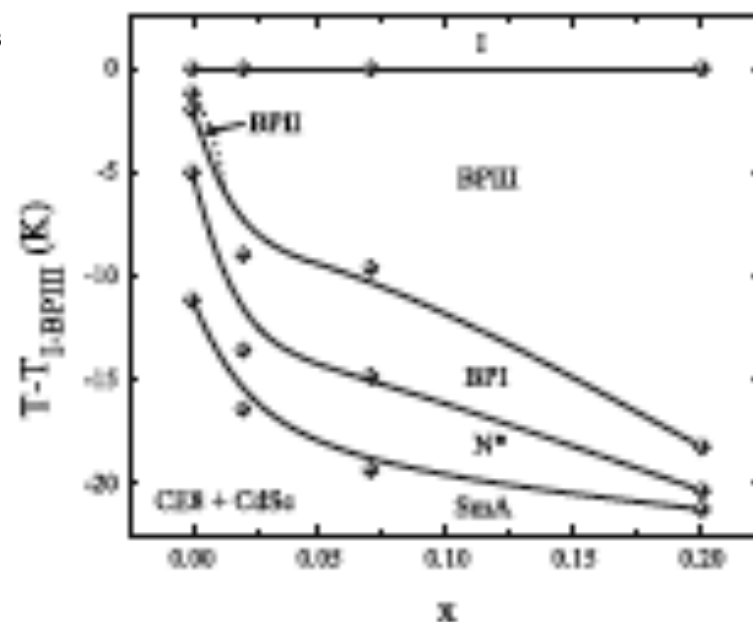
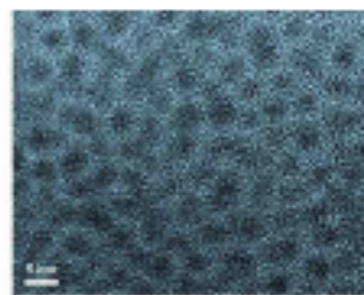
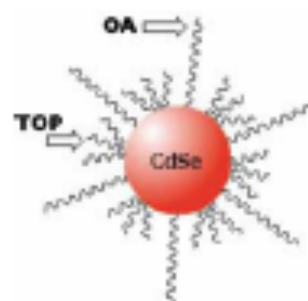
10. Liquid crystalline blue phase I observed for a bent-core molecule and its electro-optical performance (Cubic BP)

M. Lee, S-W, Choi, H. Kikuchi et al., *J. Mater. Chem.*, 2010, 20, 5813.

Nanoparticle-induced widening of the temperature range of BPIII



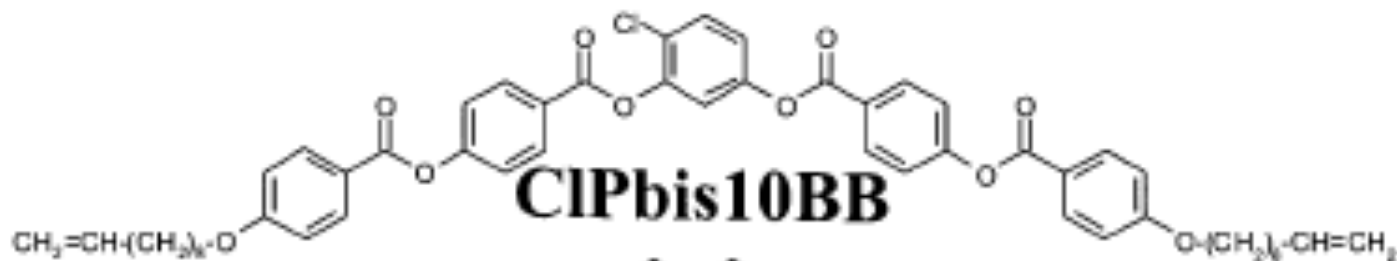
CE8



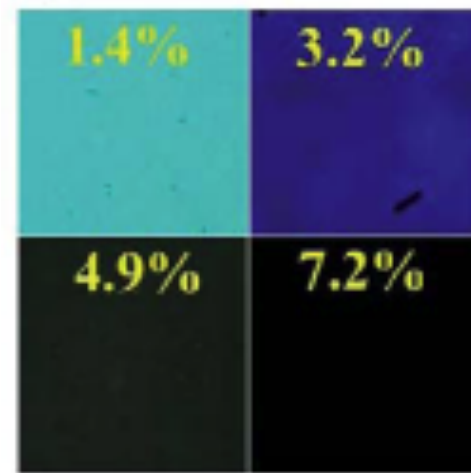
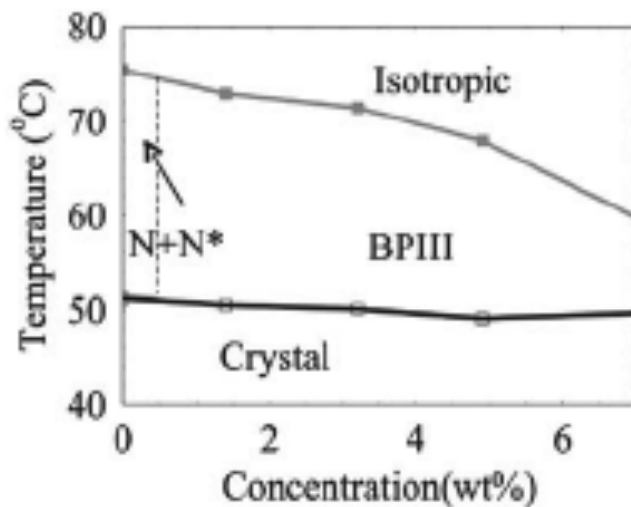
E. Karatari & Z. Kutnjak et al., *Phys. Rev. E*, 2010, 81, 041703.

Stable amorphous blue phase of bent-core nematic liquid crystals doped with a chiral material

S. Taushanoff, H. Takezoe, A. Jakli et al., *J. Mater. Chem.*, 2010, 20, 5893.

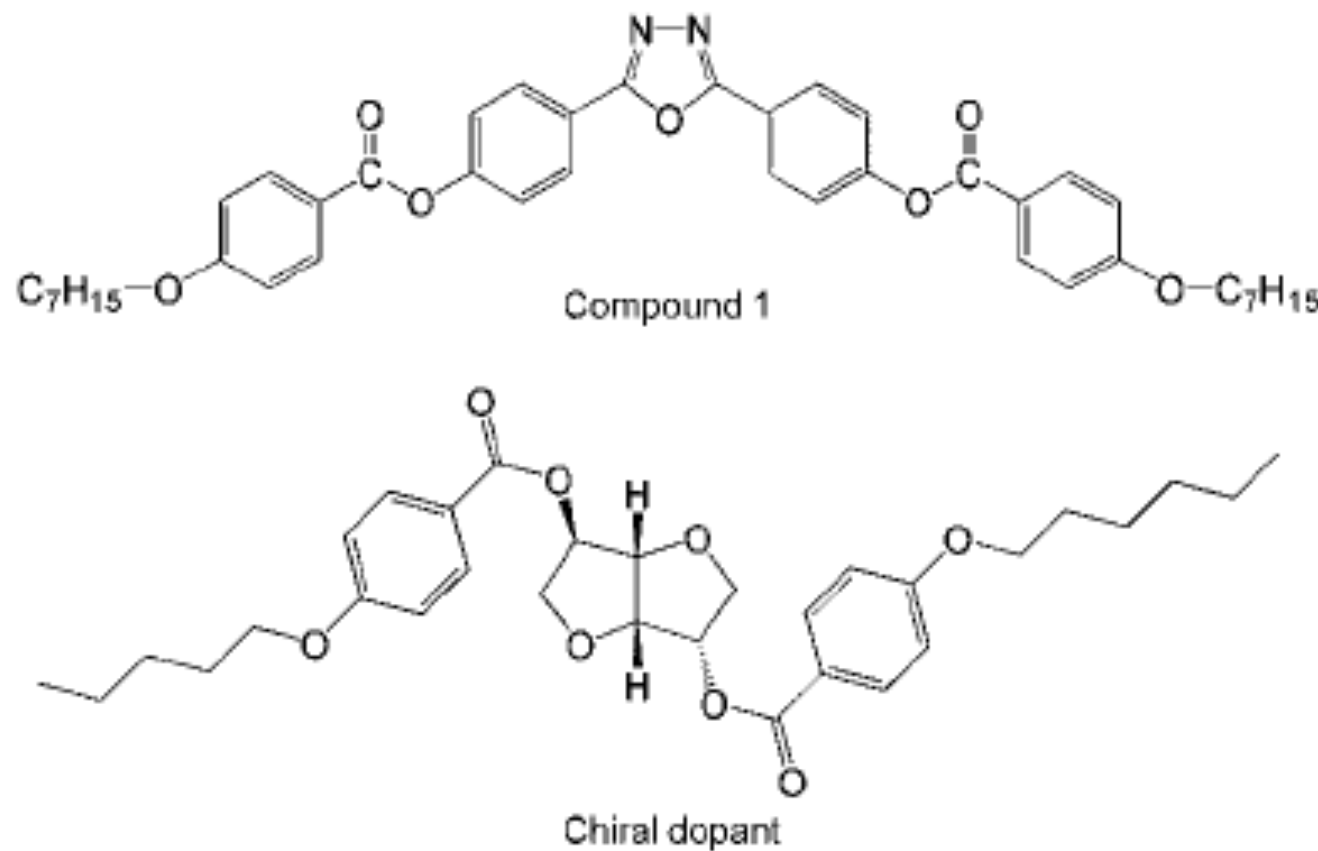


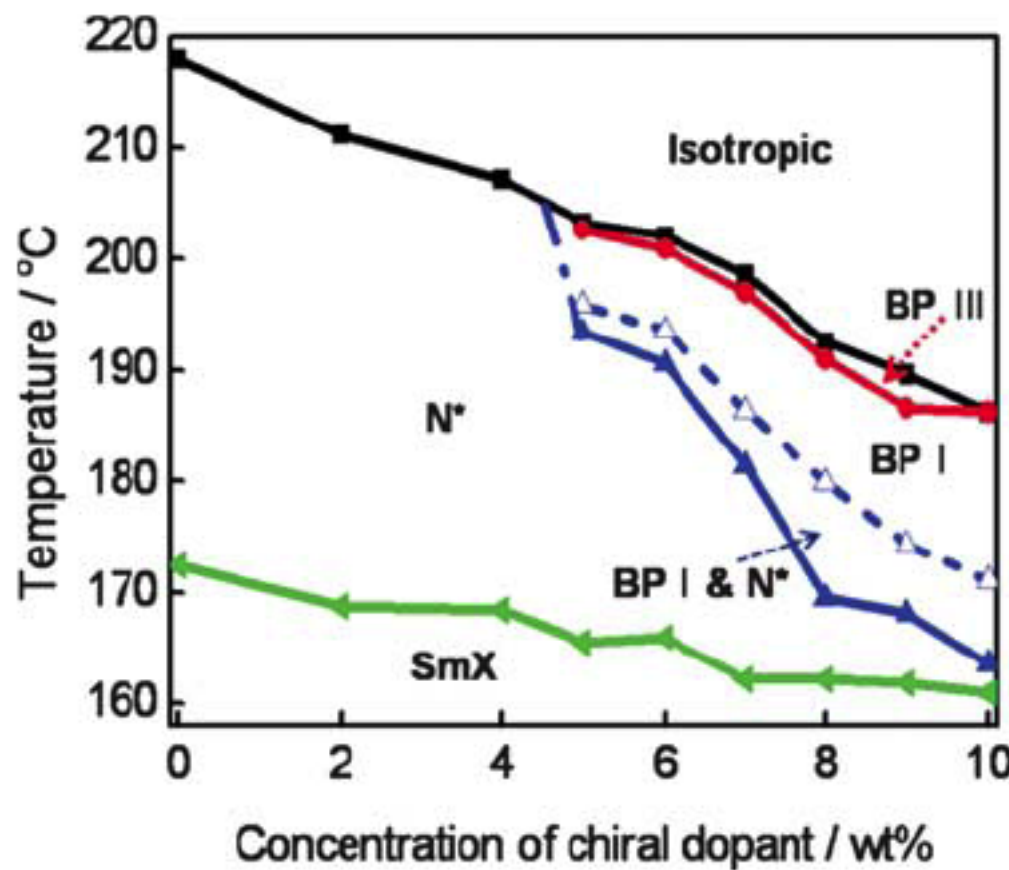
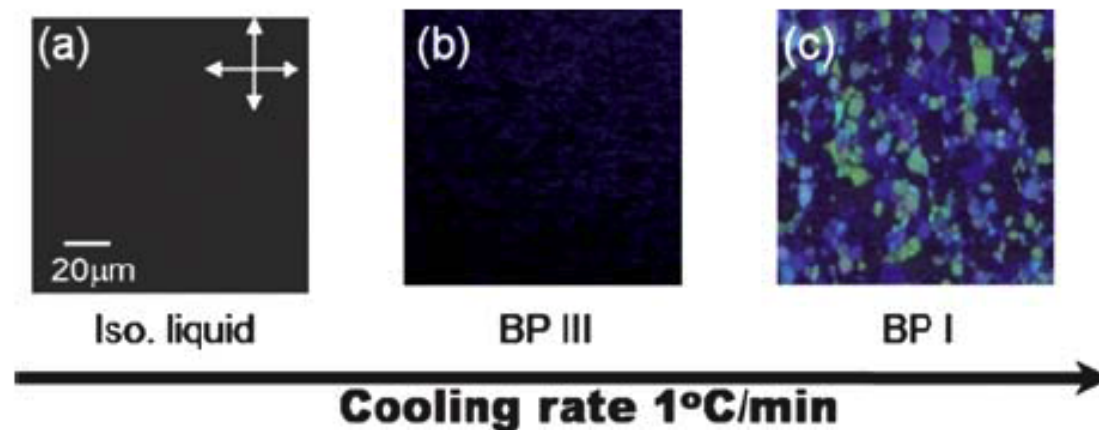
Chiral dopant: BDH1281



Liquid crystalline blue phase I observed for a bent-core molecule and its electro-optical performance

M. Lee, S-W, Choi, H. Kikuchi et al., *J. Mater. Chem.*, 2010, 20, 5813.





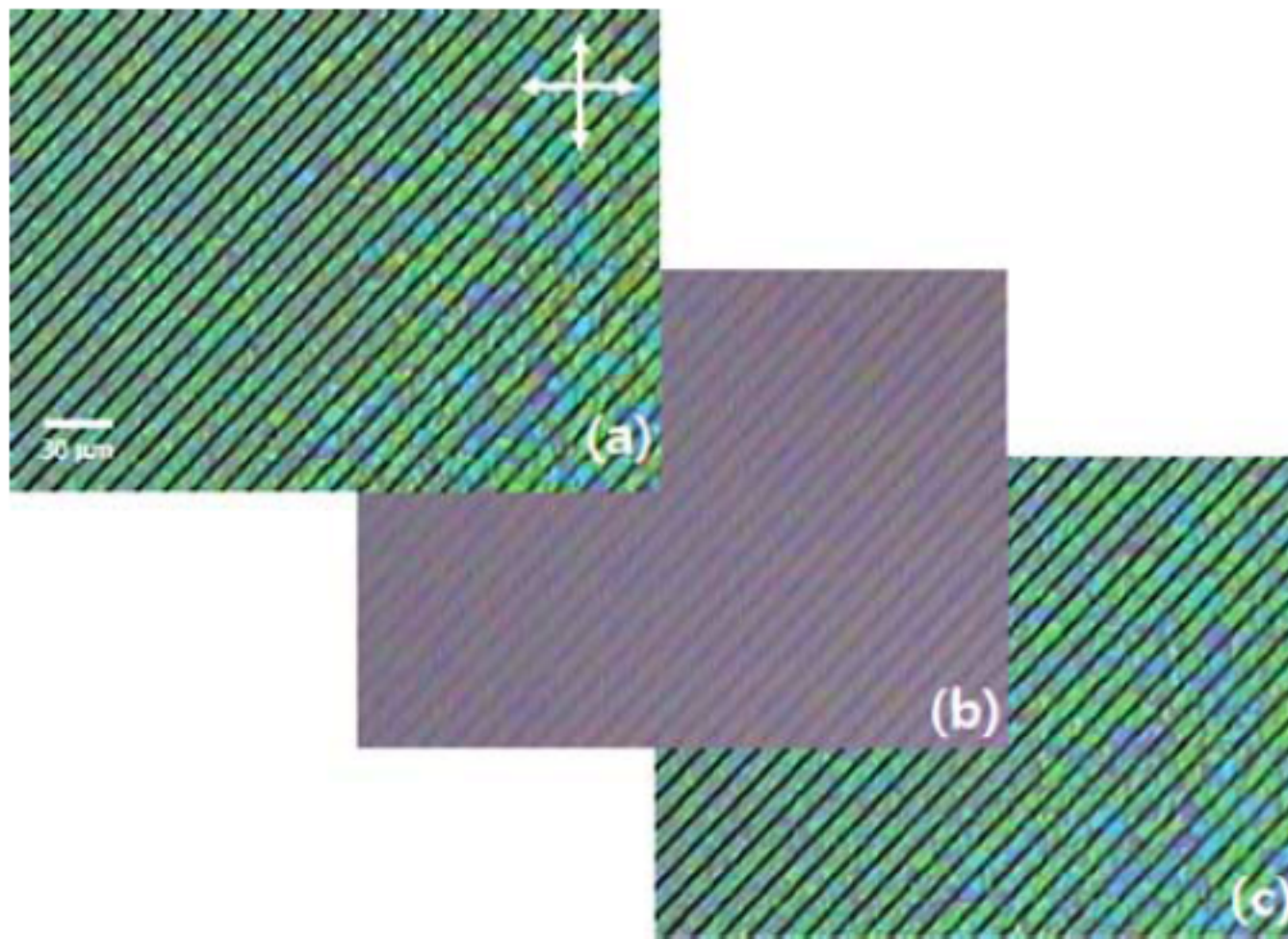
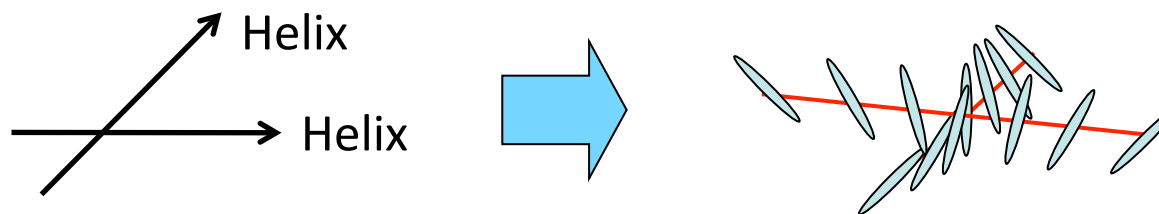


Fig. 5 Typical optical texture of the BP I of the sample composed of compound 1 with 10 wt% chiral dopant under in-plane electric field geometry (a) without the electric field, (b) with the electric field (8 V mm^{-1}), and (c) after removing the electric field. The arrows indicate the directions of the polarizers.

Theoretical prediction

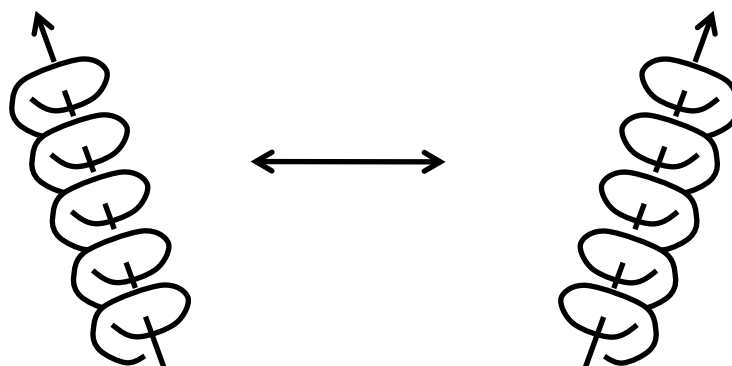
Biaxial helix

D. C. Wright and N. D. Mermin, *Rev. Mod. Phys.*, 1989, **61**, 385.

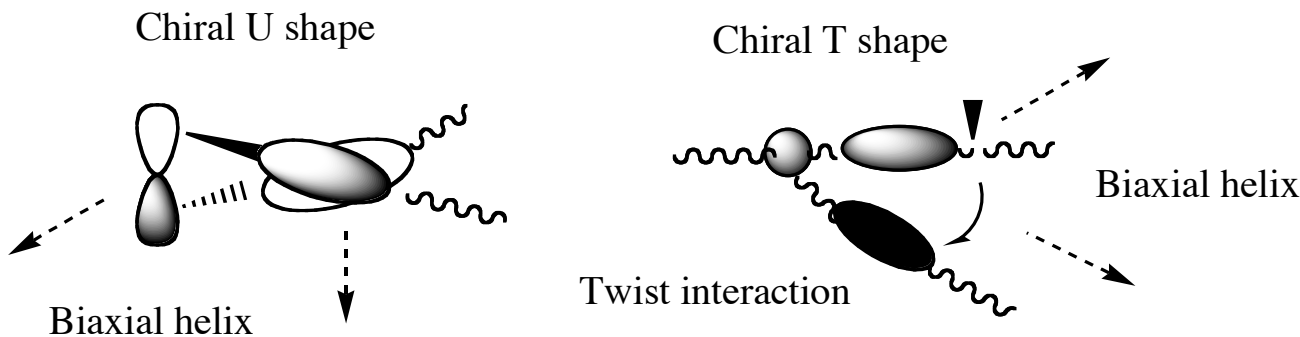


Twist inversion

G. P. Alexander and J. M. Yeomans, *Phys. Rev. E*, 2006, **74**, 061706.



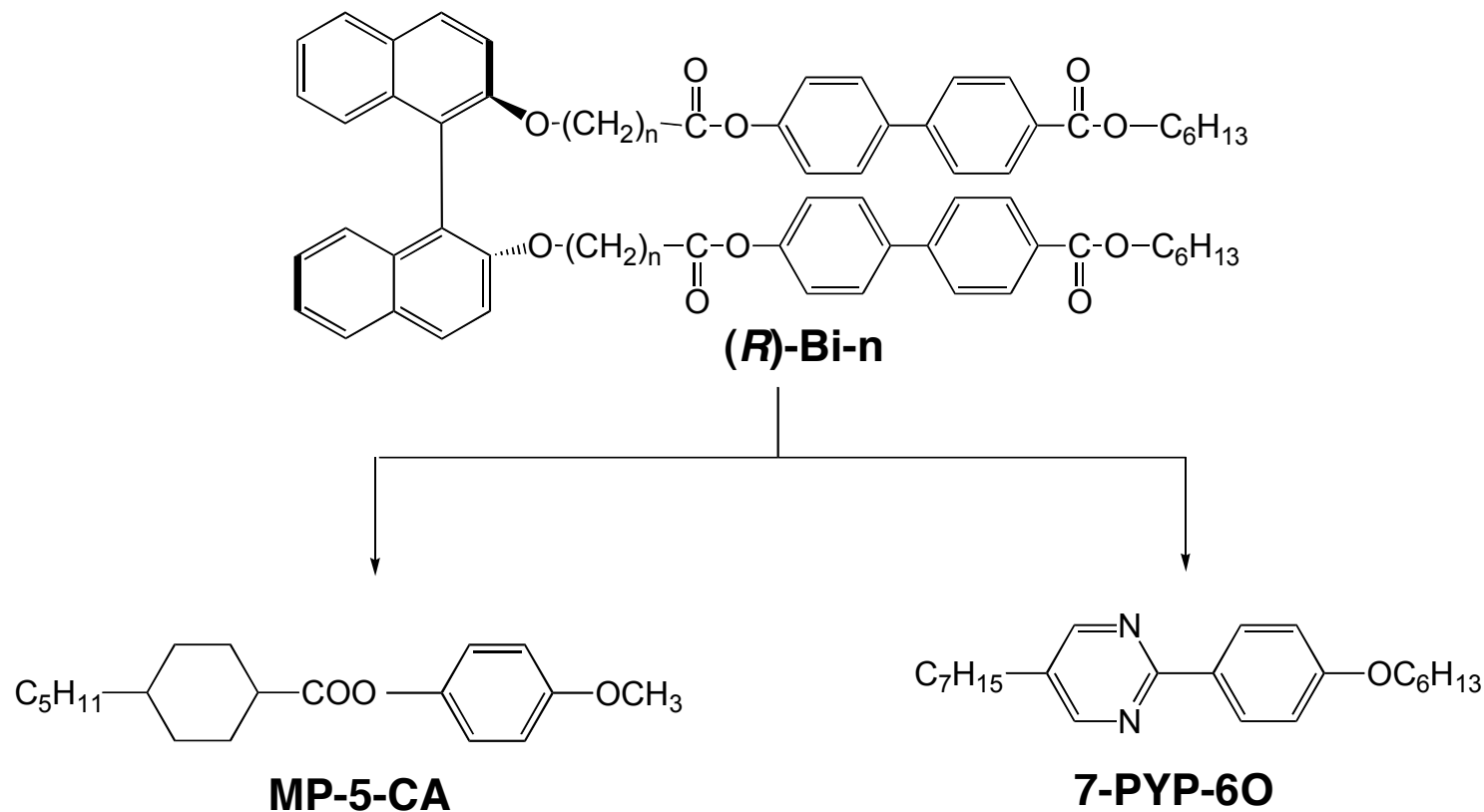
Design concepts



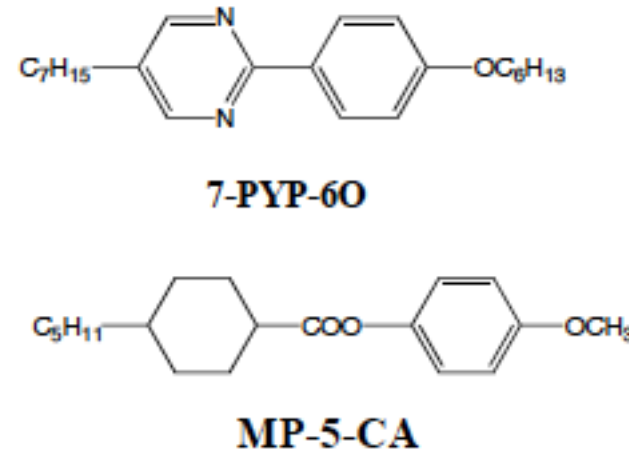
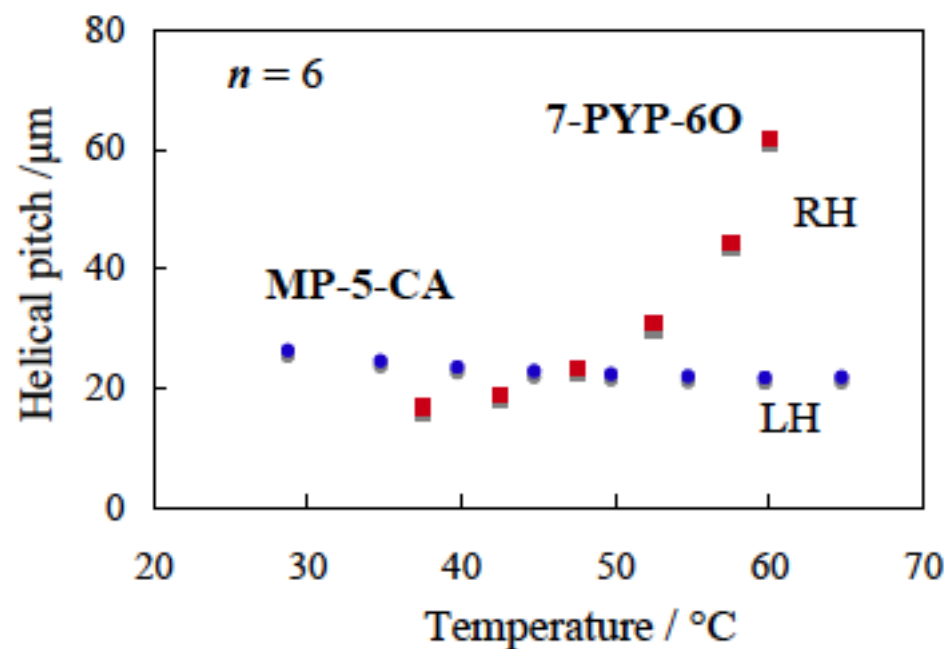
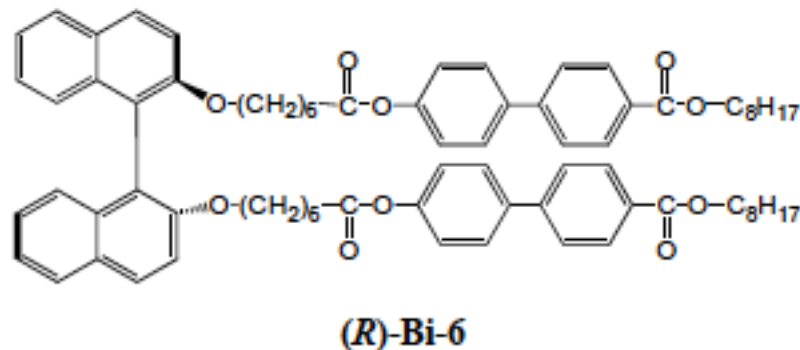
1. The two origins of the twisting power are thought to induce biaxial helix, which plays an important role in stabilizing the double twist structures.
2. A difluoro-substituted core might stabilize a cubic blue phase.
3. A liquid crystal oligomer which has a tendency to exhibit a glassy state can stabilize the amorphous phase.

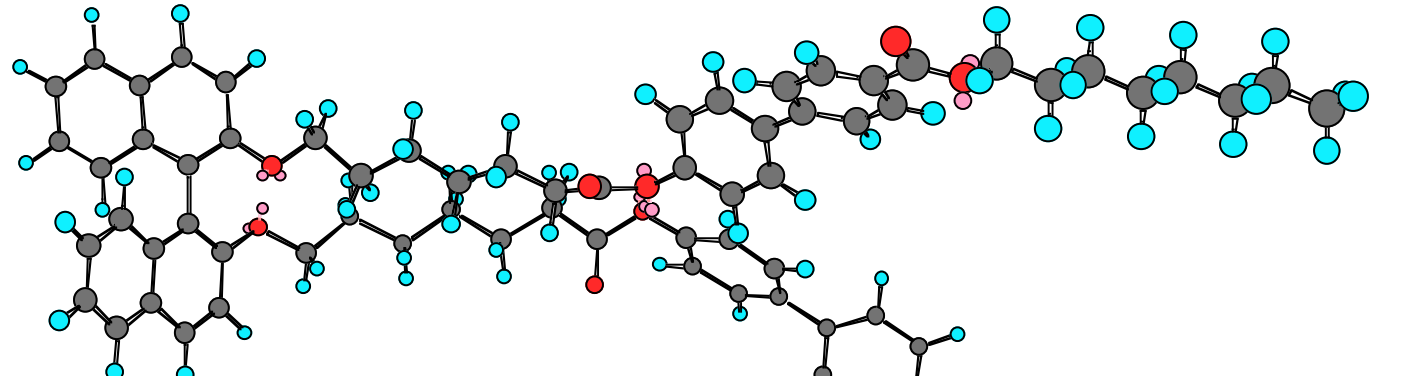
ビナフチル誘導体のねじれ力の起源

K. Kobayashi & A. Yoshizawa, *Liq. Cryst.*, 2007, **34**, 1455.



**Temperature-dependencies of N* helical pitch values induced by 2 wt% of (R)-Bi-6
in the mixture with 7-PYP-6O and that with MP-5-CA.**



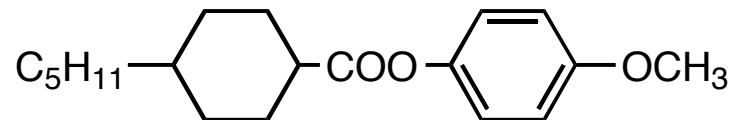


20-6

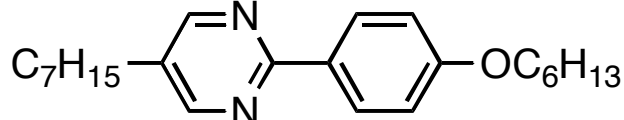
LH

RH

Core-core interactions

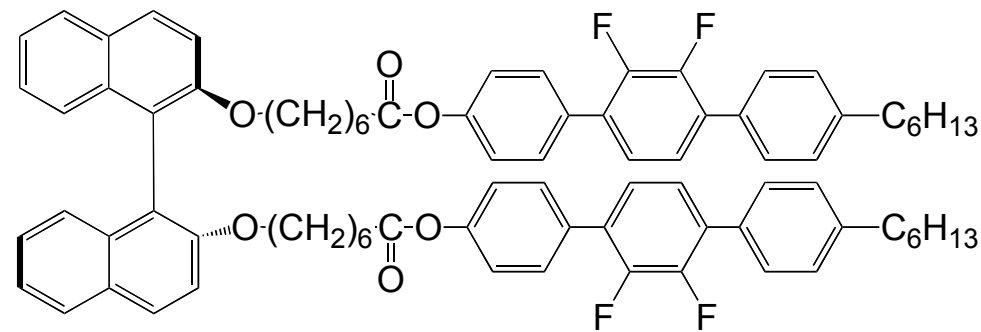


MP-5-CA

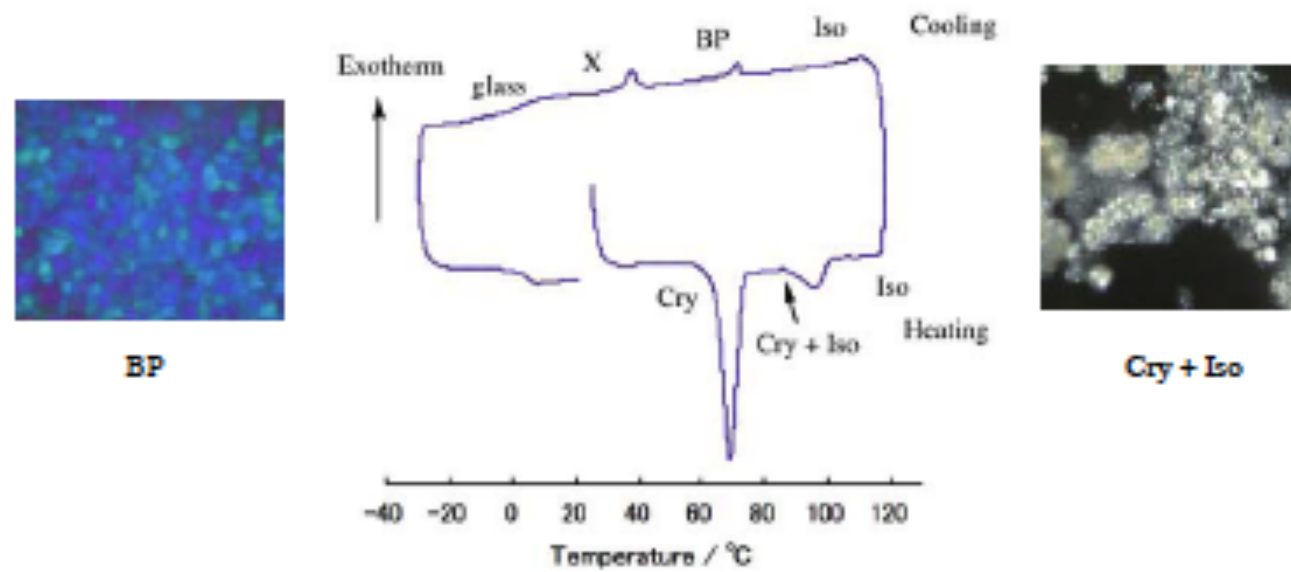


7-PYP-6O

Binaphthyl derivative with a cubic BP



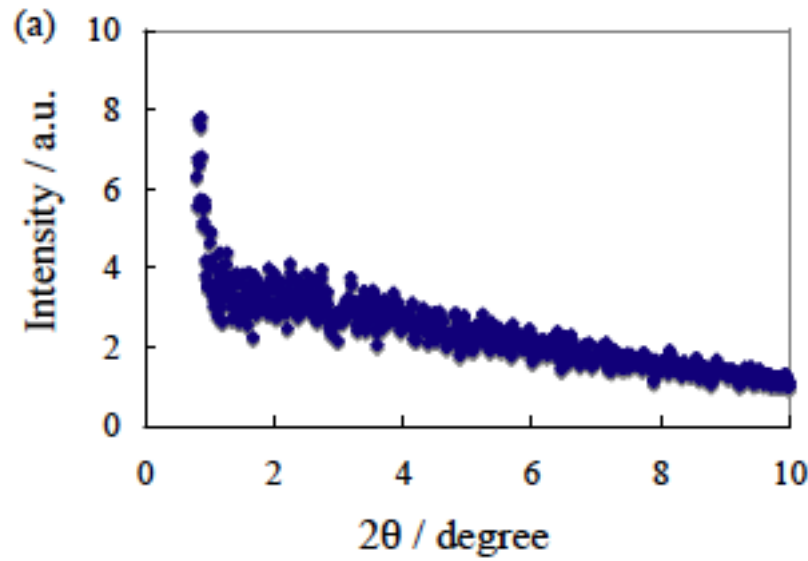
glass 8 °C X 40 °C BP 72 °C Iso



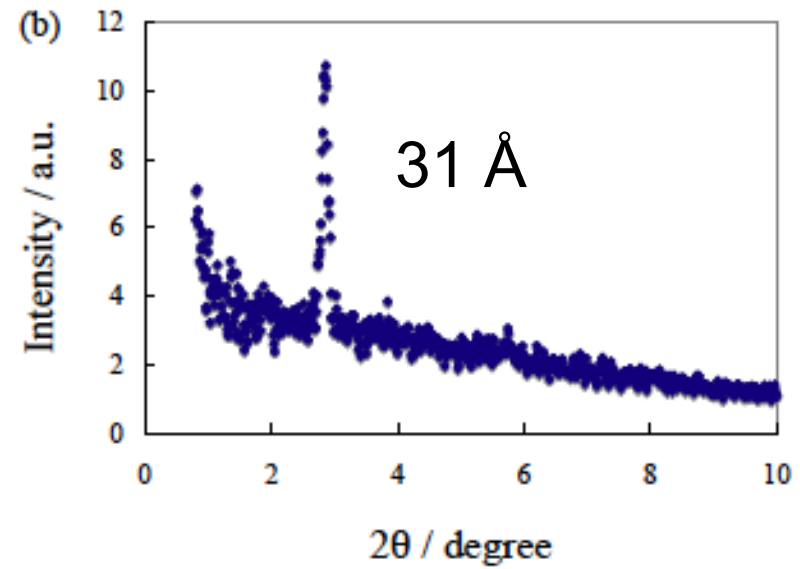
A. Yoshizawa, Y. Kogawa, K. Kobayashi, Y. Takanishi and J. Yamamoto, *J. Mater. Chem.*, 2009, 19, 5759.

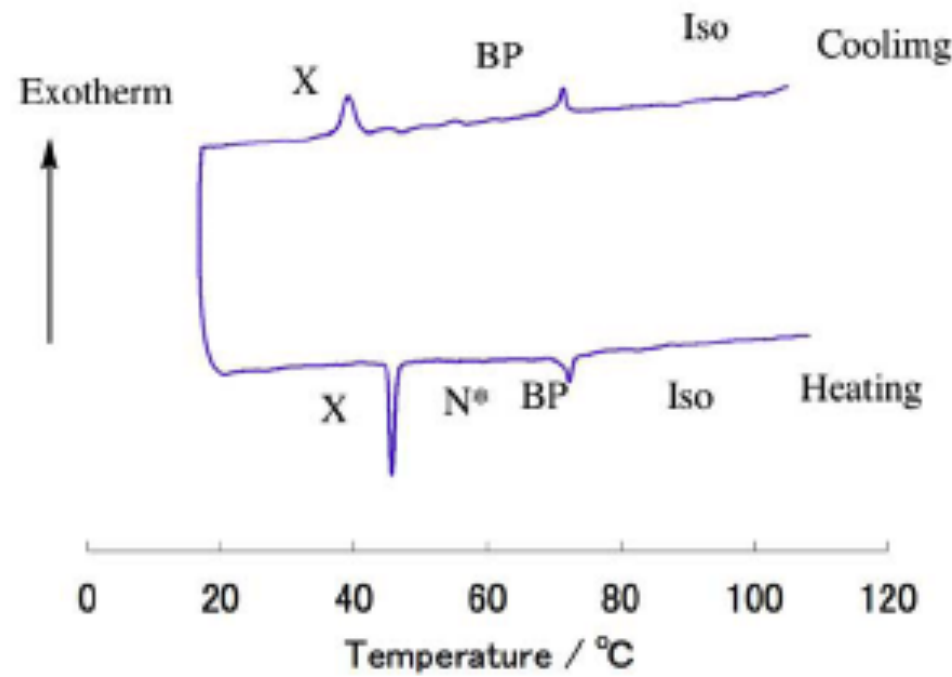
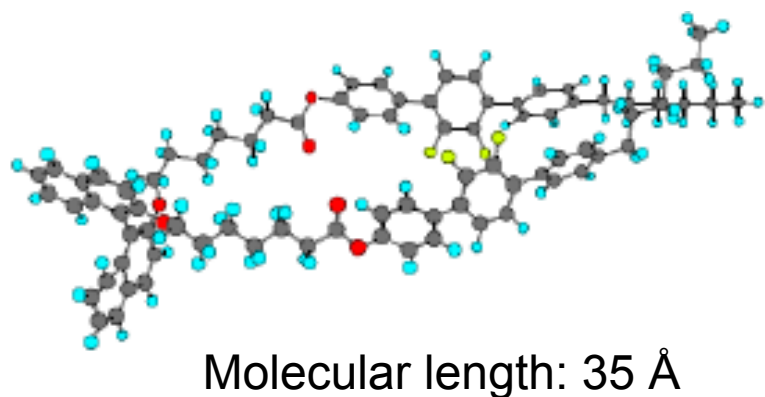
X-ray diffraction patterns

Blue phase



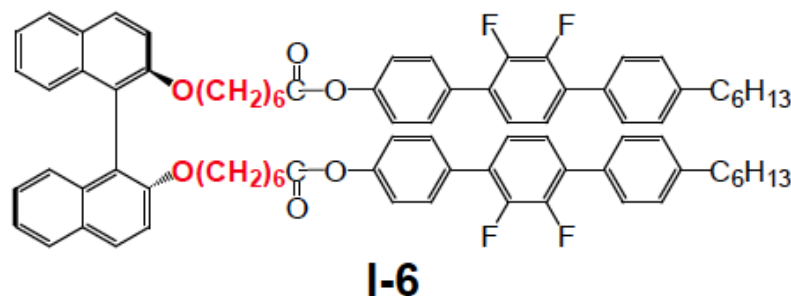
X phase



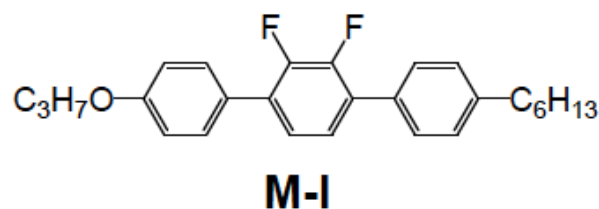


Helical twist inversion

I-6: Iso 72°C BP 40°C X

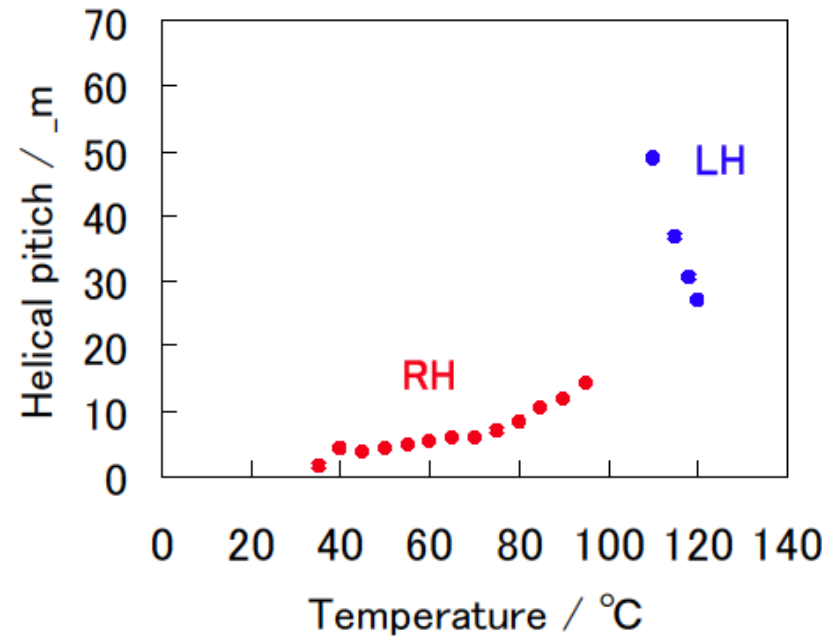


I-6

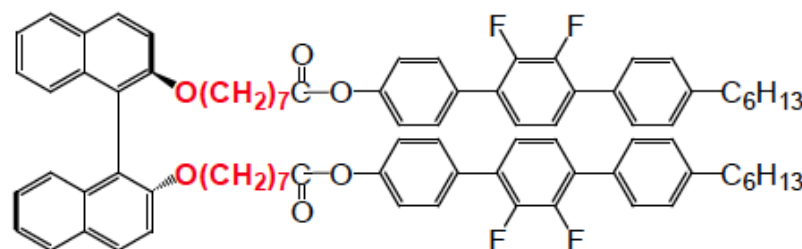


M-I

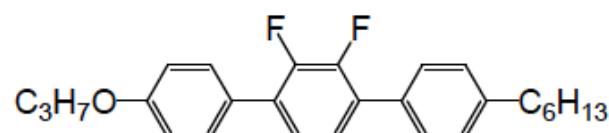
50-50 wt%



I-7: Iso 88°C N* 48°C X

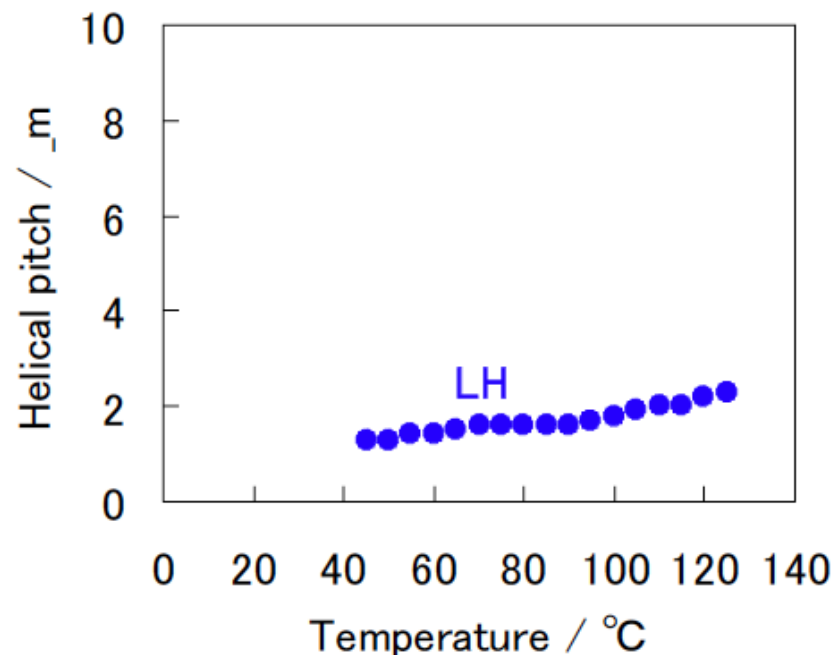


I-7

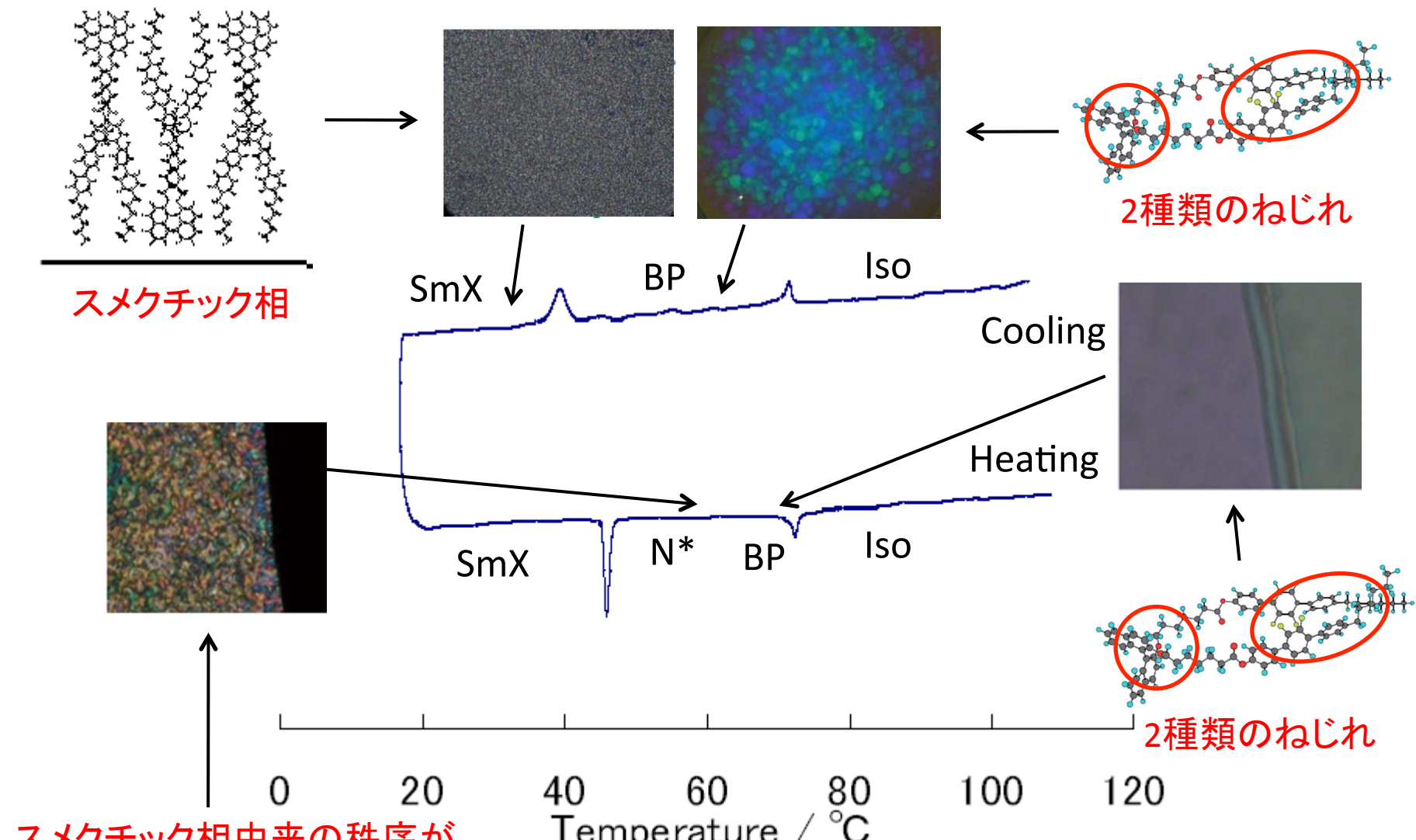


M-I

50-50 wt%



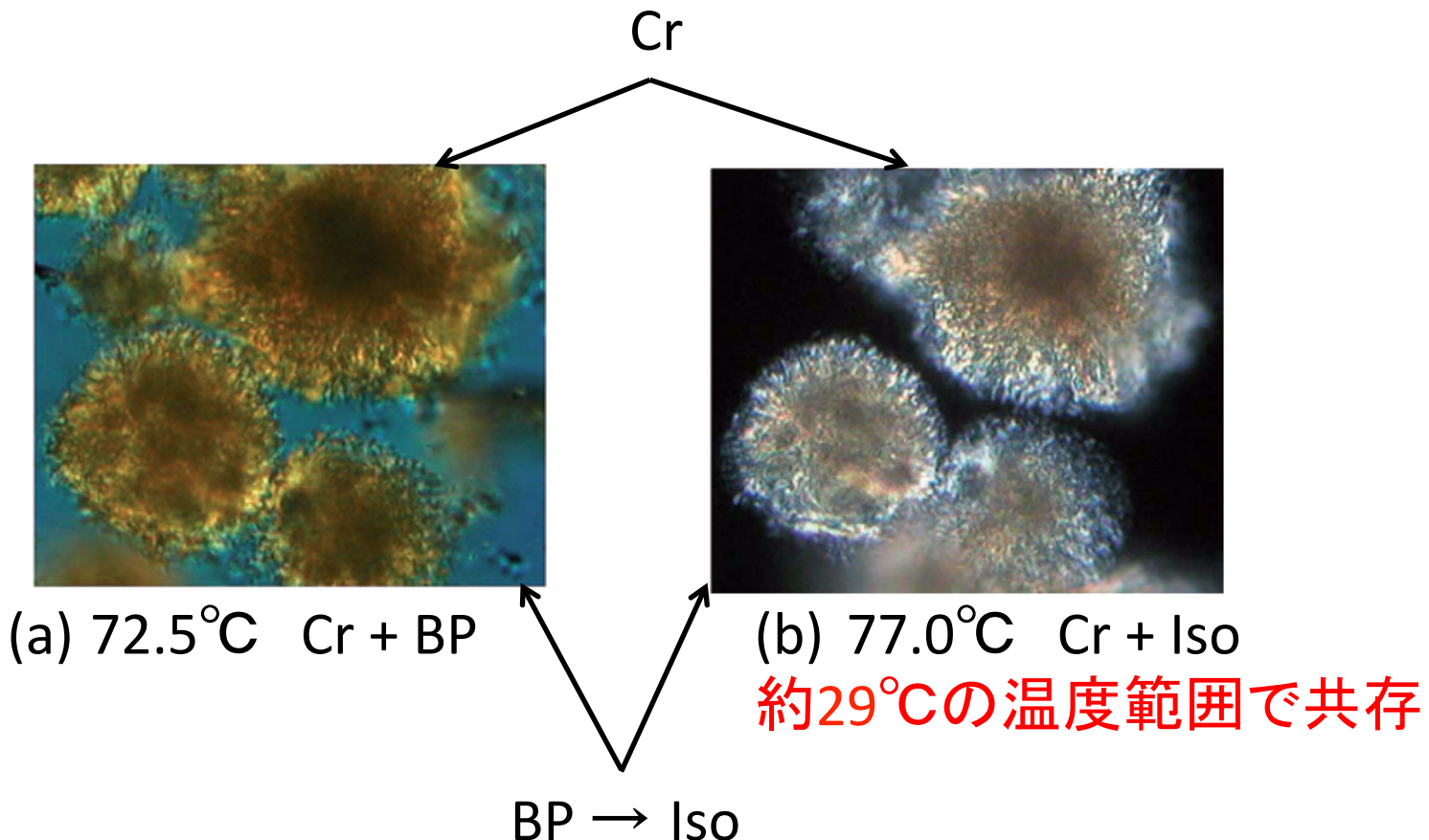
I -6の冷却・加熱過程のDSCチャート



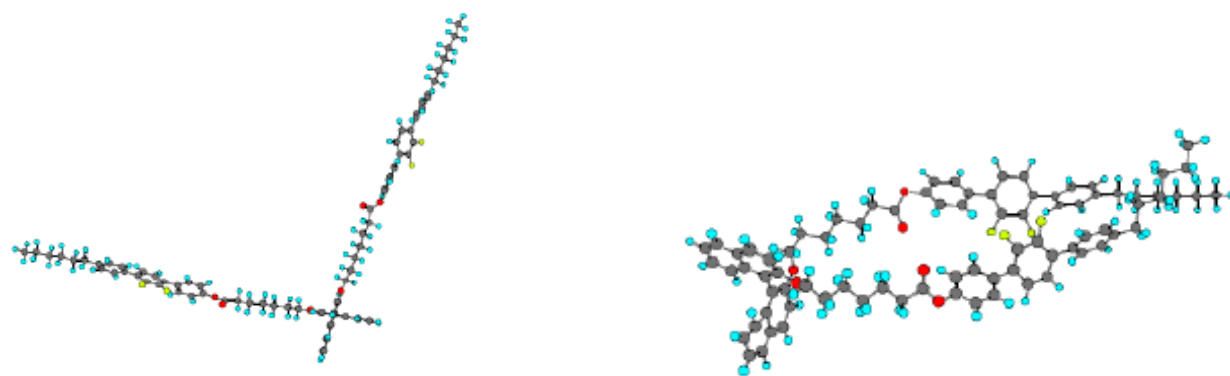
スメクチック相由来の秩序が
残っているため二軸性ヘリッ
クスが失われ N^* が発現

結晶から加熱時の顕微鏡写真

- ・ 液晶状態からではなく、結晶から加熱

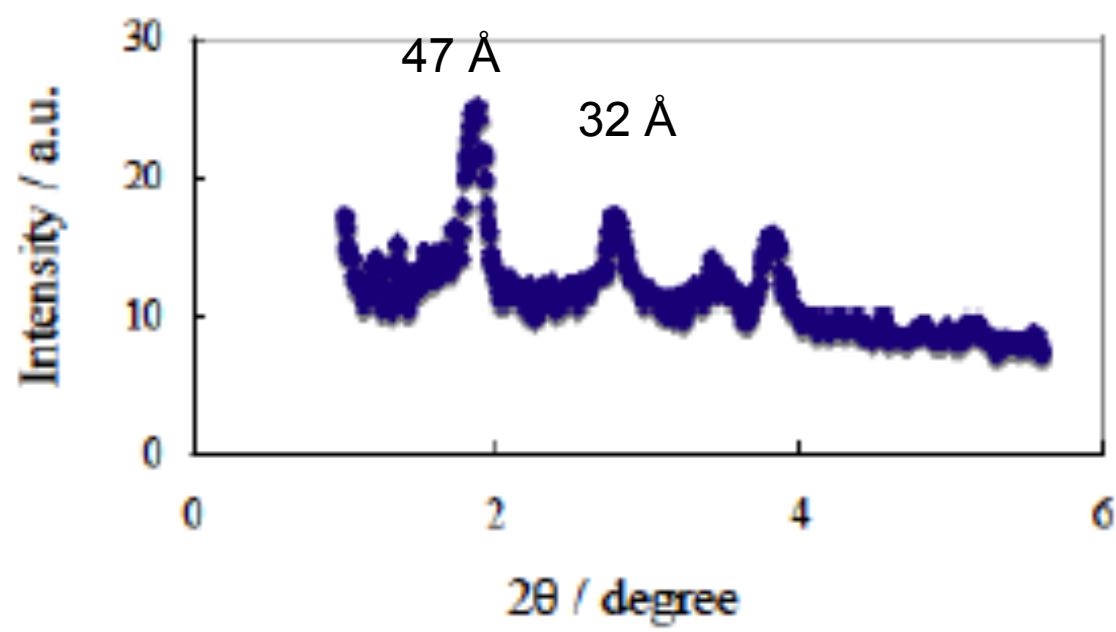


单一化合物では極めてまれな相分離を確認

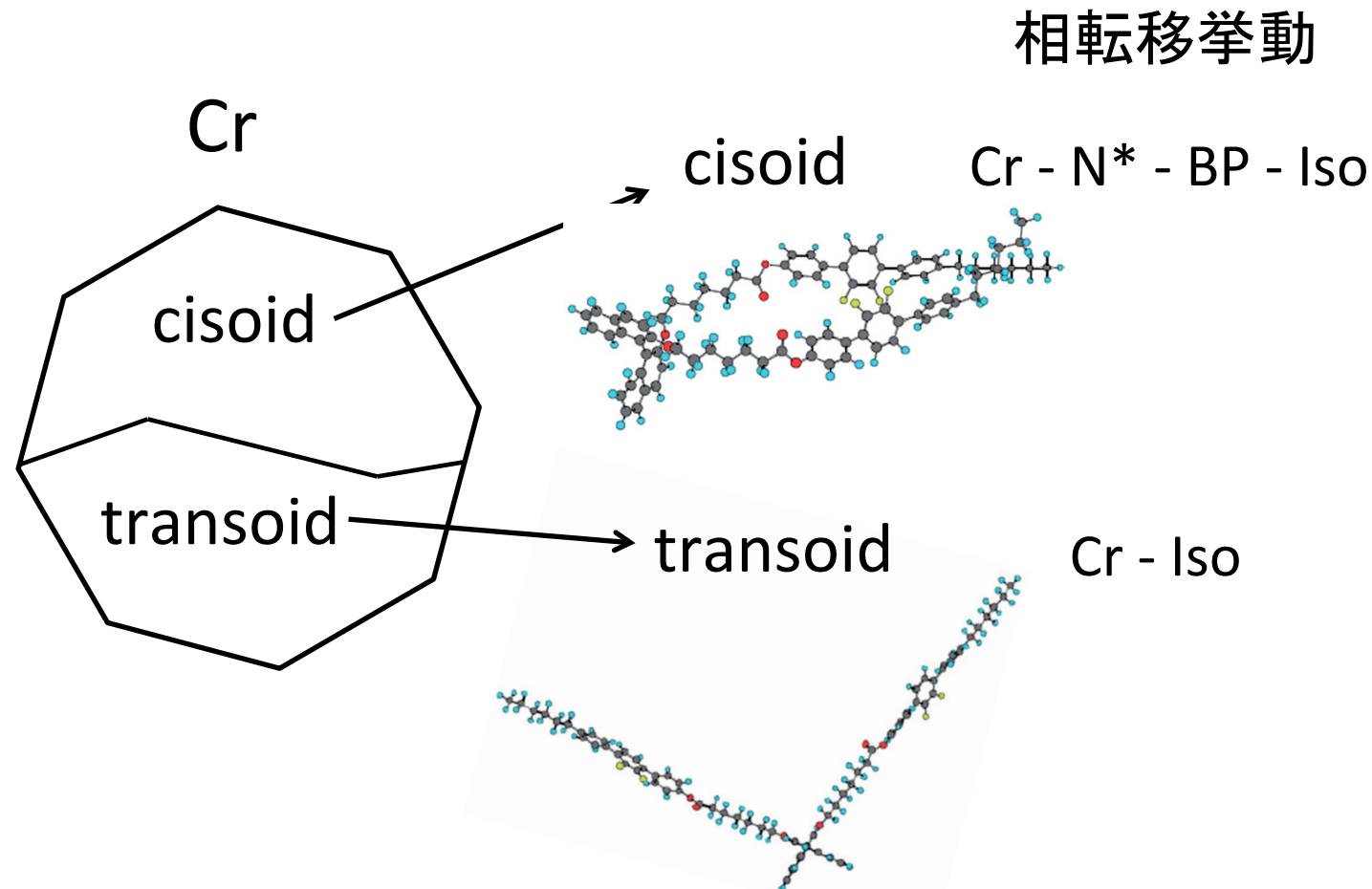


52 Å

35 Å

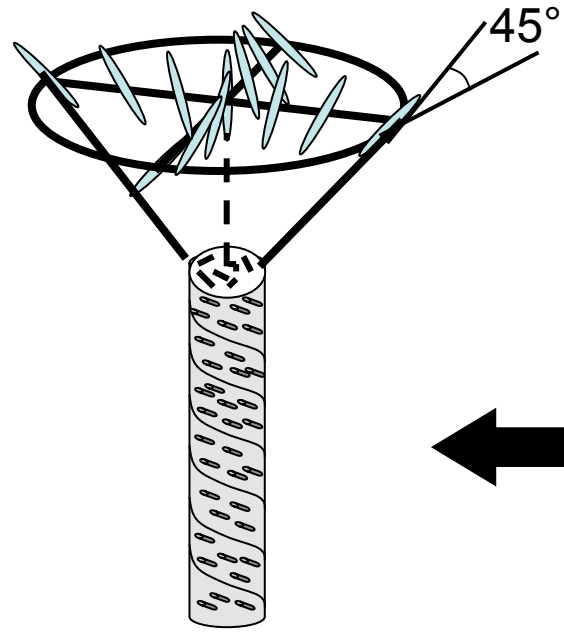


結晶からの融解挙動

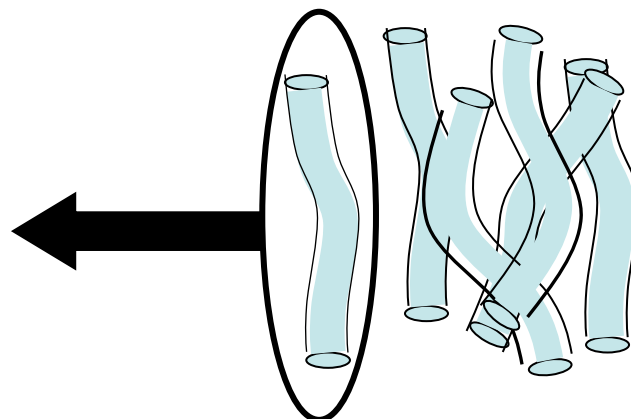


結晶状態から加熱した際に見られた相分離は、二つのコンフォメーションがそれぞれのドメインを形成したことによると考えられる。

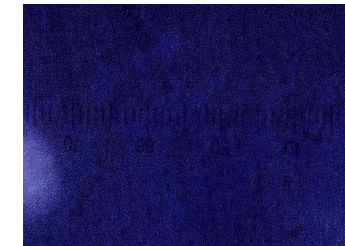
アモルファスブルー相(BPIII)



三次元らせん構造
(2重ねじれ円柱構造)



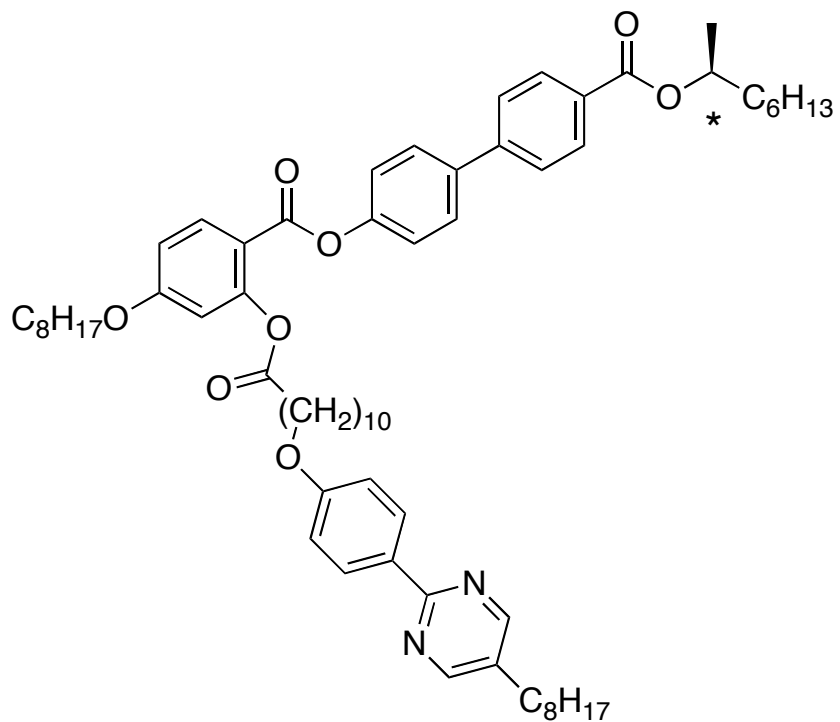
BPIII(アモルファス)



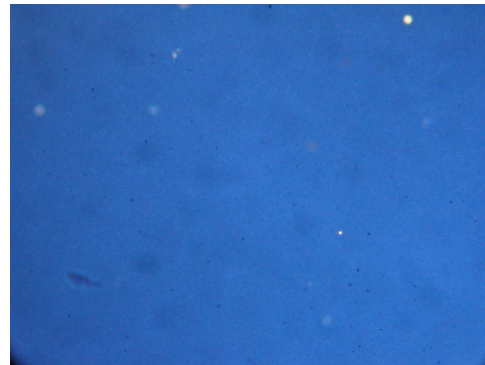
fog texture

- ・液晶分子が可能な全方位にらせん構造を形成する二重ねじれ円柱構造
- ・光学的に等方性
- ・液体と同じ対称性

T-shaped LC oligomer - Chirality & molecular biaxiality-



Cry 63 °C [N* 15 BPIII 28 (1.4 kJmol⁻¹)] Iso



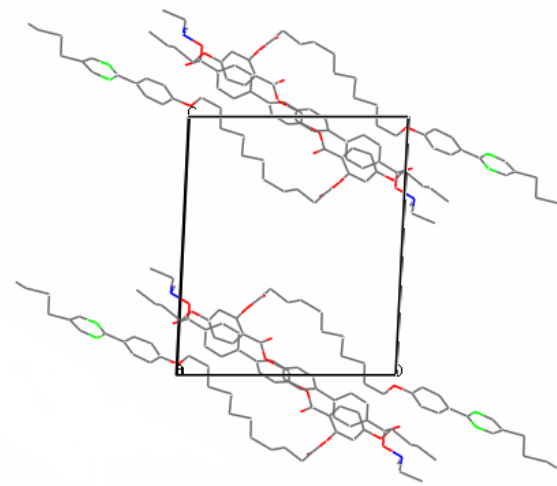
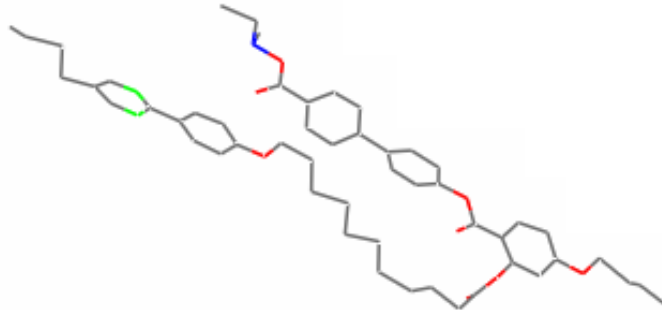
BPIII (25 °C)



N* (10 °C)

A. Yosizawa, M. Sato and J. Rokunohe, *J. Mater. Chem.*, 2005, **15**, 3285.

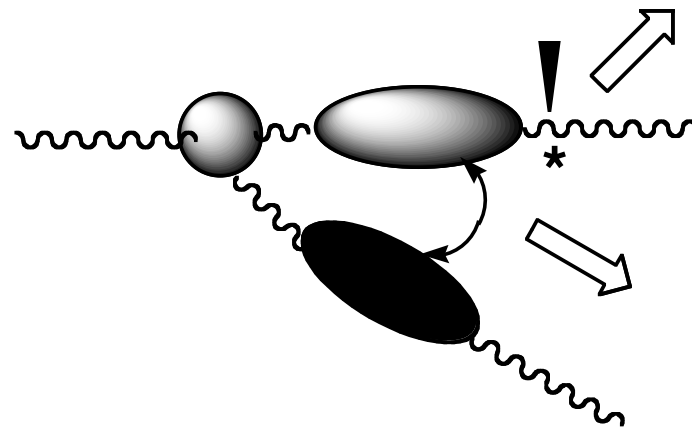
Crystal structure



1. Gauche configurations exist in the central spacer.
2. The compound has a λ-shaped structure instead of T-shaped.

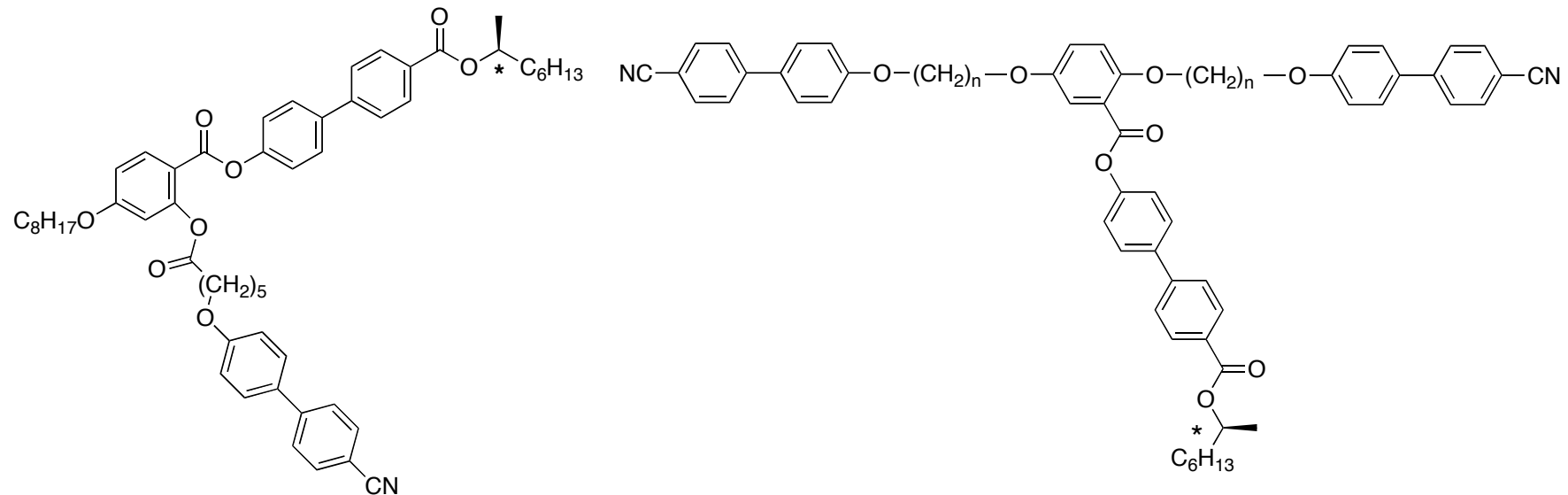
M. Sato, F. Ogasawara and A. Yoshizawa, *Mol. Cryst. Liq. Cryst.*, 2007, 475, 99.

Coupling between chirality and molecular biaxiality can organize a twisted configuration of the two mesogenic moieties within a molecule.



1. The two origins of the twisting power plays an important role in stabilizing the double twist structures.
2. A liquid crystal oligomer which has a tendency to exhibit a glassy state can stabilize the amorphous phase.

Introduction of a CN group to the T-shaped system

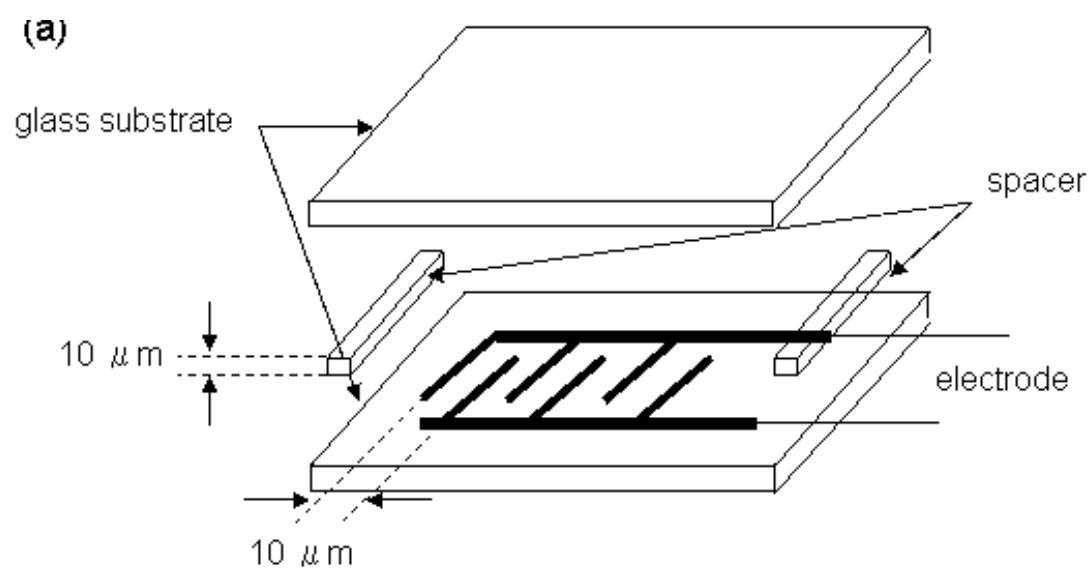
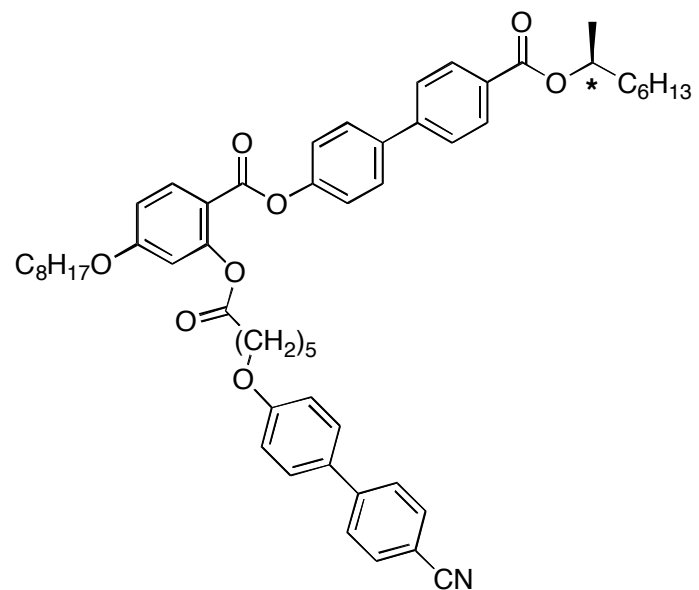


Cr 61 °C [N* 41 BP III 49] Iso

n = 6: Cr 93 °C [N* 91 BP 92] Iso

n = 7: Cr 115 °C Iso

Electrooptical switching in the amorphous BPIII



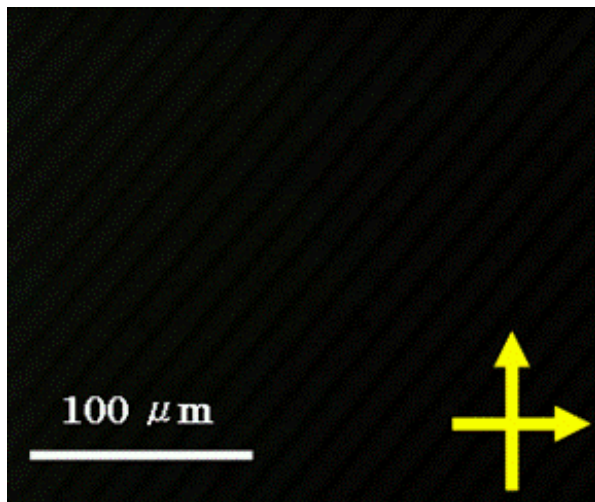
Cr 61°C [N* 41 BP III 49] Iso

Molecular structure

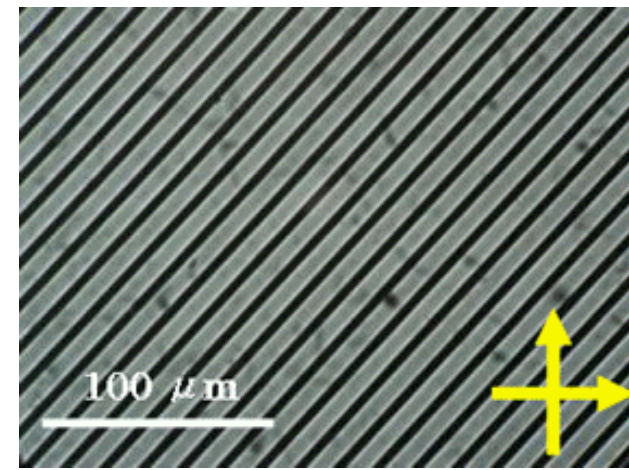
Cell geometry

M.Sato and A. Yoshizawa, *Adv. Mater.*, 2007, **19**, 4145.

Optical textures in the BP at 47 °C

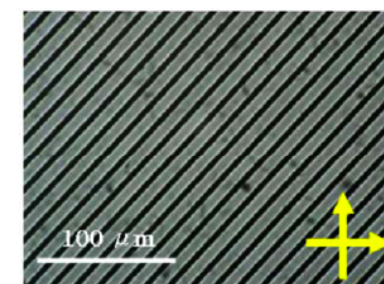
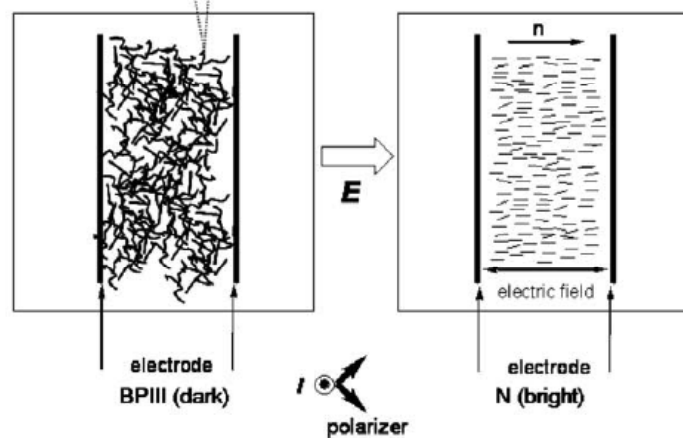
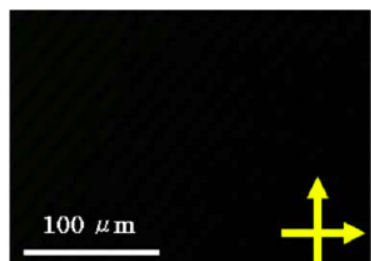
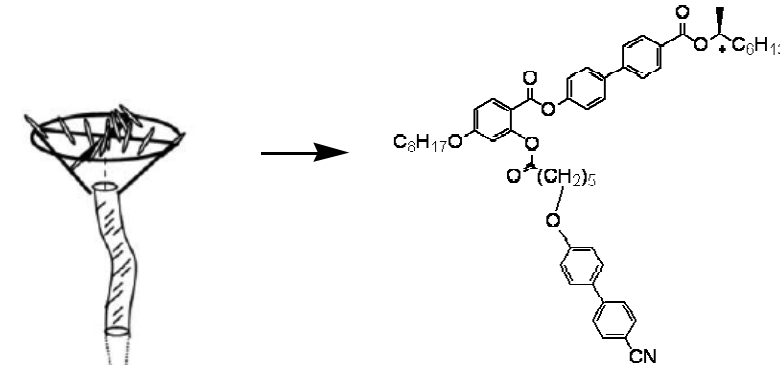


$$E = 0$$

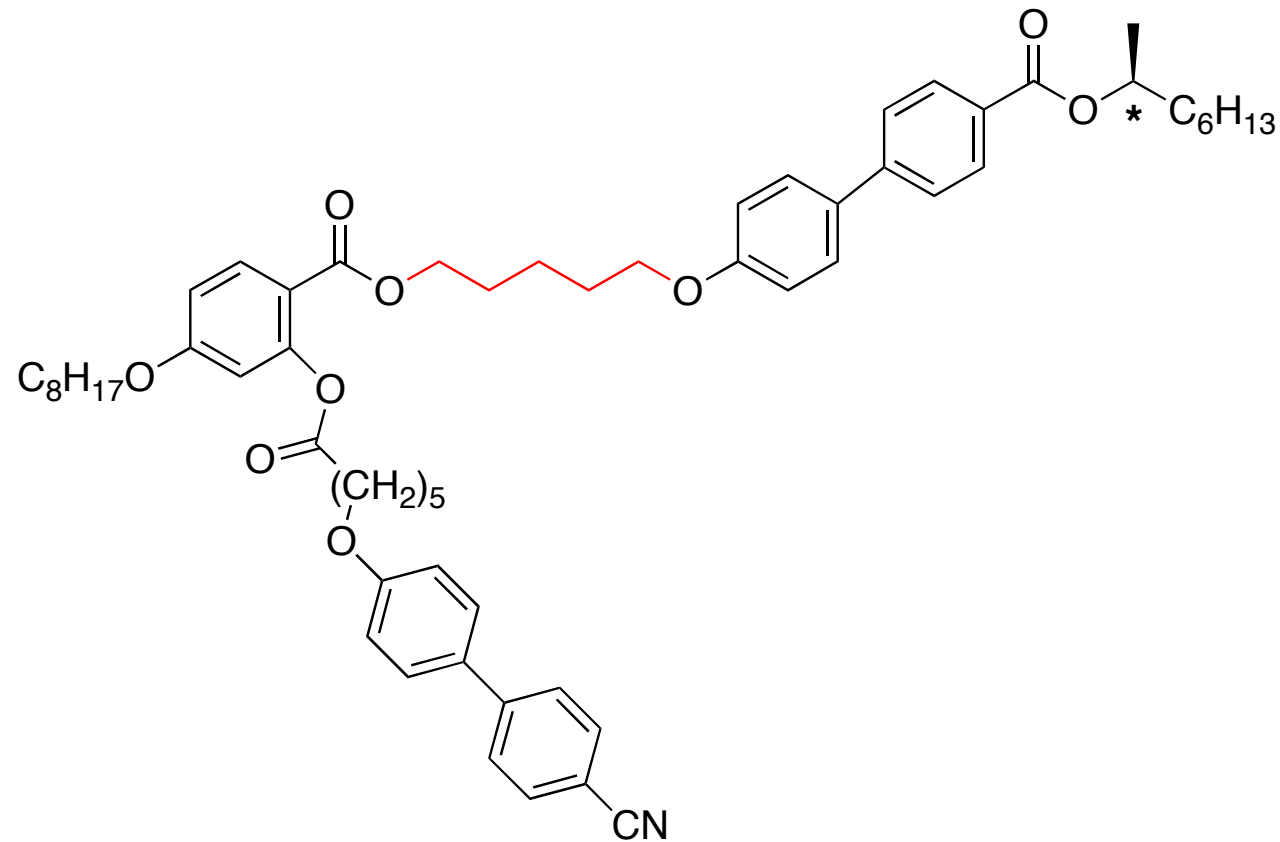


$$E = 8.2 \text{ V} \mu\text{m}^{-1}$$

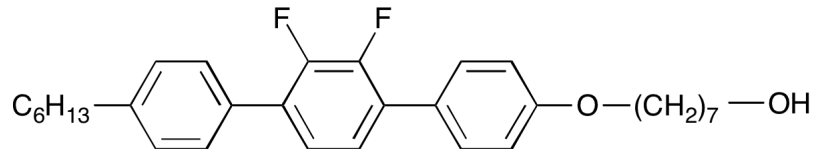
無秩序(BPIII)－秩序(N)相転移を用いた表示素子



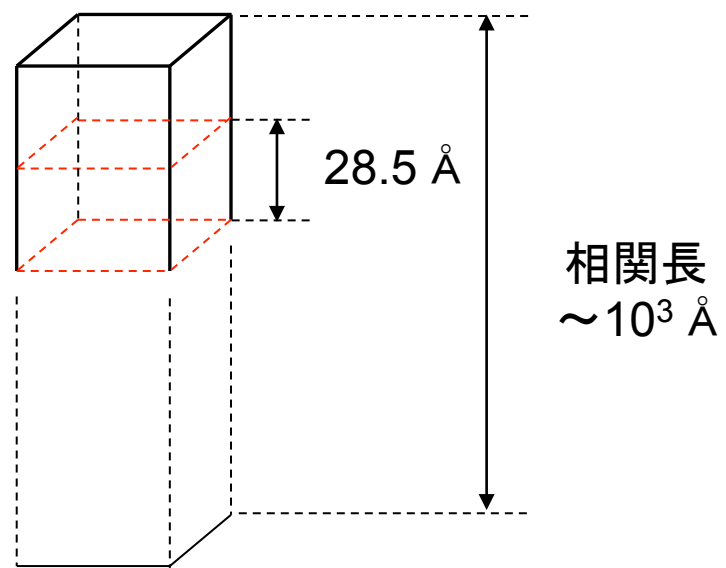
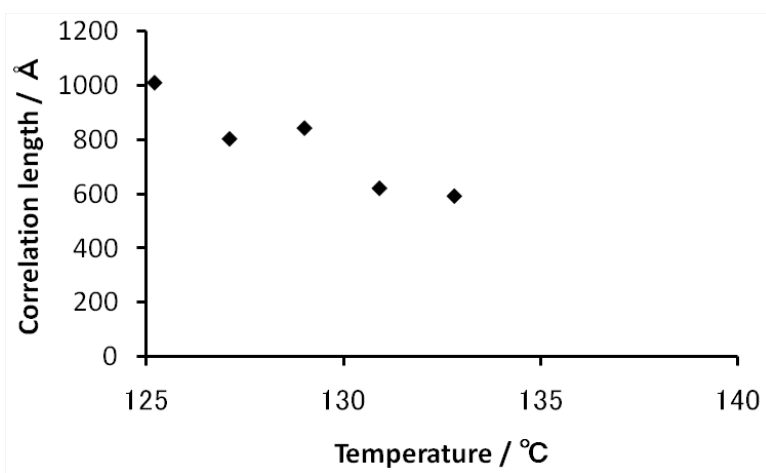
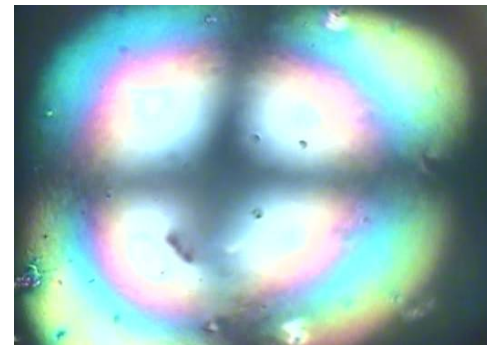
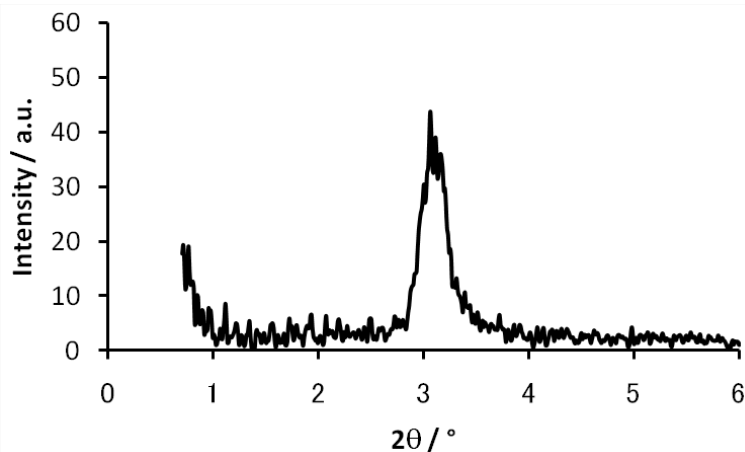
Introduction of a flexible spacer



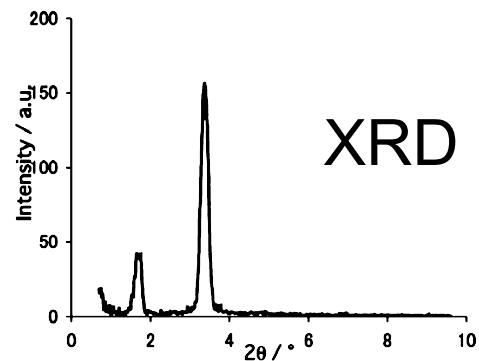
Cry 75°C [glass -0.5 BPIII 25] iso



Iso 146.5 N 124.0 SmA 117.2 SmC 109.5 SmC' 99.7 SmC'' 90 Cr



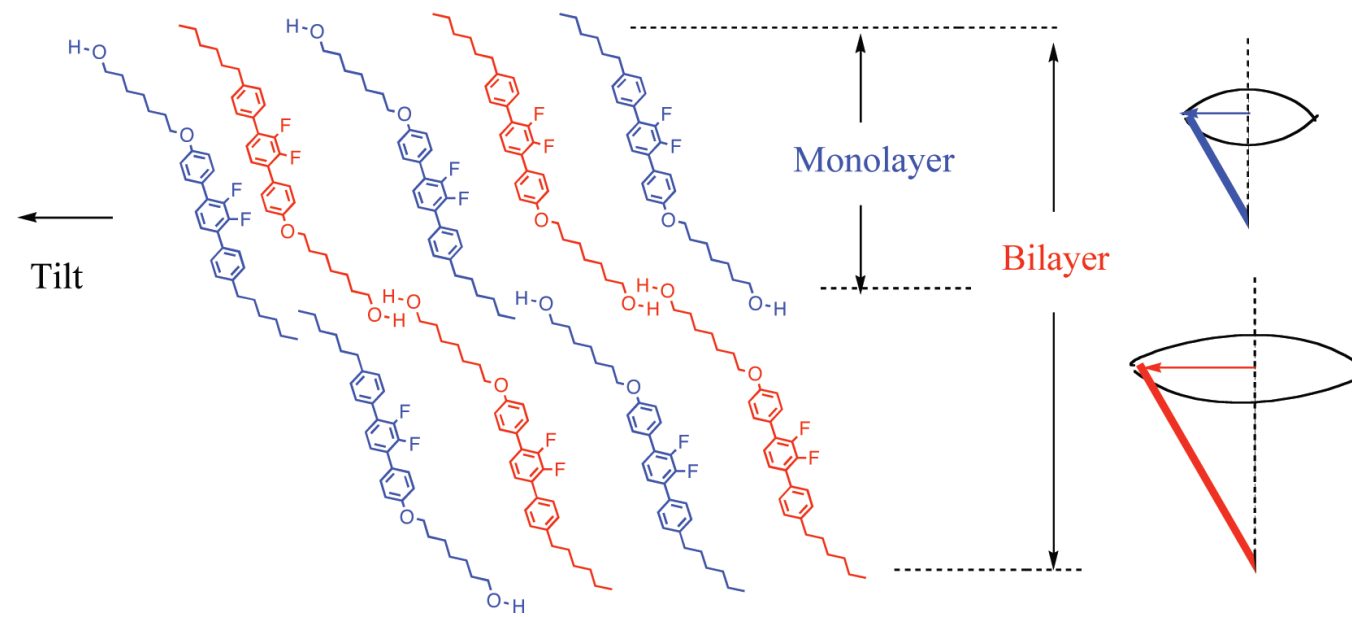
Iso 146.5 N 124.0 SmA 117.2 SmC 109.5 SmC' 99.7 SmC'' 90 Cr



Monolayer

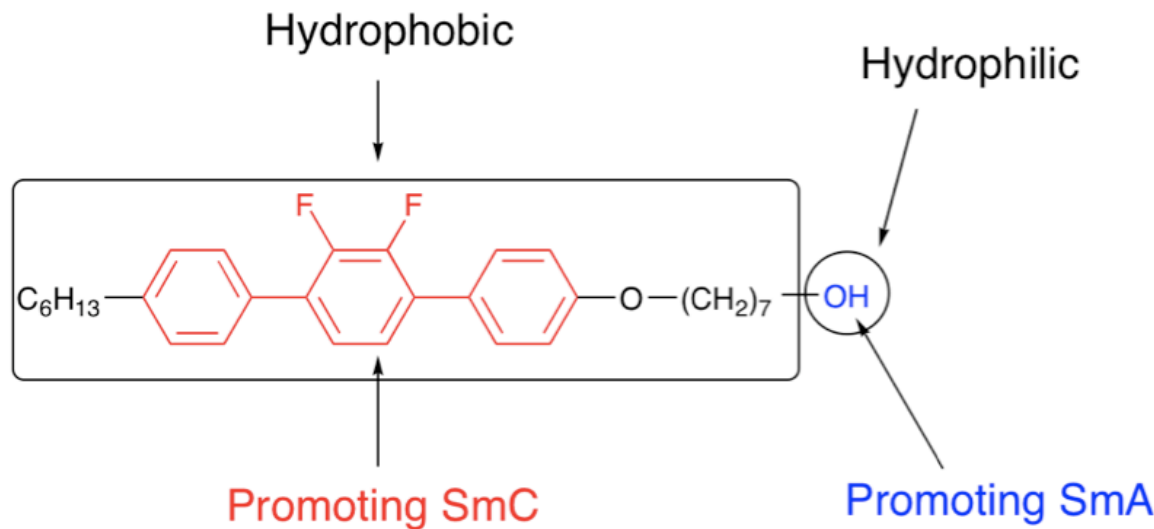
Bilayer

(b) SmC''



2つの周期を持ちながら巨視的揺らぎが存在するスメクチックC相

分子間相互作用の競合による層周期の制御



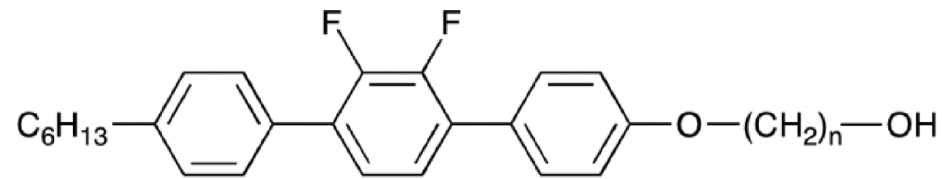
Iso 146.5 N 124.0 SmA 117.2 SmC 109.5 SmC' 99.7 SmC" 90 Cr

クラスター

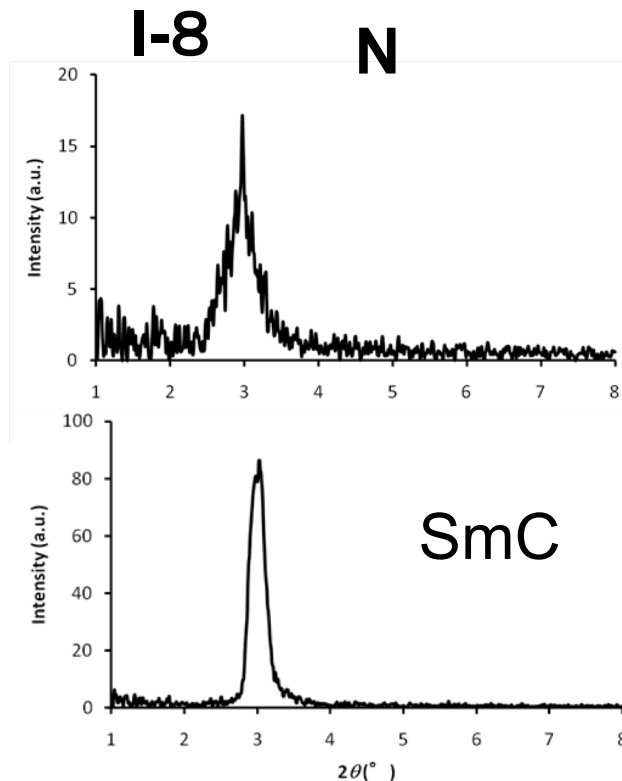
Monolayer

Monolayer & Bilayer

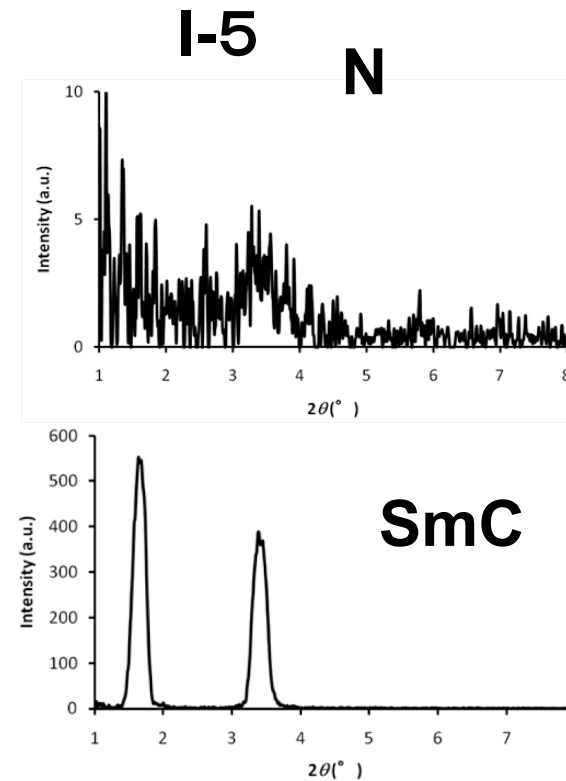
スペーサー長の効果



I-n

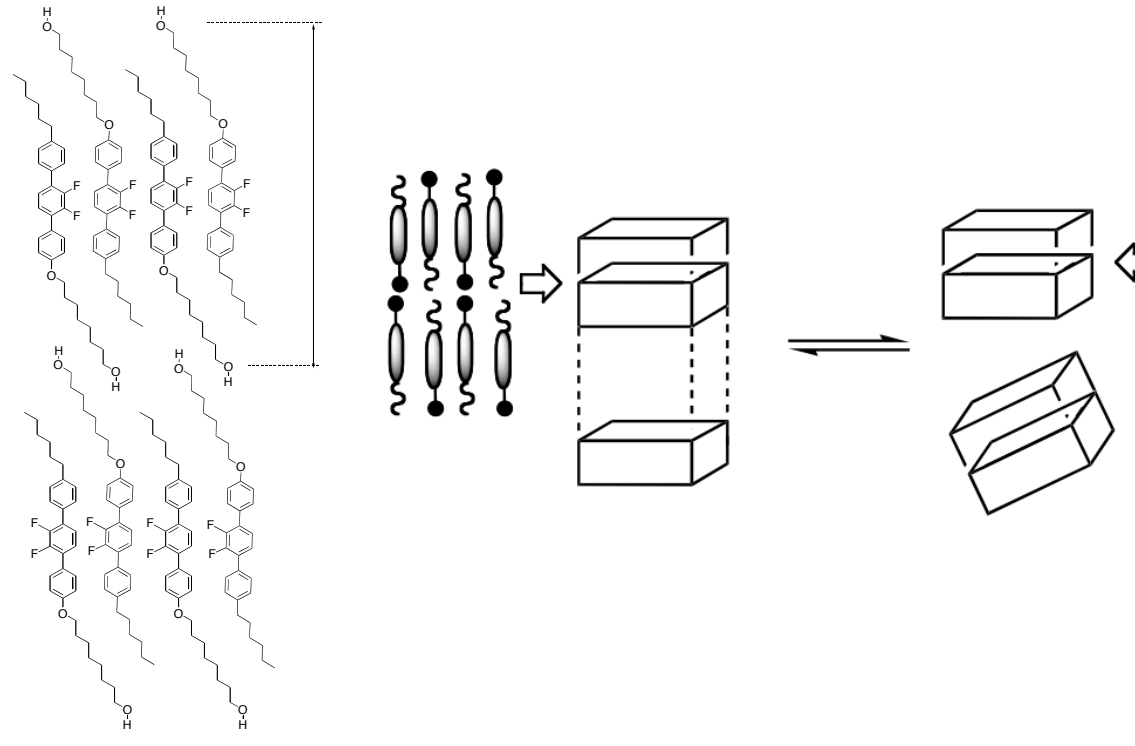


N相: クラスター秩序有り
SmC相: Monolayer



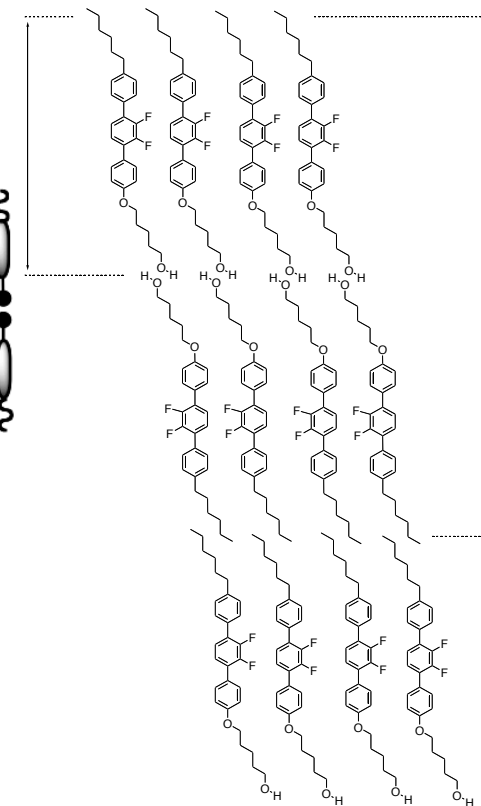
N相: クラスター秩序無し
SmC相: Bilayer & Monolayer

I-8 パッキングエントロピー



水素結合が層の両端に均一に存在
層間の相互作用が同じ
クラスター形成

I-5 ミクロ相分離



水素結合の局在化
層間の相互作用に強
クラスター形成せず